POSIVA

Assessment of the Concentration Limits for Radionuclides for Posiva

Mireia Grivé

Vansessa Montoya

Lara Duro

January 2008

Assessment of the Concentration Limits for Radionuclides for Posiva

Mireia Grivé

Vansessa Montoya

Lara Duro

Enviros Spain S.L.

January 2008

ASSESSMENT OF THE CONCENTRATION LIMITS FOR RADIONUCLIDES FOR POSIVA

ABSTRACT

The present document assesses the near-field concentration limits of the radionuclides of interest for Posiva (C, Ni, Se, Sr, Mo, Zr, Nb, Tc, Pd, Sn, Cs, Sm, Ra, Th, Pa, U, Pu, Np, Am and Cm) under the geochemical composition of the Olkiluoto groundwaters. The limits provided here are intended to be used only in the area close to the fuel given that no major solid phases other than the ones produced by the anoxic corrosion of the canister and the fuel itself are considered.

Calculations have been performed by using the PHREEQC code. Three different general cases have been considered when assessing the composition of the groundwater contacting the fuel: a) Groundwater contacts the fuel without any prior interaction with the buffer b) Groundwater is modified by interaction with Bentonite, and c) Glacial meltwater reaches the fuel. The redox state of the system has been considered to cover different evolution of the repository for the different groundwaters. Besides of the given redox potential of the groundwaters, two variations of the redox state have been accounted for in this analysis to consider the evolution of H_2 due to the anoxic corrosion of the cast iron insert: a) The maximum pH_2 overpressure is limited by the hydrostatic and swelling pressure of bentonite at repository depth, and b) The pH_2 overpressure is limited by the hematite/magnetite stability boundary. This exemplifies the corrosion of iron to magnetite in a first step, and its further evolution to hematite in a second step.

Tables summarizing the solubility and aqueous speciation of the different waters as well as the main uncertainty parameters affecting the results are provided. The concentration limits recommended in this report are based on the following assumptions: i) radionuclides will form individual solid phases, and ii) the rate of dissolution of radionuclides from spent fuel is fast enough as to ensure that equilibrium with individual solid phases is achieved for times shorter than the residence time of water in the system.

Keywords: Solubilities, Radionuclides, Asssessment, Concentration limits, Near-Field

RADIONUKLIDIEN PITOISUUSRAJOJEN ARVIOIMINEN POSIVALLE

TIIVISTELMÄ

Tässä raportissa on esitetty arvio Posivan käytetyn polttoaineen loppusijoitustilan lähialueen radionuklidien (C, Ni, Se, Sr, Mo, Zr, Nb, Tc, Pd, Sn, Cs, Sm, Ra, Th, Pa, U, Pu, Np, Am and Cm) pitoisuusrajoista Olkiluodon pohjavesiolosuhteissa. Esitetyt arviot edustavat polttoaineen lähiympäristön olosuhteita ja kapselin sekä itse polttoaineen hapettomissa olosuhteissa syntyvien korroosiotuotteiden liukoisuusarvoja.

Pitoisuusrajojen arvioimiseen on käytetty PHREEQC-ohjelmistoa. Polttoaineen kanssa kosketuksessa olevan pohjaveden koostumus on arvioitu kolmea lähestymistapaa käyttäen: a) pohjavesi on suorassa kontaktissa polttoaineen kanssa ilman vuorovaikutusta bentoniitin kanssa, b) polttoaineen kanssa kontaktissa oleva pohjavesi on muuttunut pohjavesi-bentoniitti vuorovaikutuksesta ja c) jääkauden sulamisvesi pääsee kontaktiin polttoaineen kanssa. Systeemin redox-tila kuvaa loppusijoitustilan eri kehitysvaiheita eri pohjavesien osalta. Pohjavesien mitattujen redoxpotentiaaliarvojen lisäksi on redox-tilaa määritelty sisäosan raudan korroosioreaktioihin ja syntyvään vetymäärään perustuen. Ensimmäisessä tapauksessa tarkastellaan magnetiitin muodostumista raudan korroosiossa, jolloin syntyy maksimaalinen määrä vetykaasua. Vetykaasun pitoisuutta rajoittavat hydrostaattinen paine ja bentoniitin paisuntapaine. Seuraavassa vaihessa tarkastellaan magnetiitin muuttumista hematiitiksi, jolloin vedyn osapainetta säätelee hematiitti/magnettiitti stabilisuusraja.

Liukoisuus- ja spesiaatiotulokset ja niihin vaikuttavat keskeiset epävarmuudet on koottu yhteenvetotaulukoihin. Tässä raportissa suositellut pitoisuusrajat perustuvat seuraaviin olettamuksiin: i) radionuklidit muodostavat yksittäisiä kiinteitä faaseja ja ii) polttoaineesta liukeneminen on riittävän nopeaa jotta tasapaino kiinteän faasin kanssa saavutetaan lyhyemmässä ajassa kuin veden viipymäaika systeemissä.

Avainsanat: Liukoisuudet, radionuklidit, arviointi, pitoisuusrajat, lähi-alue

TABLE OF CONTENTS

ABSTRACT
TIIVISTELMÄ

1.   BACKGROUND AND OBJECTIVES

The present document assesses the near-field concentration limits of the radionuclides of interest for Posiva under the conditions of Olkiluoto. SKB has currently conducted a new assessment of the near-field solubilities and has also reviewed the thermodynamic database to be used in the calculations based on the last NEA updates as well as on the last works appearing in the open literature (Duro et al. 2005; 2006). Since Enviros Spain has been involved in the assessment of the solubility limits for radionuclides in the near field within the SR-Can exercise (Duro et al. 2005; 2006), the consistency of the task developed is guaranteed.

The present report has been organized into 5 sections and 2 Appendices. The updated thermodynamic database used to conduct the solubility calculations is documented in Duro et al. (2005), with some modifications reported in sub-section 2.6 of the present report.

The main body of this report is conformed by the following sections:

- **Section 2. System under study**
This section presents the general problem by: i) defining the system for which the concentration limits of the radionuclides are assessed ii) presenting and documenting the different scenarios of interest for Posiva (outcome from discussions with Posiva), and iii) describing the modelling approaches.

- **Section 3. Quantification of data**
This section presents the results of the calculations conducted to select the solubility limiting solid phase for each element, under the conditions of the selected groundwaters from Olkiluoto site, bentonite waters (the resulting bentonite porewater after interaction with the groundwater), and two types of glacial meltwater. The aqueous speciation, as well as the main uncertainty parameters affecting the results of the calculations, is presented.

- **Section 4. Main Uncertainties**
This chapter presents the main uncertainties associated to the assessment of the concentration limits of each element.

- **Section 5. Solubilities for elements of interest under different cases**
In this chapter a summary of the solid phase assumed to exert the solubility control of the element in question, the concentration limit of this element, the underlying aqueous speciation and the associated uncertainty is presented.

- **Appendix A**
The compositions of the groundwaters and bentonite waters used in the modelling of solubilities are presented in Appendix A.

- **Appendix B**
Overall summary of the solubilities of the elements of interest under the conditions of the different studied groundwaters is presented in Appendix B.
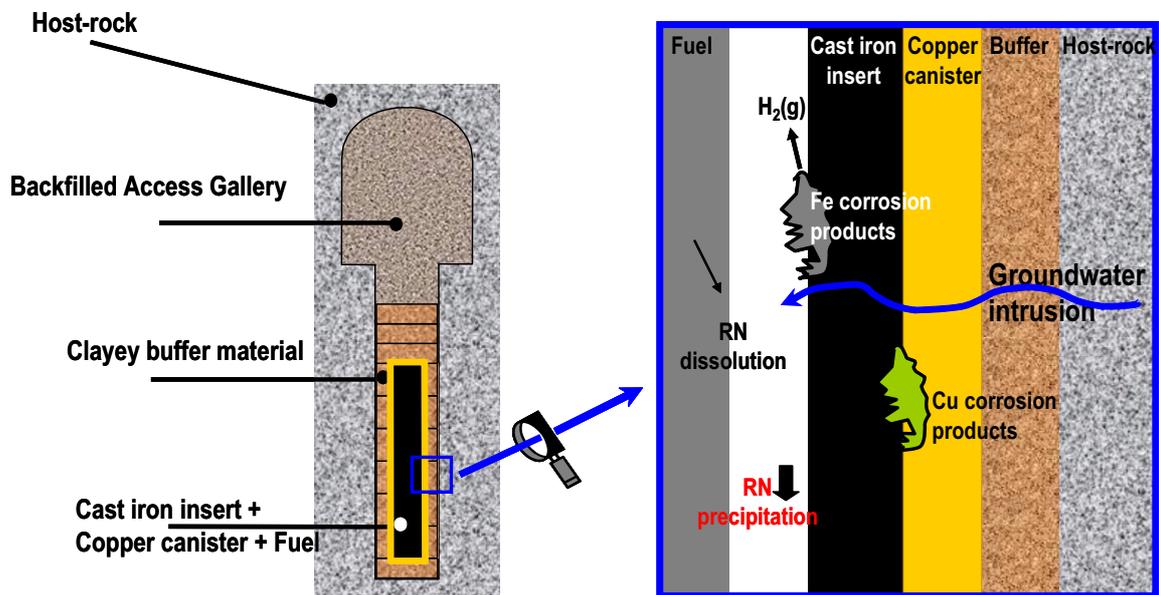
2. SYSTEM UNDER STUDY

In the following sub-sections we present a definition of the system under study, including the description of the different calculation cases and the methodology followed.

2.1 System definition

The assessment of the concentration limits of radionuclides has been done in the vicinity of the spent nuclear fuel, as it was done during the SR-Can exercise (Duro et al. 2006). The limits provided here are intended to be used only in the area close to the fuel given that the absence of major solid phases other than the ones produced by the anoxic corrosion of the canister and the fuel itself. It is assumed that the cast iron insert is corroded under anoxic conditions hence producing hydrogen. Figure 2-1 shows a schematisation of the system under study.

The assessment of the radionuclide concentration limits have been done in the very near field, i.e. in the gap in between the spent fuel and the cast iron insert, the main boundary conditions to define in the calculations are, thus:

i)   The groundwater compositions used in the solubility assessment;
ii)   The redox state of the system, and
iii)   The approaches followed during solubility calculations.

Figure 2-1. *Schematic presentation of the system under study. This figure presents the KBS-3V concept (canisters surrounded by bentonite emplaced vertically in boreholes) but can be also considered representative for the very near-field of a KBS-3H type repository (horizontal emplacements of canisters surrounded by bentonite in a supercontainer (perforated steel shell) in a long deposition drift) with the same canister and bentonite.*

These three bullet points are extensively described and discussed in the forthcoming sections.

2.2 Groundwaters, bentonite waters and glacial meltwaters

Three different general cases have been considered when assessing the composition of the groundwater contacting the fuel:

a) *Groundwater contacts the fuel without any prior interaction with the buffer*
Four selected groundwaters for the solubility calculations have been proposed (Appendix A and *Table 2-1*):

i. A brackish/saline water type that may contain water outside the test section, but still representative for baseline conditions at Olkiluoto in the sampling depth of tens of meters (water sample reference: KR20/465/1).
ii. A saline water type (water sample reference: KR10/498/1) describing the baseline conditions at Olkiluoto.
iii. The special case of upconing of brine water (water sample reference: KR12/741/1) which is dealt with in the calculations, and
iv. A dilute/brackish water type (water sample reference: KR6/58/1) as a limiting composition of the expected possible variations in future chemical conditions.

For the composition of the groundwaters the reader is referred to Table 2-1. These four types should well cover the expected conditions at the site at emplacement and the evolution from post-emplacement until the far future (Pastina & Hellä 2006).

b) *Groundwater is modified by interaction with Bentonite: Bentonite waters*
In this case, the composition of the groundwater contacting the canister has been modified mainly by its interaction with the bentonitic buffer with respect to the major cation and anion composition, and by interaction with the supercontainer steel corrosion products with respect to the redox conditions.

Three of the selected groundwaters defined above have been equilibrated with bentonite (Wersin et al. 2007). The composition of the bentonitic waters is summarized in Table 2-1 (for details see Appendix A).

c) *Infiltration of Glacial meltwater*
Water resulting from the infiltration of glacial meltwater to depth is expected to be rather diluted. Two types of glacial meltwater have been defined (Appendix 1). These waters are: the glacial meltwater used by Pitkänen et al. (2004) and the glacial meltwater (ice melting groundwater) used in SR-Can (see Duro et al. 2006). The former is the estimated Quaternary glacial melt water composition expected from ice melting processes. For Olkiluoto, pyrite/pyrrhotite are very common in fractures and thus pyrite dissolution due to oxygen present in the glacial meltwater are taken into account. This will result in a low pH value (pH 5.8). No oxygen is though expected to be transported to the repository level. The reducing conditions at the repository level have been simulated assuming long-term dynamic equilibrium between magnetite and hematite formed in the system of corroding iron insert ($pH_2 = 10^{-7}$ atm in section 5.3) . In order to

consider the eventuality of dissolved oxygen present in this water, the solubility calculations have been also conducted by assuming oxidising conditions (Eh gw in section 5.3). The second type of meltwater corresponds to the composition of a discharging dilute granitic groundwater sampled from the Migration Shear Zone at the Grimsel Test Site (GTS) in Switzerland, as analogue for the diluted groundwater composition expected from ice melting processes. This water presents a relatively high pH (9.6) due to the interaction of very diluted water with the granitic minerals, as well as a low redox potential which is the result of redox buffering processes in the rock. This high pH glacial meltwater is also closer to the expected slightly alkaline conditions buffered by bentonite.

Both variants are used in the solubility calculations as a way to address the uncertainty in the composition of glacial meltwater potentially intruding at repository depths.

The chemical composition of both groundwaters is given in Table 2-1.

Table 2-1. *Selected composition of groundwaters, bentonite waters and glacial waters. Concentrations in mM (mmol·dm^{-3}).*

Type	OLKILUOTO GROUNDWATERS				BENTONITE WATERS			GLACIAL WATER	
	Brackish Saline	Saline	Dilute brackish	Brine	Brackish saline	Saline	Dilute brackish	Glacial meltwater	Ice melting
Sample	KR20/465/1	KR10/498/1	KR6/58/1	KR12/741/1					
Depth (m)	465	498	58	741					
T(ºC)	15	15	15	15	15	15	15	15	15
Ionic strength	218	478	20	1180	315	507	220	0.0324	1.2
pH	7.4	8.0	7.6	8.2	7.82	7.66	7.39	5.8	9.6
Alkalinity	0.66	0.11	2.79	0.12	0.52	0.40	2.50		0.45
O$_2$								0.22	
DIC	0.55	0.11	2.72	0.04				2.6·10^{-3}	
SO$_4$	0.21	0.01	1.31	0.05	34.9	22.6	74.2	5.2·10^{-4}	0.061
Cl	180.5	380.8	10.4	863.2	185	386	15.1	0.020	0.16
Na	114.8	210.0	9.8	360.9	271	384	167	6.5·10^{-3}	0.69
K	0.28	0.36	0.20	0.49	0.85	1.24	0.53	3.8·10^{-3}	0.005
Ca	32.4	89.1	2.1	254.5	20.8	42.9	10.4	3.2·10^{-3}	0.14
Mg	2.6	1.6	1.1	1.5	6.32	10.9	1.1	4.1·10^{-3}	6.20·10^{-4}
Sr	0.16	0.37	0.01	1.14					2.0·10^{-3}
SiO$_2$	0.36	0.28	0.41	0.21				1.7·10^{-4}	0.25
Mn	5.8·10^{-3}	7.3·10^{-3}		9.3·10^{-3}					5.0·10^{-6}
Fe	2.5·10^{-3}	2.0·10^{-3}	0.024	3.8·10^{-4}	2.3·10^{-3}	4.2·10^{-3}	0.04	1.8·10^{-6}	3.0·10^{-6}
S^{2-}	5.61·10^{-3}	<3.12·10^{-4}	6.24·10^{-4}	1.25·10^{-3}	5.3·10^{-3}	4.8·10^{-3}			
F	1·10^{-5}	9.8·10^{-5}	3.2·10^{-5}	6.3·10^{-5}					0.36
PO$_4$	<3·10^{-7}	1·10^{-7}	5·10^{-6}	2.6·10^{-6}				3.1·10^{-6}	

Type	OLKILUOTO GROUNDWATERS				BENTONITE WATERS			GLACIAL WATER	
	Brackish Saline	Saline	Dilute brackish	Brine	Brackish saline	Saline	Dilute brackish	Glacial meltwater	Ice melting
NO_3^-								$1.1 \cdot 10^{-3}$	
Br^-								$1.2 \cdot 10^{-5}$	
Al								$3.7 \cdot 10^{-6}$	
Eh (mV)	-217 S(6)/S(-2)	-258 S(6)/S(-2)	-35 $Fe(OH)_3$/Fe(2)	-299 C(4)/C(-4)	-171 Fe_3O_4/FeS	-160 Fe_3O_4/FeS	-202 Fe_3O_4/FeCO_3	919 H_2O/O_2	-200

2.3 Redox state of the system

The redox state of the system has been considered to cover different evolution of the repository for Olkiluoto groundwaters, bentonite waters and glacial meltwater. Besides of the given redox potential of the waters, two variations of the redox state have been accounted for in this analysis to consider the evolution of H_2 due to the anoxic corrosion of the cast iron insert:

i)   The maximum pH_2 overpressure is limited by the hydrostatic and swelling pressure of bentonite at repository depth (-420 m) (only groundwaters and bentonite waters).

ii)   The pH_2 overpressure is limited by the hematite/magnetite stability boundary. This exemplifies the corrosion of iron to magnetite in a first step, and its further evolution to hematite in a second step.

A thorough description of these cases follows.

2.3.1 Maximum pH_2 overpressure formed and effect of the canister corrosion

Under anoxic conditions, and when the main oxidant present in water is water itself, Fe corrodes, in a first step, to produce $Fe(OH)_2(s)$, which, in turn can experiment the Schikorr reaction to transform into magnetite, Fe_3O_4, being the overall reaction as follows (eq. 2-1):

$$Fe(s) + 4\,H_2O = Fe_3O_4(s) + 4\,H_2 \qquad\qquad \text{(eq. 2-1)}$$
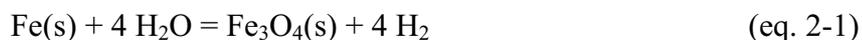
Magnetite has been proposed as the most stable corrosion product of the canister under moderately anoxic conditions. The process causes the generation of hydrogen.

Given the large availability of iron from the canister, a hydrogen overpressure can, theoretically, build up in the system, giving rise to a decrease in the redox potential of the environment. The maximum hydrogen overpressure will be limited by the maximum hydrostatic pressure at the repository depth (420 m). As discussed in the KBS-3H Evolution Report (Smith et al. 2007), gas breakthrough within bentonite has been observed to occur at a pressure approximately equal to the sum of the bentonite swelling pressure (7-8 MPa at full saturation) and the hydrostatic pressure (4 MPa at a depth of 400 m), i.e. at approximately 11-12 MPa at full saturation, which corresponds to about 100 atm[1] and gives the maximum entry pressure of hydrogen gas into bentonite. Consequently, the minimum redox potential that the system can reach will correspond to a $pH_2 = 10$ MPa which, on a redox potential scale, implies a range of Eh = -497 to -544 mV at the pH values of the groundwaters (7.4 to 8.2).

---

[1] As discussed in the KBS-3H Evolution Report (Smith et al. 2007), however, some recent experiments have shown that the breakthrough pressure of gas through bentonite can be substantially higher than this (above 20 MPa) for bentonite with a swelling pressure of ~ 6MPa.

Further corrosion of magnetite will cause the formation of Fe(III) oxides, whose most stable phase in the long term conditions of interest for PA is hematite (α-Fe_2O_3).

This means that at long-term, a dynamic equilibrium between magnetite and hematite can be established in the system, corresponding to the following reaction (eq 2-2):

$$2Fe_3O_4 + H_2O = 3\alpha\text{-}Fe_2O_3 + H_2(g) \qquad \text{(eq. 2-2)}$$
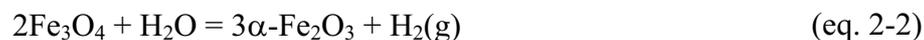
with $logK^0$ = -6.27 (Hummel et al. 2002 and Cornell & Schwertmann 1996).

The boundary between the stability field of magnetite and the one of hematite will occur, thus, at a $pH_2 = 10^{-6.27}$ atm, what would give the long-term redox potential in the system when assuming steel corrosion going-on. In order to represent the range in values in the literature for this equilibrium constant (for a detailed discussion see Hummel et al., 2002), we selected a value of $pH_2 = 10^{-7}$ atm which, at the pH values of the groundwaters (7.4 to 8.2) implies a range of Eh = -231 to -278 mV.

Table 2-2 summarizes the redox conditions used during the solubility calculations in this work, according to the previous text.

Table 2-2. *Redox conditions assumed for solubility calculations corresponding to each groundwater.*

		Conditions		
		Redox (Eh (mV))		
		Eh gw	$pH_2(g)= 10^{-7}$ **atm**	$pH_2(g)= 10^{2}$ **atm**
Groundwater	*KR20/465/1*	-217	-231	-497
	KR10/498/1	-258	-266	-532
	KR6/58/1	-35	-243	-509
	KR12/741/1	-299	-278	-544
Bentonite water	*KR20/465/1*	-171	-256	-522
	KR10/498/1	-160	-246	-512
	KR6/58/1	-202	-230	-496
Glacial meltwater		920 (*)	-136	--
Ice-melting		-200	--	--

[*]Calculated according to the oxygen content present in the composition of the glacial meltwater (see Table 2-1).

2.4 Temperature variation

The reference temperature has been fixed at 15 ºC, which is slightly above the average expected in groundwater at the repository depth (10,5 ºC) and solubility calculations have been made at 15 ºC. No important differences are foreseen for this small temperature difference and this avoids uncertainties arising from more important extrapolations from laboratory data, which is normally gathered at room temperature.

Due to the presence of the waste, it is foreseen that temperature can reach higher temperatures (up to 100 ºC) and this thermal effect can have some effect on the solubility of the radioelements of interest. Solubility calculation at temperatures different from 25 ºC require of data on reaction enthalpy. This type of data is not always available for all the aqueous complexes and solids relevant in our study (for explanations see Duro et al. 2005), and thus may introduce some uncertainty for the evaluation of the solubilities in case of an initial penetrating defect. Nevertheless, these data gaps are not expected to be very relevant to assess a change of temperatures from 25 ºC to 15 ºC, which is the temperature used in the present work.

2.5 Modelling Approaches

- **Elements of interest**

Solubility limits have been assessed for the list of 21 radioelements of interest for Posiva under the geochemical composition of the Olkiluoto groundwater, bentonite water and glacial meltwater given in Table 2-3.

- **Geochemical code**

Solubility calculations have been performed by using the PHREEQC code (Parkhurst & Appelo 2001). The PHREEQC interactive code version 2.10. (released 2nd November 2005) (Parkhurst & Appelo 2005) is a very powerful geochemical program that allows speciation and solubility calculations among other capabilities. The reason for selecting this code, among others, is that it is an open code developed by the USGS that has been widely used in multitude of geochemical calculations and is, therefore, extensively tested in many different types of problems. The PHREEQC code has the capability of calculating the solubility for all radionuclides simultaneously thus considering possible competition among complexes.

- **Ionic strength corrections**

The PHREEQC code can use two different equations to calculate the activity coefficient of a species. By default, it applies the Davies equation (eq. 2-3). But in case that the values of a and b in eq.2-3 are available, the PHREEQC code uses (eq. 2-4) Debye-Huckel for the calculation of the activity coefficients

$$\log(\gamma_i)=-0.5102\,z_i^2\left(\frac{\sqrt{I}}{1+\sqrt{I}}-0.3\,I\right) \qquad (eq.\ 2\text{-}3)$$

$$\log(\gamma_i)=-z_i^2\left(\frac{A\sqrt{I}}{1+Ba_i\sqrt{I}}\right)+b_i I \qquad (eq.\ 2\text{-}4)$$

Where γ = activity coefficient for the i species, z = charge, I = ionic strength, A and B = temeperature dependent Debye-Hückel parameters a_i= hard-core diameter and b_i = temperature dependent parameter

Both these approaches are commonly accepted to calculate activity coefficients for species at ionic strengths lower than 0.1, being in some cases, good extrapolations until I=0.2. These approaches are therefore applicable to dilute/brackish, brackish/saline groundwater, bentonite dilute/brackish, ice melting and glacial meltwater types. Nevertheless, they are not applicable to ionic strengths as high as those of the saline and brine groundwaters and the other two bentonite waters we study in this work. For these cases, according to the NEA guidelines, the Specific Ion Interaction Theory (SIT) is preferred. Unfortunately, none of the geochemical codes used can apply the SIT methodology to calculate the activity coefficient of a species as a function of the ionic strength.

Differences in ionic strengths as a function of the groundwater composition lead us to assess the extent of disagreement between different activity correction approaches. In general, we do not expect significant variations (within ± 0.3 log units for log solubility) in solubility calculations due to different activity corrections. The main differences are expected in the brine water, where the ionic strength is I=1.2 M.

- **Methodology followed in the solubility assessment**

A sensitivity analysis has been first conducted to study the influence of the main groundwater composition on the geochemistry of the selected radionuclides. To this aim we have used the MEDUSA software package (Puigdomènech 2002), which incorporates a very easy diagram drawing algorithm.

As extracted from Duro et al. (2006) "*From the sensitivity analyses, the main solid phases thermodynamically able to precipitate in the system can be identified. Nevertheless, an important contribution of expert judgement must be used when selecting, from all possible thermodynamically favourable phases, those kinetically more likely to form. This expert judgement has been conducted by using several of the sources of information, such as information from laboratory experiments and natural system*".

Table 2-3. *List of radionuclides studied in this exercise.*

Element	
C	Cs
Cl	Sm
Ni	Ra
Se	Th
Sr	Pa
Mo	U
Zr	Pu
Nb	Np
Tc	Am
Pd	Cm
Sn	

Once the solid phase has been identified, the solubility of this phase under the conditions of the groundwater was calculated by using the PHREEQC code and assuming equilibration of the corresponding metal ions with the pure solid phases considered in each case.

- **Approximations in the solubility assessment**

According to the system definition shown in chapter 2.

i)   Calculations have been undertaken at 15ºC.

ii)   The different redox states defined in section 2.3 have been considered.

iii)   No association of radionuclides with major solid phases present in the system has been considered. Initially, no other major solids, except those resulting from the corrosion of the steel, are expected to be present in this area. Thus, co-precipitation processes have been neglected.

iv)   In general, we have assumed the basic principle that the less crystalline phases are kinetically favoured and consequently they constitute the solubility limiting solid phases.

v)   We have not considered the potential microbiologically mediated reduction of sulphate although the potential effect of this process has been discussed when judged necessary.

2.6   Thermodynamic Database

The thermodynamic database used in this work has been the one used in the assessment of the radionuclide solubility limits within the SR-Can Exercise for SKB (Duro et al. 2005) with some modifications.

The improvements incorporated in the TDB used in this work relate to the latest thermodynamic data published within the NEA-TDB project on Se, Ni and Zr (Olin et al. 2005, Gamsjäger et al. 2005 and Brown et al. 2005, respectively), which were not yet available at the closing time of the SR-Can SKB TDB.

Thermodynamic data for Mo have been included from diverse literature studies (Sasaki et al. 1968, Aveston et al. 1964, Naumov et al. 1971, Robbie et al. 1979, Kaback & Runnells 1980, Wagman et al. 1982, Bard et al. 1985 and Rao 1954).

Given the delay in the publication of the NEA-TDB Thorium review, the present work has taken a more consistent and coherent update selection of Th database than that in Duro et al. (2005) by updating information that has been recently published. Data for aqueous hydroxides and solid oxides have been taken from the studies undertaken by Neck and co-workers (Neck & Kim 1999, Neck & Kim 2001, Neck et al. 2002, Neck et al. 2003 and Altmaier et al. 2005). Data for Th aqueous hydroxides have been selected from Altmaier et al. (2005), where previous values from Neck & Kim (2001) have been checked and slightly improved. Polynuclear species may form in acidic media, and have

been included in the Th selection according to the study of Neck et al. (2002). To explain the solubility of Th oxide under carbonate waters, Neck and co-workers propose a speciation scheme including hydroxides, carbonates and mixed hydroxo-carbonate complexes. This speciation scheme allows explaining solubility data obtained in the experiments of Altmaier and co-workers (Altmaier et al. 2005) as well as those experiments performed by Östhols and Bruno (Östhols et al. 1994). Data proposed in Altmaier et al. (2005) and in Altmaier et al. (2006) have been selected in the present work. LogK value for the limiting complex $Th(CO_3)_5^{6-}$ is the upper limit value recommended by Neck and co-workers.

3. QUANTIFICATION OF DATA

This section presents the results of calculations conducted to select the solubility limiting solid phase for each element, under the conditions of the different waters (groundwaters, bentonite waters, glacial meltwater and ice-melting groundwater). The aqueous speciation as well as a presentation on the main uncertainty parameters affecting calculations is also included. These uncertainty parameters are more extensively discussed in section 4. A short table summarising the results for the different redox conditions of the groundwaters is given for each element.

In section 5, different tables containing the most relevant results in terms of solubility limiting phase, concentration limits, main aqueous species and main uncertainty parameters for each element are presented under the conditions of the different waters (groundwaters, bentonite waters, glacial meltwater and ice-melting groundwater). In the Appendix section, one summary table with the solubilities calculated under the nine groundwaters considered in this study is presented.

3.1 Elements of the groups IA to VIIIA

3.1.1 Carbon

The solubility of elemental carbon under the chemical conditions of interest, in the absence of carbonate reduction, will be basically determined by calcite saturation. The solubility curves of calcite under the conditions of the groundwaters (KR20/465/1, KR10/498/1, KR6/58/1 and KR12/741/1) are shown in Figure 3-1 as a function of the calcium concentration. Figure 3-1 also includes the solubility curve of calcite corresponding to the bentonite waters in order to compare with the groundwaters.

We can see that both, the groundwaters and the bentonite waters are nearly in equilibrium with calcite, although slightly undersaturated in the case of KR20/465/1 and KR12/741/1 water, and slightly oversaturated in the KR10/498/1 for the groundwaters, and dilute/brackish water in the case of bentonite waters.

During the last years the fate of C-14 release from the metal parts and possible transport modes used in the safety assessment has been discussed. Based on the outcome of the C-14 workshop, Johnson & Schwyn (2004) pointed out that the proportion of organic C-14 vs. inorganic C-14 released upon corrosion of activated metals is high. In addition to the formation of organic acids, direct formation of methane from metal carbides is also possible (Johnson & Schwyn 2004). Identified organic compounds are e.g., short chain carboxylic acids, alcohols and aldehydes. The fate of these organic molecules is unclear: these can either be transported as such, undergo oxidation to CO_2 or reduction to CH_4 by microbial activity. The timing and the substrate in which these oxidation/reduction reactions occur are not known. Microbial reactions are likely not occurring in the buffer because of the high swelling pressure but might occur at the buffer-rock interface, in the geosphere and, most likely, in the biosphere. As the fate of
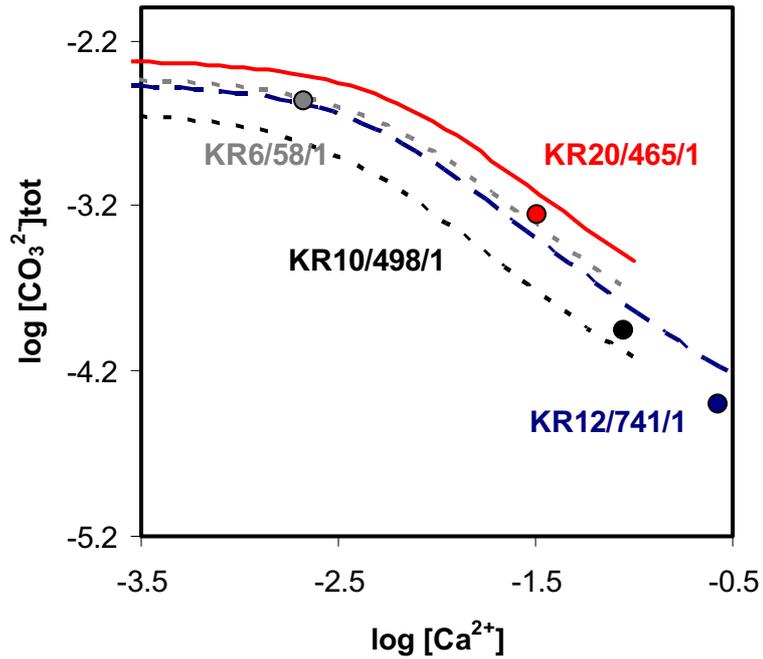
(A)
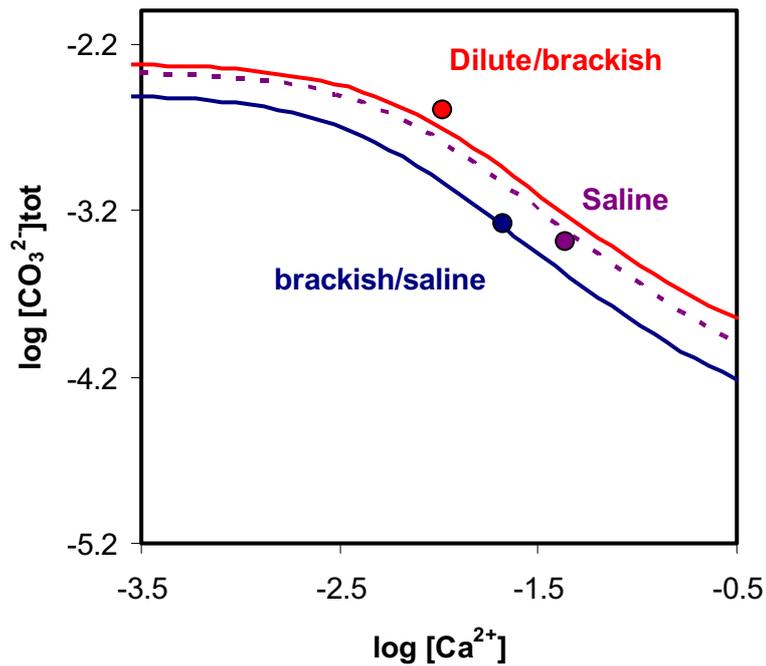
(B)

Figure 3-1. Total carbonate concentration in equilibrium with calcite. Each colour (either symbol or line) corresponding to a given gw composition. For the same colour, the symbol stands for the composition in terms of [Ca²⁺] and [CO₃²⁻] of a given groundwater while the line corresponds to the calculated solubility curve of calcite under the conditions of the gw in question A) under the composition of the different groundwaters. B) under the composition of bentonite waters.

C-14 is not definitely known generally no solubility limit is set for C-14 in the safety assessment.

Methane generation would lead to a very high solubility for total carbon in solution. In addition to the above reported direct release of C-14 from the activated metal as an organic compound, either as methane due to reduction of metal carbides or as organic acids one might also consider wether the reduction of carbonate to form methane is thermodynamically plausible. This reaction depends on:

i)   High temperature. A paper dealing with the reduction of metal carbonates to methane (Kudo and Komatsu, 1999) indicates that the yield of methane generation reaches a maximum of 17 % at 400 °C and does not occur in the absence of biological activity until the temperature exceeds 150 – 200 °C.

ii)   Presence of biological activity. This condition depends on the presence of bacteria in the vicinity of the canister, which has not been considered to occur.

According to Olkiluoto data, ongoing methanogenesis is apparent in the rock and autotrophic methanogens are present. The outcome is the reduction of carbon in the sulphate rich waters-saline waters mixing zone (Pitkänen et al. 2004).

Under the different scenarios considered in this work, autotrophic methanogens would only be efficient for the maximum pH_2 overpressures produced by the anoxic corrosion of the cast-iron insert (100 atm H_2 in this report) (see Figure 3-2).
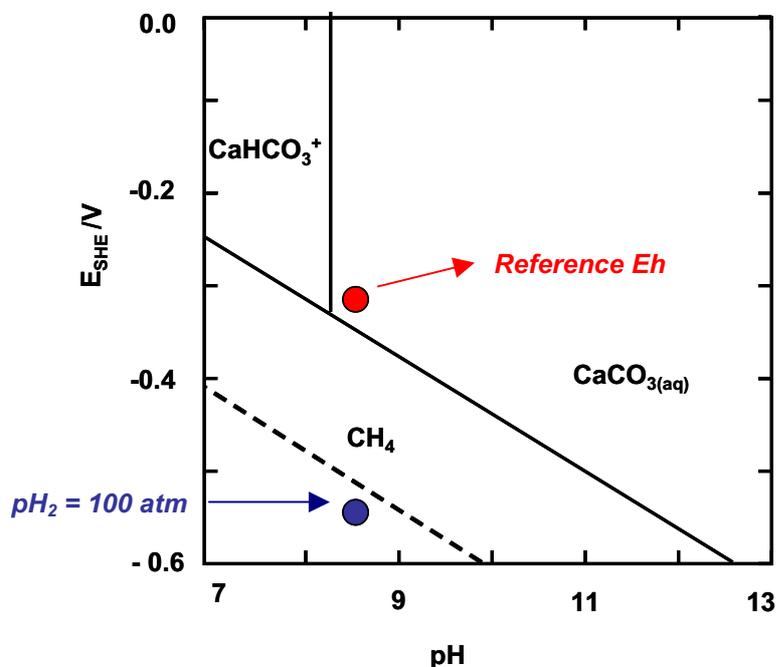
Figure 3-2. Predominance Eh vs. pH diagram of Carbon under the conditions given by brine groundwater type (KR12/741/1). The red circle indicates the conditions of the reference redox state whereas the blue circle indicates the redox state conditions for the maximum pH_2 overpressures produced by the anoxic corrosion of the cast-iron insert.

3.1.2   Caesium

This element is not solubility limited in the range of conditions of interest. The aqueous speciation in solution is dominated by the free cation Cs^+ in most natural groundwaters, with no influence of the main variables of the system, pH and carbonate content, in the range of conditions of interest for this work.

Its aqueous speciation is mainly affected by the chloride content in the water through the formation of CsCl(aq). The Figure 3-3 shows the fractional diagram with the aqueous speciation of caesium, as a function of chloride concentration under the conditions of the saline (KR10/498/1) and brine groundwater (KR12/741/1).

The fraction of CsCl(aq) in the groundwater KR10/498/1 ($[Cl^-]$ = 0.381M) is around 12% whereas the fraction of CsCl(aq) in KR12/741/1($[Cl^-]$ = 0.863M) is 20%. Cs is not solubility controlled.
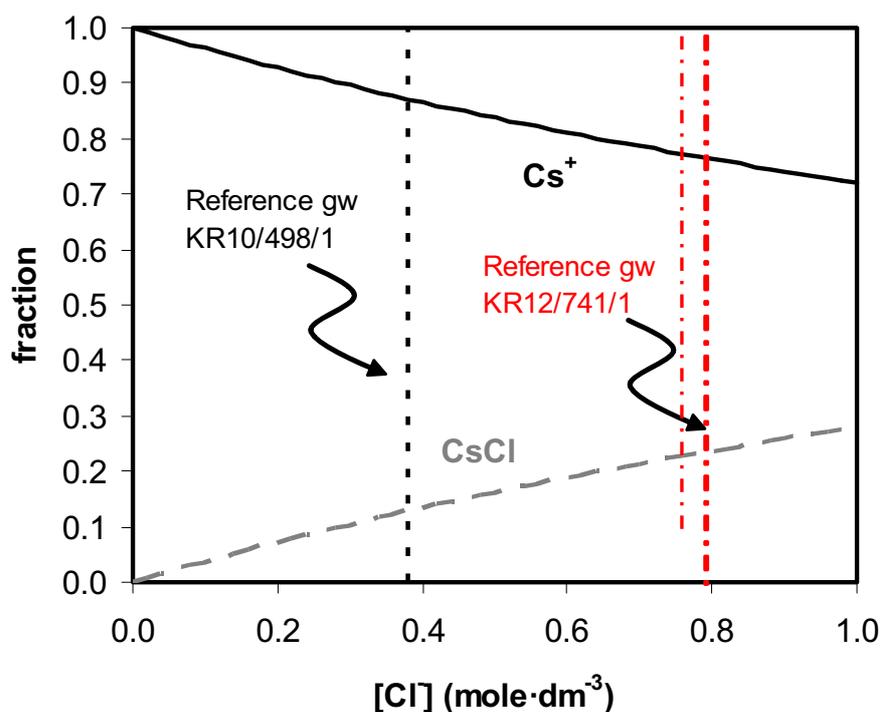
Figure 3-3. Fractional diagram showing the aqueous speciation of Caesium as a function of the chloride concentration, under the conditions of the groundwaters KR10/498/1 and KR12/741/1. Vertical black-dashed line indicates the [Cl⁻] of the KR10/498/1 groundwater whereas red indicated the chloride concentration analysed in KR12/741/1 groundwater.

3.1.3   Strontium

The aqueous speciation of strontium under the composition of the groundwaters is mainly dominated by the free Sr^{2+} cation; with some contributions of aqueous sulphate species up to ~6% for the groundwater with a higher sulphate content (dilute brackish groundwater (KR6/58/1) and all the bentonite waters).

Two different solid phases may appear as likely to control the solubility of Sr: celestite ($SrSO_4(s)$) and strontianite ($SrCO_3(s)$). The predominance of one over the other depends on the sulphate to carbonate ratio of the groundwater under study (see Figure 3-4). Due to the higher carbonate/sulphate ratio in the composition of the three groundwaters (KR20/465/1, KR10/498/1 and KR6/58/1) and the ice melting water, the pure solid phase expected to control the solubility of strontium is strontianite. In the case of the "brine-type" KR12/741/1 groundwater where the carbonate/sulphate ratio is near to 1 strontianite is the solubility controlling phase.

Increase of the sulphate/carbonate ratio would cause a change in the solubility control from strontianite to celestite (see for example, results for bentonite waters in section 5.

In the case of glacial meltwater, strontium is not solubility limited due to the low concentration of carbonate and sulphate in solution.
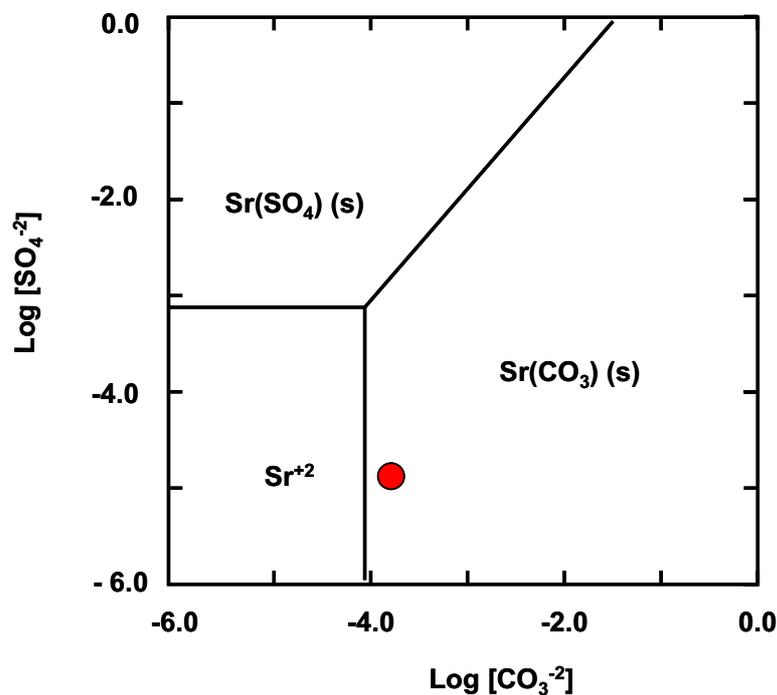
Figure 3-4. *Predominance Log [SO$_4^{-2}$] vs. log [CO$_3^{-2}$] diagram of Strontium under the conditions given by saline groundwater type (KR10/498/1) (pH = 8.0). The red circle indicates the [SO$_4^{-2}$] and [CO$_3^{-2}$] concentration given for this groundwater.*

An important conceptual uncertainty potentially affecting Sr solubility is the reduction of sulphate to sulphide. This process has not been considered here due to its very slow kinetics, favoured in the presence of sulphate reducing bacteria (SRB). SRB have been reported to be present in Olkiluoto groundwaters. Their activity in bentonite is, nevertheless, likely limited by the high density/swelling pressure of the compacted material. Studies indicate that bacterial activity will be suppressed, and both culturability and viability will decrease, at swelling pressures exceeding 2 MPa (Stroes-Gascoyne et al. 2006; Masurat 2006). It is likely that microbes are barely active under these conditions (although this is an issue that is still under investigation).

Reduction of sulphate to sulphide due to SRB would cause an increase of the celestite solubility, thus causing strontianite to exert the solubility control.

Only pure solid phases have been considered in this analysis without considering the formation of mixed solid phases. Natural analogue studies have shown that the concentration of Sr in groundwaters may be governed by co-precipitation processes with major elements, leading to smaller strontium concentrations than the ones predicted from the solubilities of solids containing that element as major component (Bruno et al. 2001). Sr is normally associated with Ca, therefore, the possibility of co-precipitation of strontium with gypsum or calcite should not be disregarded as the controlling process of the aqueous concentration of this radionuclide in the studied system.

Calculated strontium concentration limits are given in Table 3-1 under the four groundwaters conditions and under the three redox scenarios considered.

3.1.4 Radium

The aqueous speciation of radium is dominated by Ra^{2+} with small contributions the species $RaCl^+$ in the saline (KR10/498/1) and brine (KR12/741/1) groundwaters, where chloride concentrations are relatively high. In the case of the dilute/brackish groundwater, the aqueous speciation of this element is dominated by Ra^{2+} with contributions of $RaSO_4(aq)$, due to the high content of sulphate of this water. This is also the case of the speciation of the bentonite waters, where the sulphate content of the water is high (see the corresponding tables in section 5).

$RaSO_4(s)$ will exert the solubility control under the conditions of the four groundwaters.

As in the case of strontium, one of the conceptual uncertainties to consider is the reduction of sulphate to sulphide. If sulphate were allowed to reduce to sulphide, the solubility of $RaSO_4(s)$ would considerably increase. Hence, when the redox system is controlled by the event of the maximum pH_2 overpressure that could be formed ($pH_2 = 10^2$ atm) and sulphate reduction takes place, the controlling solubility solid phase is $RaCO_3(s)$, what produces a higher solubility of Ra than $RaSO_4(s)$ under the event of sulphate reduction.

Similarly to the case of strontium, the concentration of Ra in groundwaters may be governed by co-precipitation processes with major elements, leading to smaller radium

concentrations than the ones predicted from the solubilities of solids containing that element as major component. Only pure solid phases have been considered in this analysis without considering the formation of mixed solid phases, and, therefore, one uncertainty in the calculation is the possibility of co-precipitation of radium with gypsum or calcite if these solid phases form in our system.

Calculated radium concentration limits are given in Table 3-2 for the four groundwaters.

Table 3-1. *Sr solubility-controlling phases and concentration values (in M) under different redox conditions for the groundwaters.*

		$T = 15^oC$		
		Eh gw	**pH$_2$(g)= 10^{-7} atm**	**pH$_2$(g)= 10^2 atm**
Groundwaters	***Brackish saline*** *KR20/465/1*	Strontianite 5.9·10^{-3}	Strontianite 5.9·10^{-3}	Strontianite 5.9·10^{-3}
	Saline *KR10/498/1*	Strontianite 9.2·10^{-3}	Strontianite 9.2·10^{-3}	Strontianite 9.2·10^{-3}
	Dilute brackish *KR6/58/1*	Strontianite 3.1·10^{-4}	Strontianite 3.1·10^{-4}	Strontianite 3.1·10^{-4}
	Brine *KR12/741/1*	Strontianite 1.6·10^{-2}	Strontianite 1.6·10^{-2}	Strontianite 1.6·10^{-2}

Table 3-2. *Summary of Ra solubility-controlling phase and concentration values (M) under the different redox conditions for the different groundwaters. No sulphate reduction has been considered.*

		$T = 15^oC$		
		Eh gw	**pH$_2$(g)= 10^{-7} atm**	**pH$_2$(g)= 10^2 atm**
Groundwaters	***Brackish saline*** *KR20/465/1*	RaSO$_4$ 3.2·10^{-6}	RaSO$_4$ 3.2·10^{-6}	RaSO$_4$ 3.3·10^{-6}
	Saline *KR10/498/1*	RaSO$_4$ 1.1·10^{-4}	RaSO$_4$ 1.1·10^{-4}	RaSO$_4$ 1.2·10^{-4}
	Dilute brackish *KR6/58/1*	RaSO$_4$ 1.1·10^{-7}	RaSO$_4$ 1.1·10^{-7}	RaSO$_4$ 1.1·10^{-7}
	Brine *KR12/741/1*	RaSO$_4$ 3.0·10^{-5}	RaSO$_4$ 3.0·10^{-5}	RaSO$_4$ 3.0·10^{-5}

3.1.5   Tin

The aqueous speciation of tin is dominated by the hydrolysis complexes of Tin(IV): $Sn(OH)_4(aq)$ with some contribution of the species $Sn(OH)_5^-$ under the conditions of the reference (KR20/465/1, KR10/498/1 and KR6/58/1) and bentonite waters. $Sn(OH)_5^-$ is the predominant aqueous species in the more alkaline waters as the brine and ice melting groundwaters (see Figure 3-5 with contributions of $Sn(OH)_6^{2-}$ (~15%)) in the second case.

Tin solubility in the groundwaters will be most likely controlled by the fomation of $SnO_2(am)$.

Again, one uncertainty to take into consideration is the one related with the presence or not in the system of SRB (see Section 4). Indeed, if sulphate were reduced to sulphide, sulphide solid phases might exert the solubility control at reducing Eh values.

Calculated tin concentration limits are given in Table 3-3 for the groundwaters. The increase of $pH_2(g)$ to 10^2 atm translates into an increase of the solubility induced by the reduction of Sn(IV) to Sn(II) species.
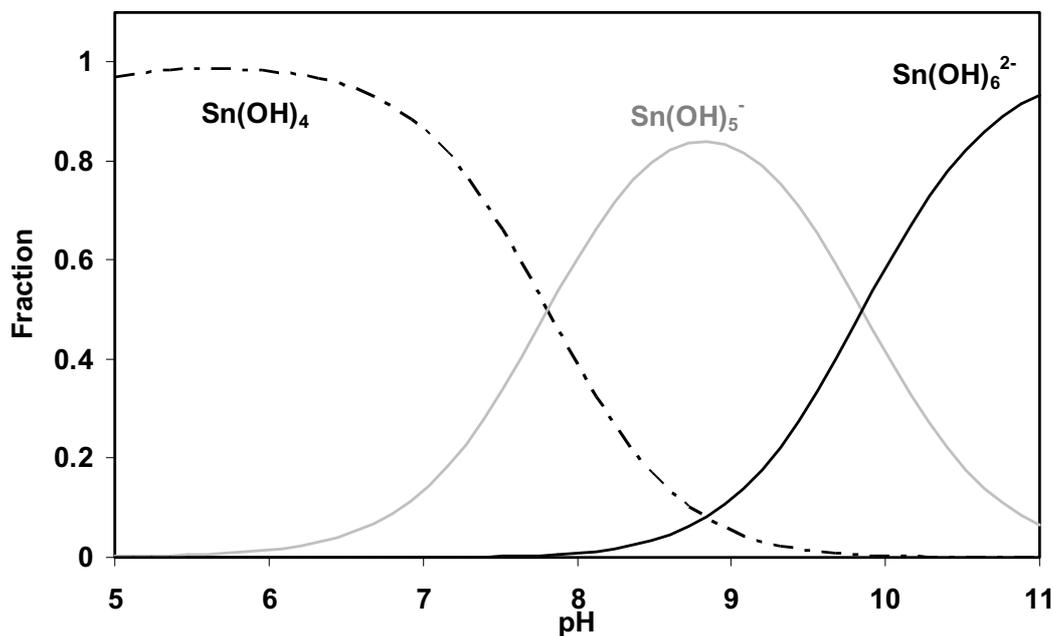
Figure 3-5. *Aqueous tin speciation as a function of the pH of the system.*

Table 3-3. *Sn solubility-controlling phases and concentration values (M) under the different redox conditions for the groundwaters.No sulphate reduction has been considered.*

T = 15ºC				
		Eh gw	**pH$_2$(g)= 10^{-7} atm**	**pH$_2$(g)= 10^2 atm**
Groundwaters	*Brackish saline* KR20/465/1	SnO$_2$ 9.6·10^{-8}	SnO$_2$ 9.6·10^{-8}	SnO$_2$ 1.2·10^{-7}
	Saline KR10/498/1	SnO$_2$ 1.4·10^{-7}	SnO$_2$ 1.4·10^{-7}	SnO$_2$ 1.7·10^{-7}
	Dilute brackish KR6/58/1	SnO$_2$ 1.1·10^{-7}	SnO$_2$ 1.1·10^{-7}	SnO$_2$ 1.4·10^{-7}
	Brine KR12/741/1	SnO$_2$ 1.5·10^{-7}	SnO$_2$ 1.5·10^{-7}	SnO$_2$ 1.8·10^{-7}

3.1.6   Selenium

Selenium is mainly found in nuclear spent fuel as selenide located predominantly in the gaps and grain boundaries and forming a volatile compound of composition Cs$_2$Se (Johnson & Tait, 1997). It will consequently dissolve from the matrix, under anoxic and reducing environments, in the form of Se(-II) species, specifically HSe$^-$ at the pH of the considered groundwaters. The presence of Fe(II) in solution may cause the formation of FeSe$_x$(s) solid phases. Therefore, the solubility of selenium will be very dependent of iron concentration. Se(IV) is dominant under the oxic conditions of glacial meltwater and selenium is not solubility limited. In case of redox determined by hematite/magnetite equilibrium (due to iron insert) in the glacial meltwater Se(-II) is dominant and selenium is solubility limited.

Another possibility would be the formation of native Se, what would imply the oxidation of the Se(-II) released from the fuel to Se(0). Recent experimental evidences have shown that Se(0) and FeSe$_2$(s) form from FeSe$_x$(s) dissolution experiments (Iida et al. 2007). The concentrations of aqueous Se measured in the experiments were, nevertheless, much higher than those expected to be driven by the Se(0) solubility control, what adds an important uncertainty to the results. Due to the reducing environment of interest in this work, we have preferred to select ferrous selenide solids as solubility limiting although the formation of Se(0) cannot be definitely ruled out and, thus, represents one important uncertainty to the selected solubility control.

Figure 3-6 shows the effect of both, the Eh of the system and the iron concentration present in groundwaters on the solid phases likely to precipitate in the studied system.
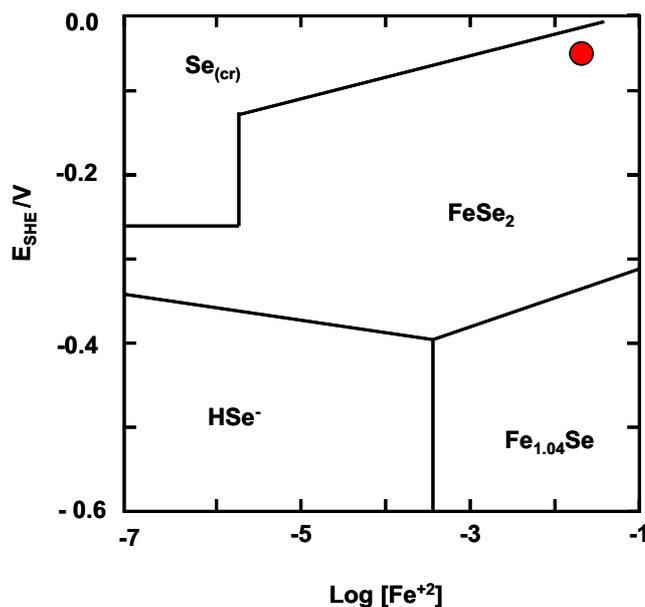
Figure 3-6. *Eh vs log[Fe^{+2}] diagram of Selenium under the conditions given by the groundwater KR6/58/1. [Se] = 1·10^{-5}M. The red circle indicates the Eh and [Fe^{+2}] given for this groundwater.*

The concentration of Se in groundwaters may be governed by co-precipitation processes with other major solid phases. Only pure solid phases have been considered in this analysis without considering the formation of mixed solid phases. The precipitation of pure solid phases of selenium is not very likely to occur under the expected concentrations released from the spent nuclear fuel and, therefore, the assumption of selenium incorporated in solid sulphides should be assessed, being one of the most important uncertainties in this calculation.

Because the ionic radius of Se^{2-} is 0.191 nm and that of S^{2-} is 0.184 nm (Shannon 1976), substitution of selenium for sulphur commonly occurs. According to mineralogical studies on sulphides, the incorporation of selenium into the crystalline cell of sulphides can occur up to a maximum of 300 ppm in pyrite (FeS$_2$(s)) and of 100 ppm in pyrrhotite (FeSe(s)) (Vaughan & Craig, 1978). If we assumed the co-precipitation of Se with iron sulphides according to this maximum values, the solubility limits would be decreased in 4 orders of magnitude.

Calculated solubilities for selenium in the groundwaters at the different redox conditions are shown in Table 3-4. Nevertheless, instead of selecting a solid as Se solubility-controlling phase, we suggest that co-precipitation processes are more likely to occur.

Table 3-4. *Se solid phases and concentration values (M) under the different redox conditions for the groundwaters. No co-precipitation with iron sulphides has been accounted for.*

			$T = 15^oC$	
		Eh gw	**pH$_2$(g)= 10^{-7} atm**	**pH$_2$(g)= 10^2 atm**
Groundwaters	*Brackish saline* KR20/465/1	FeSe$_2$ $6.0 \cdot 10^{-10}$	FeSe$_2$ $1.0 \cdot 10^{-9}$	Fe$_{1.04}$Se $1.4 \cdot 10^{-5}$
	Saline KR10/498/1	FeSe$_2$ $8.8 \cdot 10^{-10}$	FeSe$_2$ $1.2 \cdot 10^{-9}$	Fe$_{1.04}$Se $4.5 \cdot 10^{-6}$
	Dilute brackish KR6/58/1	FeSe$_2$ $6.6 \cdot 10^{-14}$	FeSe$_2$ $2.1 \cdot 10^{-10}$	Fe$_{1.04}$Se $3.8 \cdot 10^{-7}$
	Brine KR12/741/1	FeSe$_2$ $6.3 \cdot 10^{-9}$	FeSe$_2$ $2.7 \cdot 10^{-9}$	Fe$_{1.04}$Se $1.7 \cdot 10^{-5}$

3.2 Transition elements

3.2.1 Zirconium

The aqueous speciation of zirconium is dominated by Zr(OH)$_4$(aq) under the conditions of the different groundwaters, being Zr(OH)$_4$(am) the solubility controlling phase. No influence of the redox state is expected.

One of the main uncertainties affecting Zr solubility assessment is that related with the crystallinity of the solid phase formed. As explained in Section 4, the formation of the amorphous phases has been favoured in this assessment, given that many of the processes of crystallization occur through a process of dehydration or re-structuring, which are favoured both with temperature and/or with time. Figure 3-7 shows the solubility of two different zirconium hydroxides.

Calculated solubilities for zirconium for the groundwaters at the different redox conditions are shown in Table 3-5.
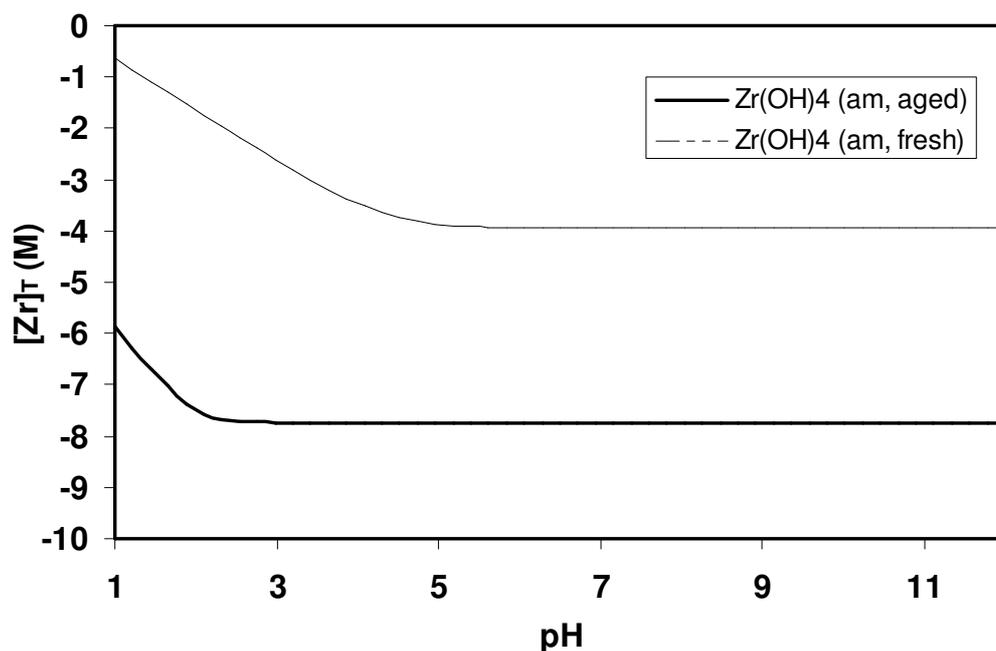
Figure 3-7. *Solubility curves of two Zr hydroxides in front of pH under the conditions of KR10/498/1 groundwater.*

Table 3-5. *Zr solubility-controlling phase and concentration values (M) under the different redox conditions for the groundwaters.*

		$T = 15^oC$		
		Eh gw	**pH$_2$(g)= 10^{-7} atm**	**pH$_2$(g)= 10^2 atm**
Groundwaters	***Brackish saline*** *KR20/465/1*	Zr(OH)$_4$ (am) 1.7·10^{-8}	Zr(OH)$_4$ (am) 1.7·10^{-8}	Zr(OH)$_4$ (am) 1.7·10^{-8}
	Saline *KR10/498/1*	Zr(OH)$_4$ (am) 1.6·10^{-8}	Zr(OH)$_4$ (am) 1.6·10^{-8}	Zr(OH)$_4$ (am) 1.6·10^{-8}
	Dilute brackish *KR6/58/1*	Zr(OH)$_4$ (am) 1.8·10^{-8}	Zr(OH)$_4$ (am) 1.8·10^{-8}	Zr(OH)$_4$ (am) 1.7·10^{-8}
	Brine *KR12/741/1*	Zr(OH)$_4$ (am) 1.4·10^{-8}	Zr(OH)$_4$ (am) 1.4·10^{-8}	Zr(OH)$_4$ (am) 1.4·10^{-8}

3.2.2 Niobium

In natural waters niobium is mainly found in the pentavalent oxidation state. There is a general lack of thermodynamic data in the literature on niobium, what constitutes an important drawback when studying the behaviour of this element.

Concentration limits of niobium are given by the solubility of $Nb_2O_5(s)$ under the conditions of interest. There is an influence of pH on the solubility of $Nb_2O_5(s)$ given the underlying aqueous speciation. The main aqueous species in equilibrium with the solid under the glacial water conditions is $Nb(OH)_5$. For all the other groundwater compositions NbO_3^- and $Nb(OH)_5^-$ dominate in solution. The solubility of the solid phase increases with pH due to the formation of the oxoanion NbO_3^- (see Table 3-6 for KR12/741/1 brine type water (pH=8.2) and Table 5-9 for the ice-melting water type (pH = 9.6)) .

Table 3-6 summarizes Nb concentration values in equilibrium with the selected solubility controlling phase under the different redox conditions studied for the different groundwaters.

3.2.3 Molybdenum

Thermodynamic data on molybdenum in the literature are scarce. Mo is a redox sensitive element that presents a rather complex chemistry due to the formation of polynuclear complexes conformed in cluster configurations.

Figure 3-8 shows the most likely solids controlling the solubility of molybdenum. As seen, a change of the Eh and/or the pH of the system may be decisive to select the solubility controlling phase. The most likely solid phase controlling the solubility of this element is $MoO_2(s)$ under most of the conditions of the groundwaters (very reducing conditions and intermediate pH values). Nevertheless, $CaMoO_4(s)$ may also control the solubility under anoxic conditions, as is the case of the KR6/58/1 dilute/ brackish water (see Table 3-7), the brackish and saline bentonite waters or the ice

Table 3-6. Nb solubility-controlling phase and concentration values (M) under the different redox conditions for the groundwaters.

		$T = 15^oC$		
		Eh gw	$pH_2(g)= 10^{-7}$ atm	$pH_2(g)= 10^2$ atm
Groundwaters	Brackish saline KR20/465/1	Nb_2O_5 $3.9 \cdot 10^{-5}$	Nb_2O_5 $3.9 \cdot 10^{-5}$	Nb_2O_5 $3.9 \cdot 10^{-5}$
	Saline KR10/498/1	Nb_2O_5 $1.2 \cdot 10^{-4}$	Nb_2O_5 $1.2 \cdot 10^{-4}$	Nb_2O_5 $1.2 \cdot 10^{-4}$
	Dilute brackish KR6/58/1	Nb_2O_5 $4.6 \cdot 10^{-5}$	Nb_2O_5 $4.6 \cdot 10^{-5}$	Nb_2O_5 $4.6 \cdot 10^{-5}$
	Brine KR12/741/1	Nb_2O_5 $2.0 \cdot 10^{-4}$	Nb_2O_5 $2.0 \cdot 10^{-4}$	Nb_2O_5 $2.0 \cdot 10^{-4}$
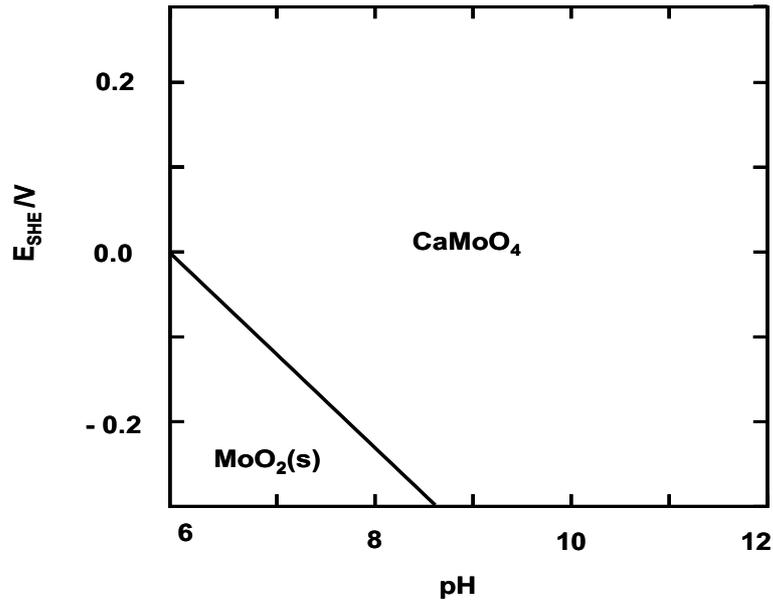
Figure 3-8. *Eh/pH diagram of Mo solids under the conditions given by the brackish/saline groundwater KR20/465/1.*

melting groundwater (see tables in section 5). Molybdenum is not solubility limited under the conditions of the glacial meltwater and $CaMoO_4$ does not precipitate due to the low calcium concentration present in this system.

The underlying aqueous speciation is dominated by the free anion MoO_4^{2-} in all cases.

Table 3-7 summarizes Mo concentration values in equilibrium with the selected solubility controlling phase under the different redox conditions studied for the different groundwaters.

Table 3-7. *Mo solubility-controlling phase and concentration values (M) under the different redox conditions for the groundwaters.*

		$T = 15^oC$		
		Eh gw	**pH$_2$(g)= 10^{-7} atm**	**pH$_2$(g)= 10^2 atm**
Groundwaters	***Brackish saline*** *KR20/465/1*	MoO_2 $7.9 \cdot 10^{-9}$	MoO_2 $2.8 \cdot 10^{-9}$	*MoO_2 $(2.8 \cdot 10^{-18})$
	Saline *KR10/498/1*	MoO_2 $8.5 \cdot 10^{-8}$	MoO_2 $4.5 \cdot 10^{-8}$	*MoO_2 $(4.5 \cdot 10^{-17})$
	Dilute brackish *KR6/58/1*	$CaMoO_4$ $1.9 \cdot 10^{-5}$	MoO_2 $3.7 \cdot 10^{-9}$	*MoO_2 $(3.8 \cdot 10^{-18})$
	Brine *KR12/741/1*	MoO_2 $1.3 \cdot 10^{-8}$	MoO_2 $6.7 \cdot 10^{-8}$	*MoO_2 $(6.7 \cdot 10^{-17})$

*The formation of MoO_2 under 100 atm of H_2 is not very likely to control the solubility of Mo in this system, therefore no solubility limit is recommended at this stage.

3.2.4 Technetium

Technetium may be immobilised under reducing conditions due to the high stability of Tc(IV) phases. Under oxidising conditions, though, it is not solubility limited given the large stability of aqueous Tc(VII) complexes, mainly in the form of TcO_4^- (see glacial meltwater, for instance).

The aqueous Tc speciation under the different water conditions is mainly dominated by $TcO(OH)_2(aq)$, except in the case of the ice melting water (containing a 7% of TcO_4^-) and the acidic oxidant glacial meltwater with a speciation dominated by TcO_4^-. The solid phase likely to control technetium concentrations in the different waters is technetium dioxide ($TcO_2 \cdot 1.63H_2O(s)$).

The precipitation of metallic technetium has not been considered due to the slow kinetics normally associated to the formation of metals from solution. Tc oxides are easily formed in laboratory conditions while Tc(cr) is only obtained by prolonged reductions of previous oxides.

Table 3-9 summarizes Tc concentrations values in equilibrium with the controlling solid phase under the different redox conditions for the different groundwaters.

3.2.5 Nickel

Nickel is mainly found in the +2 oxidation state in aqueous and solid states. The aqueous nickel speciation is dominated by free Ni^{2+} with some contributions of chloride species under the conditions of the brackish saline, brine and saline groundwaters. For the dilute brackish groundwater and all bentonite waters, the main aqueous species is free Ni^{2+} with contribution of the sulphate species. Under the ice melting groundwater conditions (pH=9.6) $Ni(OH)_2$ (aq) dominate the aqueous speciation.

Table 3-8. *Tc solubility-controlling phases and concentration values (M) under the different redox conditions for the different groundwaters.*

		Eh gw	$pH_2(g)= 10^{-7}$ atm	$pH_2(g)= 10^2$ atm
		$T = 15^oC$		
Groundwaters	*Brackish saline* KR20/465/1	$TcO_2 \cdot 1.6H_2O$ $4.0 \cdot 10^{-9}$	$TcO_2 \cdot 1.6H_2O$ $4.0 \cdot 10^{-9}$	$TcO_2 \cdot 1.6H_2O$ $4.0 \cdot 10^{-9}$
	Saline KR10/498/1	$TcO_2 \cdot 1.6H_2O$ $4.0 \cdot 10^{-9}$	$TcO_2 \cdot 1.6H_2O$ $4.1 \cdot 10^{-9}$	$TcO_2 \cdot 1.6H_2O$ $4.1 \cdot 10^{-9}$
	Dilute brackish KR6/58/1	$TcO_2 \cdot 1.6H_2O$ $5.0 \cdot 10^{-9}$	$TcO_2 \cdot 1.6H_2O$ $4.2 \cdot 10^{-9}$	$TcO_2 \cdot 1.6H_2O$ $4.2 \cdot 10^{-9}$
	Brine KR12/741/1	$TcO_2 \cdot 1.6H_2O$ $4.1 \cdot 10^{-9}$	$TcO_2 \cdot 1.6H_2O$ $4.1 \cdot 10^{-9}$	$TcO_2 \cdot 1.6H_2O$ $4.0 \cdot 10^{-9}$

Nickel carbonates have been disregarded as solubility controlling solid phases likely for the reasons given below:

- gaspeite ($NiCO_3$ (s)) is only formed at high temperature.
- hellyerite ($NiCO_3 \cdot 6H_2O$) presents a solubility much higher than the one of gaspeite, giving unrealistic nickel concentrations.

$Ni(OH)_2$(s) is the solid phase most likely to exert the solubility control of this element, although due to the low hydrozability of Ni, the formation of this solid does not lead to effective solubility control until more alkaline pH values than the ones of interest in the groundwaters. Indeed, nickel is not solubility limited in the glacial meltwater given its low pH (pH = 5.8).

As discussed in Section 4, one of the conceptual uncertainties that may affect Ni solubility is the reduction of sulphate to sulphide. If sulphate is allowed to reduce to sulphide in the system, the solubility of $Ni(OH)_2$(s) would increase for reducing redox potentials due to the formation of aqueous nickel sulphides.

Table 3-9 summarizes nickel concentrations values in equilibrium with the controlling solid phase under the different redox conditions for the different groundwaters.

3.2.6   Palladium

Palladium may be found at several redox states, 0, +2 and +4, although the common redox state is +2 in aqueous media.

The main aqueous palladium species is $Pd(OH)_2$(aq) with some small contributions of chloride species under the conditions of the brine groundwater and saline bentonite water.

Table 3-9. *Ni solubility-controlling phases and concentration values (M) under the different redox conditions for the groundwaters.*

		T = 15ºC		
		Eh gw	**pH$_2$(g)= 10^{-7} atm**	**pH$_2$(g)= 10^2 atm**
Groundwaters	*Brackish saline* KR20/465/1	$Ni(OH)_2$ $2.0 \cdot 10^{-3}$	$Ni(OH)_2$ $2.0 \cdot 10^{-3}$	$Ni(OH)_2$ $2.0 \cdot 10^{-3}$
	Saline KR10/498/1	$Ni(OH)_2$ $1.4 \cdot 10^{-4}$	$Ni(OH)_2$ $1.4 \cdot 10^{-4}$	$Ni(OH)_2$ $1.4 \cdot 10^{-4}$
	Dilute brackish KR6/58/1	$Ni(OH)_2$ $4.4 \cdot 10^{-4}$	$Ni(OH)_2$ $4.4 \cdot 10^{-4}$	$Ni(OH)_2$ $4.4 \cdot 10^{-4}$
	Brine KR12/741/1	$Ni(OH)_2$ $4.4 \cdot 10^{-5}$	$Ni(OH)_2$ $4.4 \cdot 10^{-5}$	$Ni(OH)_2$ $4.4 \cdot 10^{-5}$

The solid phases most likely to precipitate are palladium oxides. Two solid oxides are reported in the literature, PdO and $Pd(OH)_2$(s). According to the Ostwald's rule, the amorphous solid has been selected as exerting the solubility control. Metallic Pd is not considered due to the slow kinetics normally associated to the formation of metals from solution.

Table 3-10 summarizes the calculated solubilities for palladium under the different redox conditions studied for the different groundwaters.

3.3   Lanthanides

3.3.1   Samarium

This element is not redox sensitive and its chemical behaviour is basically controlled by the pH, the carbonate and the sulphate content of the waters. The free cation Sm^{3+} with some contribution of $SmCO_3^+$ dominate the aqueous speciation of Sm in bracklish saline and saline groundwaters (KR20/465/1 and KR10/498/1), while carbonate species are the dominant aqueous species in the case of the dilute brackish groundwater (KR6/58/1) due to the higher carbonate content of this water. In the case of the brine groundwater (KR12/741/1) with higher chloride concentration, some contributions of chloride species ($SmCl^{2+}$) are observed.

Sulphate species dominate in the brackish saline and dilute brackish bentonite waters, whereas the free cation Sm^{3+} dominates in saline bentonite water and in glacial meltwater. $Sm(CO_3)_2^-$ is the dominant aqueous species in the ice-melting groundwater.

Table 3-10. *Pd solubility-controlling phases and concentration values (M) under the different redox conditions for the different groundwaters.*

		$T = 15^oC$		
		Eh gw	**pH$_2$(g)= 10^{-7} atm**	**pH$_2$(g)= 10^2 atm**
Groundwaters	*Brackish saline* KR20/465/1	Pd(OH)$_2$ $2.6 \cdot 10^{-6}$	Pd(OH)$_2$ $2.6 \cdot 10^{-6}$	Pd(OH)$_2$ $2.6 \cdot 10^{-6}$
	Saline KR10/498/1	Pd(OH)$_2$ $2.5 \cdot 10^{-6}$	Pd(OH)$_2$ $2.5 \cdot 10^{-6}$	Pd(OH)$_2$ $2.5 \cdot 10^{-6}$
	Dilute brackish KR6/58/1	Pd(OH)$_2$ $2.7 \cdot 10^{-6}$	Pd(OH)$_2$ $2.7 \cdot 10^{-6}$	Pd(OH)$_2$ $2.7 \cdot 10^{-6}$
	Brine KR12/741/1	Pd(OH)$_2$ $2.4 \cdot 10^{-6}$	Pd(OH)$_2$ $2.4 \cdot 10^{-6}$	Pd(OH)$_2$ $2.4 \cdot 10^{-6}$

The most likely precipitating solid phases are samarium phosphate, samarium hydroxide, samarium carbonate and the mixed samarium hydroxo-carbonate, depending on the water composition.

Phosphates have been identified to form both, strong aqueous complexes in solution and stable solid phases with lanthanides, leading to lower lanthanide concentrations in natural waters than those calculated assuming that solid carbonates are the limiting solid phases. Calculations undertaken under the composition of the four groundwaters and the glacial meltwater -where phosphate measurements are available- show that solid phosphates may exert the solubility control. This assumption leads to samarium concentrations in line with those measured in natural waters (see Duro et al., 2006). One of the conceptual uncertainties important to consider in the case of Sm is, therefore, the presence of phosphate in groundwater. When ignoring phosphates (bentonite and ice melting groundwaters), the mixed hydroxo-carbonate solid phase ($SmOHCO_3$ (s)) controls the solubility of samarium.

Table 3-10 summarizes the calculated solubilities for samarium under the different redox conditions studied for the different groundwaters.

3.4 Actinides

3.4.1 Thorium

This radionuclide is mainly found in the redox state +4 and is non redox sensitive. The concentration of Thorium in groundwater seems to be limited by the solubility of hydrous thorium oxide ($ThO_2 \cdot 2H_2O(am)$).

The main aqueous species in the groundwaters, KR20/465/1 (brackish saline), KR10/498/1 (saline), KR6/58/1 (dilute brackish), all the bentonite waters and ice melting groundwater is the mixed hydroxo-carbonate $ThCO_3(OH)_3^-$, which is, at the same time, the main aqueous species in equilibrium with the solid phase. This mixed hydroxocarbonate complex have been recently de fined by Altmaier et al. (2006) to

Table 3-11. Sm solubility-controlling phases and concentration values (M) under the different redox conditions for the groundwaters.

			$T = 15^oC$	
		Eh gw	**pH$_2$(g)= 10^{-7} atm**	**pH$_2$(g)= 10^2 atm**
Groundwaters	*Brackish saline* KR20/465/1	$SmPO_4$ $9.3 \cdot 10^{-9}$	$SmPO_4$ $9.3 \cdot 10^{-9}$	$SmPO_4$ $9.3 \cdot 10^{-9}$
	Saline KR10/498/1	$SmPO_4$ $7.8 \cdot 10^{-9}$	$SmPO_4$ $7.8 \cdot 10^{-9}$	$SmPO_4$ $7.8 \cdot 10^{-9}$
	Dilute brackish KR6/58/1	$SmPO_4$ $9.2 \cdot 10^{-10}$	$SmPO_4$ $9.2 \cdot 10^{-10}$	$SmPO_4$ $9.2 \cdot 10^{-10}$
	Brine KR12/741/1	$SmPO_4$ $1.2 \cdot 10^{-10}$	$SmPO_4$ $1.2 \cdot 10^{-10}$	$SmPO_4$ $1.2 \cdot 10^{-10}$

describe the solubility of thorium in carbonated waters. In the case of brine groundwater, with lower carbonate concentration, the main aqueous species is $Th(OH)_4$ with a slight contribution of the mixed carbonate species. The aqueous speciation is dominated by $Th(OH)_3^+$, $Th(OH)_2^{2+}$ in the glacial meltwater, containing a lower pH and carbonate concentration.

The influence of carbonate on the $ThO_2 \cdot 2H_2O$ solubility at the pHs of the groundwaters results in an increase on the solubility when increasing the total carbonate concentration of the system. This is in agreement with the results presented in Table 3-12, where Th concentrations are higher, in agreement with the carbonate content of the considered groundwater (Dilute brackish [Th] KR6/58/1> [Th] Brackish saline KR20/465/1 > [Th] Saline KR10/498/1 > Brine KR12/741/1).

Due to the low phosphate concentration (~10^{-9} M), no effect of phosphate is seen in this case.

Table 3-10 summarizes the calculated solubilities for thorium under the different redox conditions studied for the different groundwaters.

3.4.2 Protactinium

Pa can occur in the +IV and +V oxidation state. Under the conditions of the different waters, the aqueous speciation is dominated by $PaO_2OH(aq)$ in all cases. The solid phase that may exert the solubility control is $Pa_2O_5(s)$.

The most important uncertainty concerning protactinium is the scarcity of thermo-dynamic data available in the literature.

Table 3-10 summarizes the calculated solubilities for protactinium under the different redox conditions studied for the different groundwaters.

Table 3-12. *Th solubility-controlling phases and concentration values (M) under the different redox conditions for the different groundwaters.*

		$T = 15^oC$		
		Eh gw	**pH$_2$(g)= 10^{-7} atm**	**pH$_2$(g)= 10^2 atm**
Groundwaters	*Brackish saline* KR20/465/1	$ThO_2 \cdot 2H_2O$ $1.0 \cdot 10^{-9}$	$ThO_2 \cdot 2H_2O$ $1.0 \cdot 10^{-9}$	$ThO_2 \cdot 2H_2O$ $1.0 \cdot 10^{-9}$
	Saline KR10/498/1	$ThO_2 \cdot 2H_2O$ $2.0 \cdot 10^{-10}$	$ThO_2 \cdot 2H_2O$ $2.0 \cdot 10^{-10}$	$ThO_2 \cdot 2H_2O$ $2.0 \cdot 10^{-10}$
	Dilute brackish KR6/58/1	$ThO_2 \cdot 2H_2O$ $6.9 10^{-9}$	$ThO_2 \cdot 2H_2O$ $6.9 10^{-9}$	$ThO_2 \cdot 2H_2O$ $6.9 10^{-9}$
	Brine KR12/741/1	$ThO_2 \cdot 2H_2O$ $7.5 \cdot 10^{-11}$	$ThO_2 \cdot 2H_2O$ $7.5 \cdot 10^{-11}$	$ThO_2 \cdot 2H_2O$ $7.5 \cdot 10^{-11}$

Table 3-13. Pa solubility-controlling phases and concentration values (M) under the different redox conditions for the groundwaters.

		Eh gw	pH$_2$(g)= 10^{-7} atm	pH$_2$(g)= 10^2 atm
		T = 15°C		
Groundwaters	*Brackish saline* KR20/465/1	Pa$_2$O$_5$ 3.0·10^{-7}	Pa$_2$O$_5$ 3.0·10^{-7}	*Pa$_2$O$_5$* *3.0·10^{-7}*
	Saline KR10/498/1	Pa$_2$O$_5$ 2.8·10^{-7}	Pa$_2$O$_5$ 2.8·10^{-7}	*Pa$_2$O$_5$* *2.8·10^{-7}*
	Dilute brackish KR6/58/1	Pa$_2$O$_5$ 3.1·10^{-7}	Pa$_2$O$_5$ 3.1·10^{-7}	Pa$_2$O$_5$ 3.1·10^{-7}
	Brine KR12/741/1	Pa$_2$O$_5$ 2.4·10^{-7}	Pa$_2$O$_5$ 2.4·10^{-7}	Pa$_2$O$_5$ 2.3·10^{-7}

3.4.3 Uranium

Uranium aqueous speciation is very dependent on the redox potential and pH of the studied system. Under reducing conditions, uranium is predominantly in the tetravalent state. In general terms, the aqueous chemistry of uranium at reducing conditions is mainly dominated by U(OH)$_4$(aq) in the brackish saline and saline (KR20/465/1 and KR10/498/1 respectively) and brine (KR12/741/1) groundwaters. Under less reducing conditions such as those of the dilute/brackish (KR6/58/1),all bentonite waters and the ice melting groundwater, at the pH and carbonate concentrations of interest, the predominant aqueous species of uranium are carbonates of hexavalent uranium (see Figure 3-9).

U(VI) carbonate complexes are very stable and they may dominate the aqueous speciation even at slightly reducing conditions. This is the case of the dilute brackish bentonite water, which contains a high carbonate concentration and the uranium aqueous speciation is mainly dominated by UO$_2$(CO$_3$)$_3^{-4}$ although the redox is potential is slightly lower than -200mV (see Table 5-7 and Figure 3-10).

In very diluted oxidizing waters (glacial meltwater), the U(VI) hydrolysis dominate the aqueous speciation.

The solid phases that may form in the system are strongly dependent on the composition of the groundwaters. Under reducing conditions, UO$_{2+x}$ phases can appear. The very stable UO$_{2.0}$ can accept excess oxygen in its cubic fluorite structure up to a non-stoichiometric composition corresponding to x = 0.33, i.e., UO$_{2.33}$ or U$_3$O$_7$. Under oxidising conditions, hexavalent uranium solids appear. The precipitation of U(VI) oxyhydroxides is very fast and, thus, not kinetically limited. Under the presence of silicate in the groundwater, as it is the case of interest for this analysis, different silicate solid phases can also form. Uranophane, (Ca(UO$_2$)$_2$(SiO$_3$OH)$_2$ •5H$_2$O) has been found

37
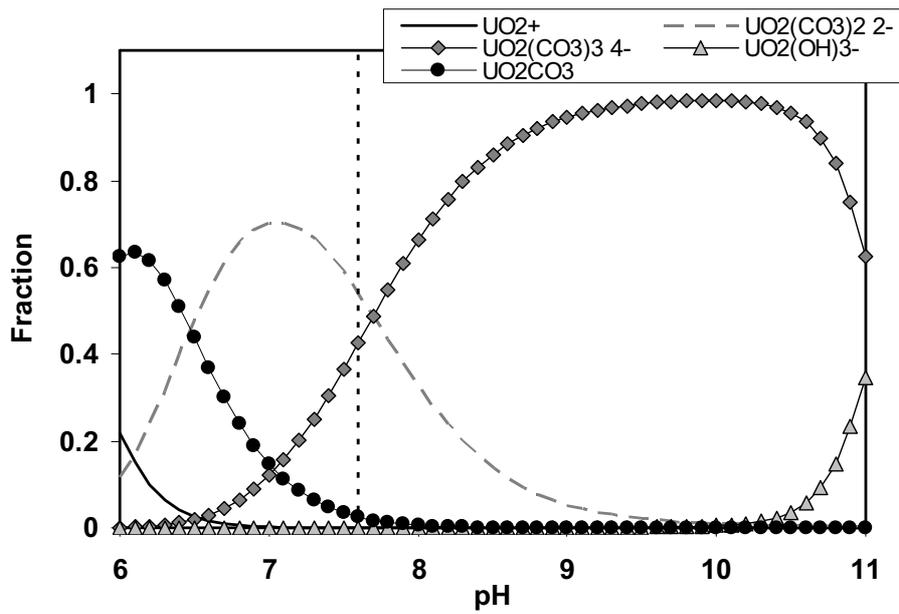
Figure 3-9. *Fractional diagram showing the aqueous speciation of Uranium as a function of pH, under the conditions of the dilute/brackish groundwater KR6/58/1. Vertical black-dashed line indicates the pH of the groundwater.*
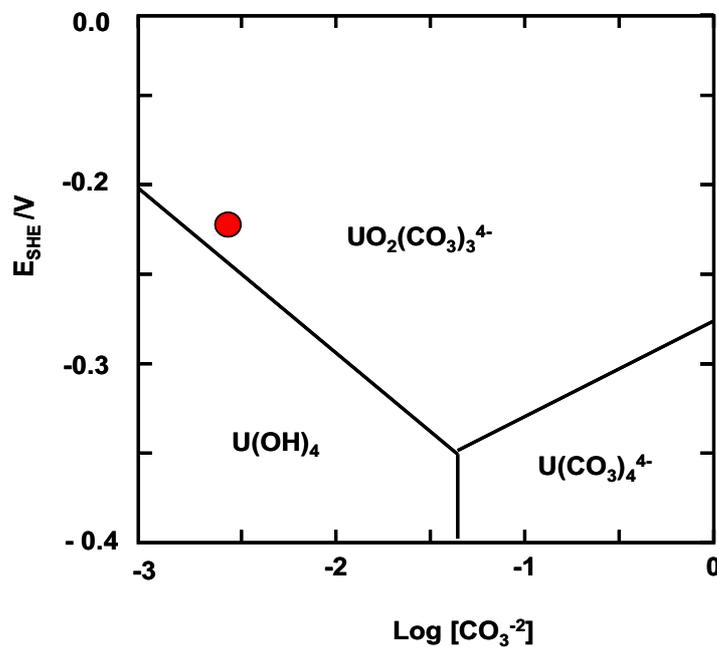
Figure 3-10. *Eh/log[CO$_3^{-2}$] predominance diagram of the aqueous species underlying UO$_2$·2H$_2$O solubility under the conditions given by the dilute/brackish bentonite water. The red circle indicates the Eh and [CO$_3^{-2}$] given for this groundwater.*

to form as secondary phase in the vicinity of massive uranium ores and, therefore, its formation can be possible under the flow regimes expected in the surroundings of the repository.

Under reducing conditions, solids of the type UO_{2+x} are the ones able to control the aqueous concentration of uranium. Under more oxidising conditions, though, uranophane may form under the appropriated silicon concentrations. When the silicon concentration in water is very low (glacial meltwater), becquerelite is the solid phase presenting the lowest solubility.

One of the main uncertainties arising from the study of this element is related with the precipitation of calcium uranates and coffinite, which were omitted in the present calculations due to the few thermodynamic data available. Although both solids have been observed in laboratory experiments and natural systems respectively, the only thermodynamic data available are coming from few experimental data and calorimetric studies performed with crystalline solid phases respectively, which gives unrealistic low uranium concentrations. The lack of thermodynamic data from solubility experiments with less crystalline solid phases leads to disregard these solids for giving uranium concentration limits.

Calculated concentrations of uranium in equilibrium with the different selected solid phases are summarized in Table 3-14 for the groundwaters.

Table 3-14. *U solubility-controlling phase and concentration values (M) under the different redox conditions for the different groundwaters. Selected solid phases in bold.*

		T = 15ºC		
		Eh gw	**pH$_2$(g)= 10^{-7} atm**	**pH$_2$(g)= 10^2 atm**
Groundwaters	*Brackish saline* KR20/465/1	**UO$_2$·2H$_2$O** **7.0·10^{-10}** Uranophane 3.2·10^{-7}	**UO$_2$·2H$_2$O** **6.8·10^{-10}** Uranophane 9.1·10^{-7}	**UO$_2$·2H$_2$O** **6.5·10^{-10}**
	Saline KR10/498/1	**UO$_2$·2H$_2$O** **6.1·10^{-10}** Uranophane 9.0·10^{-8}	**UO$_2$·2H$_2$O** **6.1·10^{-10}** Uranophane 1.7·10^{-7}	**UO$_2$·2H$_2$O** **6.1·10^{-10}**
	Dilute brackish KR6/58/1	UO$_2$·2H$_2$O 2.2·10^{-3} **Uranophane** **2.7·10^{-7}**	**UO$_2$·2H$_2$O** **8.0·10^{-10}** Uranophane 1.6·10^{-6}	**UO$_2$·2H$_2$O** **6.8·10^{-10}**
	Brine KR12/741/1	**UO$_2$·2H$_2$O** **5.2·10^{-10}** Uranophane 3.3·10^{-7}	**UO$_2$·2H$_2$O** **5.2·10^{-10}**	**UO$_2$·2H$_2$O** **5.1·10^{-10}**

3.4.4   Neptunium

Neptunium may be found at different oxidation states: +3, +4, +5 and +6 depending on the redox environment.

Neptunium concentrations under the conditions of interest for this work (except the oxidising glacial meltwater conditions) are expected to be controlled by the precipitation of neptunium(IV) dioxide. This solid is stable over a relatively wide redox potential range, from very reducing to slightly oxidising conditions. According to the Ostwald's rule, the amorphous phase will precipitate first, so, amorphous NpO_2 has been the one selected for the solubility calculations.

The underlying aqueous speciation of neptunium for all the other waters is mainly dominated by $Np(OH)_4$ with important contributions of $NpCO_3(OH)_3^-$ in higher carbonate concentrations groundwaters (for instance dilute brackish groundwater (KR6/58/1)).

The effect of phosphate present in the groundwater on the solubility of Np is negligible. There are no experimental data for the Np(III) phosphate system and no data have been selected in the NEA book (Lemire et al. 2001). If assumed that the stability of Np(III)-phosphates can be estimated by analogy to Pu(III)-phosphates, the role of Np(III) phosphates would not be relevant under the conditions of the groundwaters of interest.

Calculated concentrations of neptunium in equilibrium with the different selected solid phases are summarized in Table 3-15 for the groundwaters.

Table 3-15. *Np solubility-controlling phases and concentration values (M) under the different redox conditions for the different groundwaters.*

		$T = 15^oC$		
		Eh gw	**pH$_2$(g)= 10^{-7} atm**	**pH$_2$(g)= 10^2 atm**
Groundwaters	***Brackish saline*** *KR20/465/1*	$NpO_2 \cdot 2H_2O$ $8.0 \cdot 10^{-10}$	$NpO_2 \cdot 2H_2O$ $8.0 \cdot 10^{-10}$	$NpO_2 \cdot 2H_2O$ $8.0 \cdot 10^{-10}$
	Saline *KR10/498/1*	$NpO_2 \cdot 2H_2O$ $6.9 \cdot 10^{-10}$	$NpO_2 \cdot 2H_2O$ $6.9 \cdot 10^{-10}$	$NpO_2 \cdot 2H_2O$ $6.9 \cdot 10^{-10}$
	Dilute brackish *KR6/58/1*	$NpO_2 \cdot 2H_2O$ $1.2 \cdot 10^{-9}$	$NpO_2 \cdot 2H_2O$ $1.2 \cdot 10^{-9}$	$NpO_2 \cdot 2H_2O$ $1.2 \cdot 10^{-9}$
	Brine *KR12/741/1*	$NpO_2 \cdot 2H_2O$ $5.7 \cdot 10^{-10}$	$NpO_2 \cdot 2H_2O$ $5.7 \cdot 10^{-10}$	$NpO_2 \cdot 2H_2O$ $5.7 \cdot 10^{-10}$

3.4.5   Plutonium

The chemical behaviour of plutonium is quite similar to the one of neptunium and this radionuclide may be also found at different oxidation states, +3, +4, +5 and +6 depending on the environmental redox conditions.

The aqueous speciation will mainly depend on the master variables Eh and pH, although the groundwater composition i.e. carbonates, sulphates, phosphates will also have an important role on determining the aqueous complexes dominating Pu species in solution.

The aqueous speciation of plutonium under the conditions of the brackish saline, saline (KR20/465/1 and KR10/498/1 respectively) and brine (KR12/741/1) groundwaters is dominated by the Pu(III) species (Pu^{3+} and $PuOH^{2+}$). Pu(III) sulphates dominate in bentonite and $Pu(OH)_4$ in the dilute/brackish (KR6/58/1) and ice melting water conditions.

Pu(V) and Pu(VI) dominate the aqueous speciation under the glacial meltwater conditions (see Table 5-8).

Two different solids are the most likely to govern the solubility of this actinide under reducing to slightly oxidising conditions (all the waters in the present work except for the glacial meltwater): $PuO_2 \cdot (am)$ and $PuPO_4(s)$. Although a more crystalline form of tetravalent Pu oxide is selected in Guillaumont et al. (2003), the experimental data available in the literature fall in between the solubility calculated by equilibrating waters with the $PuO_2(am, hyd)$ selected by Guillaumont et al. (2003) and the one obtained with the $Pu(OH)_4(am)$ solid selected in Lemire and Garisto (1989) (see Duro et al., 2005). For the sake of conservatism of the results, solubility calculations have been conducted with the amorphous form of $Pu(OH)_4(am)$, although also the results obtained with $PuO_2 \cdot (am,hyd)$ are reported here.

Phosphates have been identified to form stable Pu(III) solid phases leading to lower Pu concentrations. Therefore, a phosphate of plutonium (III) might be the solid phase controlling the solubility in neutral and reducing waters if phosphates were present.

Indeed, plutonium phosphate has been selected as the Pu solubility controlling phase in the case of the brackish saline (KR20/465/1) and brine (KR12/741/1) groundwater. Under the conditions of the saline groundwater KR10/498/1 both, $PuPO_4$ and $Pu(OH)_4(am)$ could exert the solubility control. The solubility of Pu, though, is governed by $Pu(OH)_4(am)$ under the conditions of the dilute/brackish groundwater, bentonite waters, and ice melting water where the Eh of the system is higher.

Under the conditions of the bentonitic groundwaters (see Table 5-5 to Table 5-7) no aqueous phosphate is reported and therefore, one of the main uncertainties is the effect of phosphate on the solubility of Pu. Sulphate Pu(III) aqueous species are the predominant aqueous species in this case, producing an increase of the $Pu(OH)_4(am)$ solubility.

The limiting solid phase in the case of the glacial meltwater (see Table 5-8) is $PuO_2(OH)_2 \cdot H_2O$ given the high oxygen content of the water.

Table 3-16 summarizes the Pu solubility-controlling phases as well as the concentration values under the different redox conditions studied in the reference case. Pu is a redox sensitive element and because of this, the solubility-limiting phase varies depending on the redox potential considered.

3.4.6 Americium and Curium

Given the chemical analogy existing between americium and curium, we present in this section the discussion undertaken for americium, and the same analyses will apply to curium. For most TDBs and compilations Am and Cm are considered equivalent and data of Am are used for Cm and viceversa.

Americium is one of the so-called trivalent actinides, given that its most stable oxidation state in waters is +3. Am(IV) solid phases are also reported in the literature although americium species in aqueous solutions have not been identified. Am(V) hydroxides have been investigated; nevertheless they have not been included in the database because they are only relevant at very high redox potentials, which is out of the scope of the present work.

Table 3-16. *Pu solubility-controlling phases and concentration values (M) under the different redox conditions for the different groundwaters. Selected in bold.*

		Eh gw	pH$_2$(g)= 10^{-7} atm	pH$_2$(g)= 10^2 atm
		$T = 15^oC$		
Groundwaters	**Brackish saline** *KR20/465/1*	**PuPO$_4$** **8.0·10^{-9}**	**PuPO$_4$** **8.0·10^{-9}**	**PuPO$_4$** **8.0·10^{-9}**
		Pu(OH)$_4$ 4.0·10^{-8}	Pu(OH)$_4$ 6.8·10^{-8}	Pu(OH)$_4$ 2.0·10^{-3}
	Saline *KR10/498/1*	PuPO$_4$ 1.0·10^{-8}	PuPO$_4$ 1.0·10^{-8}	**PuPO$_4$** **9.5·10^{-9}**
		Pu(OH)$_4$ **1.3·10^{-9}**	**Pu(OH)$_4$** **1.8·10^{-9}**	Pu(OH)$_4$ 5.3·10^{-5}
	Dilute brackish *KR6/58/1*	PuPO$_4$ 4.1·10^{-9}	**PuPO$_4$** **5.1·10^{-10}**	**PuPO$_4$** **5.1·10^{-10}**
		Pu(OH)$_4$ **1.5·10^{-10}**	Pu(OH)$_4$ 6.2·10^{-8}	Pu(OH)$_4$ 9.6·10^{-4}
	Brine *KR12/741/1*	PuPO$_4$ 2.3·10^{-10}	PuPO$_4$ 2.7·10^{-10}	PuPO$_4$ 2.0·10^{-10}
		Pu(OH)$_4$ 7.4·10^{-10}	Pu(OH)$_4$ 3.8·10^{-10}	Pu(OH)$_4$ 8.9·10^{-6}

Am aqueous species dominating under the selected groundwater conditions are $AmOSi(OH)_3^{2+}$ with contributions of carbonate species. This aqueous speciation is very similar in the ice melting water.

Free Am^{3+}, sulphate and carbonate complexes are the main aqueous species in the bentonite waters, while only free Am^{3+} is present in the glacial meltwater.

Several solid phases could exert the solubility control in the different waters depending on the pH range considered as well as on the water composition. These solids are the hydroxide, mixed hydroxo-carbonate, $Am(CO_3)_2Na \cdot 5H_2O$, $Am_2(CO_3)_3(s)$ and $AmPO_4 \cdot xH_2O$ phases. Phosphates form stable solid phases with Am, leading to lower and more realistic concentrations than those calculated with the carbonate solid phases. Calculations undertaken show that solid phosphates may exert the solubility control when phosphate concentrations are considered.

When no phosphates are present in the water composition (bentonite waters) $Am(CO_3)_2Na \cdot 5H_2O$ controls the solubility of americium. $Am(OH)_3$ is the limiting solid phase under the ice melting water conditions.

Table 3-17 summarizes the calculated Am concentrations in equilibrium with the different solid phases able to exert the solubility control under the different groundwater compositions.

One of the main conceptual uncertainties important to include during the discussion of this element is the effect of phosphate concentration.

Table 3-17. *Am solubility-controlling phases and concentration values (M) under the different redox conditions for the different groundwaters.*

T = 15ºC				
		Eh gw	**pH$_2$(g)= 10^{-7} atm**	**pH$_2$(g)= 10^2 atm**
Groundwaters	***Brackish saline*** *KR20/465/1*	$AmPO_4$ $1.7 \cdot 10^{-7}$	$AmPO_4$ $1.7 \cdot 10^{-7}$	$AmPO_4$ $1.7 \cdot 10^{-7}$
	Saline *KR10/498/1*	$AmPO_4$ $4.4 \cdot 10^{-7}$	$AmPO_4$ $4.4 \cdot 10^{-7}$	$AmPO_4$ $4.4 \cdot 10^{-7}$
	Dilute brackish *KR6/58/1*	$AmPO_4$ $3.3 \cdot 10^{-9}$	$AmPO_4$ $3.5 \cdot 10^{-9}$	$AmPO_4$ $3.2 \cdot 10^{-9}$
	Brine *KR12/741/1*	$AmPO_4$ $1.2 \cdot 10^{-8}$	$AmPO_4$ $1.2 \cdot 10^{-8}$	$AmPO_4$ $1.2 \cdot 10^{-8}$

4. UNCERTAINTY ASSESSMENT

The solubility concentrations calculated in this work contain an important level of uncertainty. It is of the utmost relevance to identify which type of uncertainty may affect each one of the radionuclides under study.

The main uncertainties can be classified as conceptual uncertainties and numerical uncertainties.

4.1 Conceptual uncertainties

Most of the conceptual uncertainties are related to the choice of models selected to conduct the solubility assessment. We intend to assess solubility limits applicable to the *very-near field* of the repository, when water enters the canister gap and interacts with the waste (see section 2.1). Therefore, it must be clearly stated that the solid phases selected as likely to precipitate apply to the conditions found in the vicinity of the fuel and the canister.

The most relevant uncertainties affecting the system under study are following detailed:

- **Composition of the interacting groundwater**

In this work, we have considered that the compositions of the groundwaters interacting with the waste are those of the groundwaters representative for baseline conditions at Olkiluoto and upcoming of a brine type water (see section 2.2). These types should well cover the expected conditions at the site at emplacement and the evolution from post-emplacement until the far future (Pastina & Hellä 2006).

Groundwater will probably interact with the engineering barriers before contacting the waste, and therefore bentonite waters, corresponding to the groundwaters interacted with the buffer have also been defined as based on calculations by Wersin et al. (2007).

The effect of the corrosion of iron insert and resulting hydrogen overpressure has been considered in both the solubility calculations for groundwaters and bentonite waters.

Two glacial waters resulting from the infiltration of melting of ice to deeper areas have been considered.

- **Precipitation of pure solid phases**

One of the hypotheses enunciated in this work deals with the assumption of the precipitation of pure solid phases of the elements. We have not conducted calculations implying formation of mixed solid phases, although we have commented on this possibility for those elements likely to be incorporated in other major solids.

- **Precipitation of amorphous solid phases**

Another conceptual uncertainty deals with the fact that we have credited the precipitation of amorphous, or less crystalline solid phases, over crystalline solids.

This assumption is partly based on the Ostwald Step Rule. This rule postulates that the precipitate with the highest solubility, that is, the least stable solid phase will form first.

The nucleation of a more soluble phase is kinetically favoured over that of the less soluble phase. Small particles have a higher ratio surface area to particle mass than large particles and therefore will have high surface energy, thus dissolving preferentially. The higher solubility of small particles produces solutions which are supersaturated relative to large particles.

No metallic of native phases have been in principle considered, except for Se(0). This decision has been taken in the light of the very slow formation kinetics of this type of phases under the conditions of interest. This has, nevertheless, a certain level of uncertainty.

- **Sulphate to sulphide reduction process**

Multi-electron transfers only occurs by one electron at a time and, therefore, take place in several steps which require many successive encounters between electron donor and electron acceptor, resulting in a slow global reaction. The reduction of sulphate (eq 4-1):

$$SO_4^2 + 9\,H^+ + 8\,e = HS + 4\,H_2O \qquad\qquad (eq.\ 4\text{-}1)$$

implies the transfer of 8 electrons. This process is so slow that equilibrium between hydrogen sulphide and sulphate has never been observed in any abiotic system below 200 ºC (Grenthe & Puigdomenech, 1997). The reaction is accelerated, though, in the presence of bacterial activity. In fact, inorganic sulphur species more oxidized than sulphide can act as electron acceptors in the oxidation of organic matter by bacteria. In the process the sulphur is reduced to sulphide.

In the system we deal with in this work, the presence of sulphate reducing bacteria (SRB) has not been clearly evidenced so far. SRB are present in Olkiluoto groundwaters but the activity should be restricted in bentonite due to its high density/swelling pressure. Therefore, we have decoupled the +VI from the –II oxidation states of sulphur, precluding the possibility of reduction of sulphate to sulphide. Should the bacterial activity be considered, different solubilities would be suggested for some of the radionuclides studied here. This uncertainty will mainly affect to those elements whose solubility is considered to be limited by sulphate solids, such as Sr.

In some cases, we have coupled the +VI and –II oxidation states of sulphur in order to test which would be the influence of sulphate reduction in the radionuclide behaviour. Only when working at the highest pH_2 (100 atm) the process would have any effect on the solubility of the studied radionuclides.

4.2   Numerical uncertainties

The main numerical uncertainties are described below.

- **Thermodynamic database**

An important numerical uncertainty is the Thermodynamic Database used in the calculations. The TDB used is reported in Duro et al. (2005) where the procedure for

data selection and uncertainty assignment is fully documented. As explained in section 2.6, that TDB has been modified according the latest publications within the NEA TDB project on Ni, Se and Zr. Furthermore, thermodynamic data on Mo have been added since no data for this element was present and new data for Th has been considered. The most relevant uncertainty associated with the TDB is the effect of temperature on the stability of aqueous species and solid compounds. In the mentioned report, a selection of reaction enthalpy is included, although in some cases no enthalpy data are available. The approach to correct the equilibrium constants for temperature effects follows the Van't Hoff equation, where constant $\Delta_r H^0$ is considered. This approach is valid under the temperature regime expected in the studied system (10-25 °C).

- **Activity corrections**

The treatment of activity corrections also represents an uncertainty to the current solubility assessment. The range of ionic strength (I) in the groundwaters used in this work spans from 10^{-5} to 1.2 M. The most appropriated procedure to conduct activity corrections in this range would be the Specific Interaction Theory (SIT), as recommended by the NEA guidelines, which is expressed by (eq. 4-2).

$$\log(\gamma_i) = -z_i^2 \left(\frac{A\sqrt{I}}{1 + Ba_i\sqrt{I}} \right) + \sum_k \varepsilon_{(i,k,I)} m_k \qquad \text{(eq. 4-2)}$$

where log (γI) is the logarithm of the activity coefficient of species I, a_i is the effective diameter of the hydrated ion, $\varepsilon_{(I,k,I)}$ is the ion interaction coefficient and m_k is the molality of the background electrolyte.

Nevertheless, this approach is not still implemented in the geochemical codes that we have used in our calculations and, therefore, the extended Debye-Hückel theory (see eq. 4-3) has been used for activity corrections in this report.

$$\log(\gamma_i) = -z_i^2 \left(\frac{A\sqrt{I}}{1 + Ba_i\sqrt{I}} \right) + b_i I \qquad \text{(eq. 4-3)}$$

where Z_i is the charge of the ion, I the ionic strength (m), A is a constant equal to 0.5100 $mol^{-0.5}$ $kg^{0.5}$ at 25 °C, B is a parameter defined by temperature, pressure and the dielectric constant of water and b is a parameter dependent on temperature and pressure.

5. SOLUBILITIES FOR THE ELEMENTS OF INTEREST UNDER DIFFERENT SCENARIOS

In this chapter several tables summarize the solid phases assumed to control the aqueous concentration of the element in question, the concentration limit of this element, the underlying aqueous speciation and the uncertainty parameters associated for all the nine waters (groundwaters, bentonite waters, and glacial waters (glacial melt water and ice melting water)).

5.1 Groundwaters

The following tables detail the solid phase assumed to control the concentration of the element in question, the concentration limit of this element, the underlying aqueous speciation and the uncertainty parameters associated for each groundwater type and redox state defined.

Table 5-1. *Solubilities for elements of interest. Brackish Saline groundwater(KR20/465/1).*

Element	Solubility limiting phase and reaction	Redox states	M(mol·dm^{-3})	Main complexes formed	Associated uncertainty parameters
Cs		Eh gw	n.s.l.	Cs$^+$ (93%), CsCl (7%)	
		pH$_2$(g) = 10^{-7} atm	n.s.l.	Cs$^+$ (93%), CsCl (7%)	
		pH$_2$(g) = 10^2 atm	n.s.l.	Cs$^+$ (93%), CsCl (7%)	
Sr	Strontianite $SrCO_3 + H^+ = Sr^{2+} + HCO_3^-$	Eh gw	5.9·10^{-3}	Sr^{2+} (99.7%)	Possibility of coprecipitation with other elements carbonates SO$_4^{2-}$ to HS$^-$ reduction
		pH$_2$(g) = 10^{-7} atm	5.9·10^{-3}	Sr^{2+} (99.7%)	
		pH$_2$(g) = 10^2 atm	5.9·10^{-3}	Sr^{2+} (99.7%)	
Ra	$RaSO_4(s) = Ra^{2+} + SO_4^{2-}$	Eh gw	3.2·10^{-6}	Ra^{2+} (97%)	Possibility of coprecipitation with other elements carbonates SO$_4^{2-}$ to HS$^-$ reduction
		pH$_2$(g) = 10^{-7} atm	3.2·10^{-6}	Ra^{2+} (97%)	
		pH$_2$(g) = 10^2 atm	3.3·10^{-6}	Ra^{2+} (96%)	
Sn	$SnO_2 (am) + 4H^+ = 2\,H_2O + Sn^{4+}$	Eh gw	9.6·10^{-8}	Sn(OH)$_4$ (81.3%), Sn(OH)$_5^-$ (19%)	SO$_4^{2-}$ to HS$^-$ reduction
		pH$_2$(g) = 10^{-7} atm	9.6·10^{-8}	Sn(OH)$_4$ (81.3%), Sn(OH)$_5^-$ (19%)	
		pH$_2$(g) = 10^2 atm	1.2·10^{-7}	Sn(OH)$_4$ (65%), Sn(OH)$_2$ (25%), Sn(OH)$_5^-$ (15%)	
Se	$FeSe_2 + 2\,H^+ + 2\,e^- = Fe^{2+} + 2HSe^-$	Eh gw	6.0·10^{-10}	HSe$^-$ (99.9%)	Formation of native Se^o SO$_4^{2-}$ to HS$^-$ reduction
	$FeSe_2 + 2\,H^+ + 2\,e^- = Fe^{2+} + 2HSe^-$	pH$_2$(g) = 10^{-7} atm	1.0·10^{-9}	HSe$^-$ (99.9%)	Possibility of coprecipitation with

Element	Solubility limiting phase and reaction	Redox states	$M(mol \cdot dm^{-3})$	Main complexes formed	Associated uncertainty parameters
	$Fe_{1.04}Se + H^+ = 1.04Fe^{2+} + HSe^- + 0.08e^-$	$pH_2(g) = 10^2$ atm	$1.4 \cdot 10^{-5}$	HSe^- (99.9%)	coprecipitation with sulphides Uncertainty in measured iron concentrations
Zr	$Zr(OH)_4$ (am) $Zr(OH)_4 + 4 H^+ = 4 H_2O + Zr^{4+}$	Eh gw	$1.7 \cdot 10^{-8}$	$Zr(OH)_4$ (100%)	Crystallinity of the solid phase
		$pH_2(g) = 10^{-7}$ atm	$1.7 \cdot 10^{-8}$	$Zr(OH)_4$ (100%)	
		$pH_2(g) = 10^2$ atm	$1.7 \cdot 10^{-8}$	$Zr(OH)_4$ (100%)	
Nb	$Nb_2O_5 + H_2O = 2 NbO_3^- + 2 H^+$	Eh gw	$3.9 \cdot 10^{-5}$	NbO_3^- (64%), $Nb(OH)_5$ (36%)	Scarcity of TDB
		$pH_2(g) = 10^{-7}$ atm	$3.9 \cdot 10^{-5}$	NbO_3^- (64%), $Nb(OH)_5$ (36%)	
		$pH_2(g) = 10^2$ atm	$3.9 \cdot 10^{-5}$	NbO_3^- (64%), $Nb(OH)_5$ (36%)	
Mo	$MoO_2(s) + 2 H_2O = MoO_4^{2-} + 4H^+ + 2e^-$	Eh gw	$7.9 \cdot 10^{-9}$	MoO_4^{2-} (100%)	Scarcity of TDB
		$pH_2(g) = 10^{-7}$ atm	$2.8 \cdot 10^{-9}$	MoO_4^{2-} (100%)	
		$pH_2(g) = 10^2$ atm	-		
Tc	$TcO_2 \cdot 1.6H_2O = TcO(OH)_2 + 0.6 H_2O$	Eh gw	$4.0 \cdot 10^{-9}$	$TcO(OH)_2$ (98.9%)	Formation of metallic Tc^o
		$pH_2(g) = 10^{-7}$ atm	$4.0 \cdot 10^{-9}$	$TcO(OH)_2$ (98.9%)	
		$pH_2(g) = 10^2$ atm	$4.0 \cdot 10^{-9}$	$TcO(OH)_2$ (98.9%)	
Ni	$Ni(OH)_2(s) + 2 H^+ = Ni^{2+} + 2 H_2O$	Eh gw	$2.0 \cdot 10^{-3}$	Ni^{2+}(94%), $NiCl^+$(6%)	SO_4^{2-} to HS^- reduction
		$pH_2(g) = 10^{-7}$ atm	$2.0 \cdot 10^{-3}$	Ni^{2+}(94%), $NiCl^+$(6%)	
		$pH_2(g) = 10^2$ atm	$2.0 \cdot 10^{-3}$	Ni^{2+}(94%), $NiCl^+$(6%)	
Pd	$Pd(OH)_2(s) + 2 H^+ = 2 H_2O + Pd^{2+}$	Eh gw	$2.6 \cdot 10^{-6}$	$Pd(OH)_2$ (99.9%)	Formation of metallic Pd^o
		$pH_2(g) = 10^{-7}$ atm	$2.6 \cdot 10^{-6}$	$Pd(OH)_2$ (99.9%)	
		$pH_2(g) = 10^2$ atm	$2.6 \cdot 10^{-6}$	$Pd(OH)_2$ (99.9%)	

Element	Solubility limiting phase and reaction	Redox states	$M(mol \cdot dm^{-3})$	Main complexes formed	Associated uncertainty parameters
Sm	$SmPO_4(s) + 2H^+ = H_2PO_4^- + Sm^{3+}$	Eh gw	$9.3 \cdot 10^{-9}$	Sm^{3+} (75%), $SmCO_3^+$ (14%), $Sm(CO_3)_2^-$ (4%), $SmCl^{2+}$ (4%)	Reliability of phosphate measurements
		$pH_2(g) = 10^{-7}$ atm	$9.3 \cdot 10^{-9}$	Sm^{3+} (75%), $SmCO_3^+$ (14%), $Sm(CO_3)_2^-$ (4%), $SmCl^{2+}$ (4%)	
		$pH_2(g) = 10^2$ atm	$9.3 \cdot 10^{-9}$	Sm^{3+} (75%), $SmCO_3^+$ (14%), $Sm(CO_3)_2^-$ (4%), $SmCl^{2+}$ (4%)	
Th	$ThO_2 \cdot 2H_2O + 4H^+ = Th^{4+} + 4H_2O$	Eh gw	$1.0 \cdot 10^{-9}$	$ThCO_3(OH)_3^-$ (82%), $Th(CO_3)_2(OH)_2^{2-}$ (8%)	Stability of the solid phase Uncertain thermodynamic data for aqueous carbonates
		$pH_2(g) = 10^{-7}$ atm	$1.0 \cdot 10^{-9}$	$ThCO_3(OH)_3^-$ (82%), $Th(CO_3)_2(OH)_2^{2-}$ (8%)	
		$pH_2(g) = 10^2$ atm	$1.0 \cdot 10^{-9}$	$ThCO_3(OH)_3^-$ (82%), $Th(CO_3)_2(OH)_2^{2-}$ (8%)	
Pa	$Pa_2O_5(s) + 2H^+ = 2PaO_2^+ + H_2O$	Eh gw	$3.0 \cdot 10^{-7}$	PaO_2OH (99.8%)	Lack of thermodynamic data
		$pH_2(g) = 10^{-7}$ atm	$3.0 \cdot 10^{-7}$	PaO_2OH (99.8%)	
		$pH_2(g) = 10^2$ atm	$3.0 \cdot 10^{-7}$	PaO_2OH (99.8%)	
U	$UO_2 \cdot 2H_2O + 4H^+ = U^{4+} + 4H_2O$	Eh gw	$7.0 \cdot 10^{-10}$	$U(OH)_4$ (92%), UO_2^+ (5%)	Silicate solid precipitation TDB data on solid stability
		$pH_2(g) = 10^{-7}$ atm	$6.8 \cdot 10^{-10}$	$U(OH)_4$ (96%)	
		$pH_2(g) = 10^2$ atm	$6.5 \cdot 10^{-10}$	$U(OH)_4$ (98%)	
Np	$NpO_2 \cdot 2H_2O + 4H^+ = Np^{4+} + 4H_2O$	Eh gw	$8.0 \cdot 10^{-10}$	$Np(OH)_4$ (89%), $NpCO_3(OH)_3^-$ (9%)	
		$pH_2(g) = 10^{-7}$ atm	$8.0 \cdot 10^{-10}$	$Np(OH)_4$ (89%), $NpCO_3(OH)_3^-$ (8%)	Crystallinity of the solid

Element	Solubility limiting phase and reaction	Redox states	$M(\text{mol·dm}^{-3})$	Main complexes formed	Associated uncertainty parameters
		$pH_2(g) = 10^2$ atm	$8.0·10^{-10}$	$Np(OH)_4$ (89%), $NpCO_3(OH)_3^-$ (8%)	phase
Pu	$PuPO_4(s) + 2H^+ = Pu^{3+} + H_2PO_4^-$	Eh gw	$8.0·10^{-9}$	Pu^{3+} (69%), $PuOH^{2+}$ (17%), $PuCO_3^+$ (10%)	Reliability of phosphate measurements
		$pH_2(g) = 10^{-7}$ atm	$8.0·10^{-9}$	Pu^{3+} (69%), $PuOH^{2+}$ (17%), $PuCO_3^+$ (10%)	
		$pH_2(g) = 10^2$ atm	$8.0·10^{-9}$	Pu^{3+} (69%), $PuOH^{2+}$ (17%), $PuCO_3^+$ (10%)	
Am/Cm	$AmPO_4{:}xH_2O(am)$ $AmPO_4 + 2H^+ = Am^{3+} + H_2PO_4^-$	Eh gw	$1.7·10^{-7}$	$AmOSi(OH)_3^{2+}$ (96.6%)	Reliability of phosphate measurements
		$pH_2(g) = 10^{-7}$ atm	$1.7·10^{-7}$	$AmOSi(OH)_3^{2+}$ (96.6%)	
		$pH_2(g) = 10^2$ atm	$1.7·10^{-7}$	$AmOSi(OH)_3^{2+}$ (96.6%)	

Table 5-2. *Solubilities for elements of interest. Saline groundwater (KR10/498/1).*

Element	Solubility limiting phase and reaction	Redox states	M(mol·dm^{-3})	Main complexes formed	Associated uncertainty parameters
Cs		Eh gw	n.s.l.	Cs$^+$ (88%), CsCl(aq) (12%)	
		pH$_2$(g) = 10^{-7} atm	n.s.l.	Cs$^+$ (88%), CsCl(aq) (12%)	
		pH$_2$(g) = 10^2 atm	n.s.l.	Cs$^+$ (88%), CsCl(aq) (12%)	
Sr	Strontianite SrCO$_3$ + H$^+$= Sr^{2+} + HCO$_3^-$	Eh gw	9.2·10^{-3}	Sr^{2+} (100%)	Possibility of coprecipitation with other elements' carbonates SO$_4^{2-}$ to HS$^-$ reduction
		pH$_2$(g) = 10^{-7} atm	9.2·10^{-3}	Sr^{2+} (100%)	
		pH$_2$(g)= 10^2 atm	9.2·10^{-3}	Sr^{2+} (100%)	
Ra	RaSO$_4$(s) = Ra^{2+} + SO$_4^{2-}$	Eh gw	1.1·10^{-4}	Ra^{2+}(93%), RaCl$^+$(7%)	Possibility of coprecipitation with other elements' carbonates SO$_4^{2-}$ to HS$^-$ reduction
		pH$_2$(g) = 10^{-7} atm	1.1·10^{-4}	Ra^{2+}(93%), RaCl$^+$(7%)	
		pH$_2$(g)= 10^2 atm	1.2·10^{-4}	Ra^{2+}(93%), RaCl$^+$(7%)	
Sn	SnO$_2$ (am) + 4H$^+$ = 2H$_2$O +Sn^{4+}	Eh gw	1.4·10^{-7}	Sn(OH)$_4$ (50%), Sn(OH)$_5^-$ (49%)	
		pH$_2$(g)= 10^{-7} atm	1.4·10^{-7}	Sn(OH)$_4$ (51%), Sn(OH)$_5^-$ (49%)	SO$_4^{2-}$ to HS$^-$ reduction
		pH$_2$(g)= 10^2 atm	1.7·10^{-7}	Sn(OH)$_4$ (42%), Sn(OH)$_5^-$ (41%), Sn(OH)$_2$ (16%)	
Se	FeSe$_2$(s) +2H$^+$ +2e$^-$ =Fe^{2+} + 2HSe$^-$	Eh gw	8.8·10^{-10}	HSe$^-$ (100%)	Formation of native Se^o SO$_4^{2-}$ to HS$^-$ reduction
	FeSe$_2$(s) +2H$^+$ +2e$^-$ = Fe^{2+} +2HSe$^-$	pH$_2$(g)= 10^{-7} atm	1.2·10^{-9}	HSe$^-$ (100%)	

Element	Solubility limiting phase and reaction	Redox states	M(mol·dm^{-3})	Main complexes formed	Associated uncertainty parameters
	$Fe_{1.04}Se + H^+ = 1.04Fe^{2+} + HSe^- + 0.08e^-$	pH$_2$(g)= 10^2 atm	$4.5\cdot10^{-6}$	HSe$^-$ (100%)	Possibility of coprecipitation with sulphides Uncertainty in measured iron concentrations
Zr	Zr(OH)$_4$ (aged) $Zr(OH)_4 + 4 H^+ = 4 H_2O + Zr^{4+}$	Eh gw	$1.6\cdot10^{-8}$	Zr(OH)$_4$(aq) (99.9%)	Crystallinity of the solid phase
		pH$_2$(g)= 10^{-7} atm	$1.6\cdot10^{-8}$	Zr(OH)$_4$(aq) (100%)	
		pH$_2$(g)= 10^2 atm	$1.6\cdot10^{-8}$	Zr(OH)$_4$(aq) (100%)	
Nb	$Nb_2O_5 + H_2O = 2 NbO_3^- + 2 H^+$	Eh gw	$1.2\cdot10^{-4}$	NbO$_3^-$ (90%), Nb(OH)$_5$ (10%)	Scarcity of TDB
		pH$_2$(g)= 10^{-7} atm	$1.2\cdot10^{-4}$	NbO$_3^-$ (89%), Nb(OH)$_5$ (11%)	
		pH$_2$(g)= 10^2 atm	$1.2\cdot10^{-4}$	NbO$_3^-$ (89%), Nb(OH)$_5$ (11%)	
Mo	$MoO_2(s) + 2H_2O = MoO_4^{2-} + 4H^+ + 2e^-$	Eh gw	$8.5\cdot10^{-8}$	MoO$_4^{2-}$ (100%)	Scarcity of TDB
		pH$_2$(g)= 10^{-7} atm	$4.5\cdot10^{-8}$	MoO$_4^{2-}$ (100%)	
		pH$_2$(g)= 10^2 atm	-		
Tc	$TcO_2\cdot1.6H_2O = TcO(OH)_2 + 0.6 H_2O$	Eh gw	$4.0\cdot10^{-9}$	TcO(OH)$_2$(aq) (99.7%)	Formation of metallic Tc^o
		pH$_2$(g)= 10^{-7} atm	$4.0\cdot10^{-9}$	TcO(OH)$_2$(aq) (99.8%)	
		pH$_2$(g)= 10^2 atm	$4.0\cdot10^{-9}$	TcO(OH)$_2$(aq) (99.8%)	
Ni	$Ni(OH)_2(s) + 2H^+ = Ni^{2+} + 2H_2O$	Eh gw	$1.4\cdot10^{-4}$	Ni^{2+}(88%),NiCl$^+$(11%)	SO$_4^{2-}$ to HS$^-$ reduction
		pH$_2$(g)= 10^{-7} atm	$1.4\cdot10^{-4}$	Ni^{2+}(88%),NiCl$^+$(11%)	
		pH$_2$(g)= 10^2 atm	$1.4\cdot10^{-4}$	Ni^{2+}(88%),NiCl$^+$(11%)	
Pd	$Pd(OH)_2(s) + 2H^+ = 2H_2O + Pd^{2+}$	Eh gw	$2.5\cdot10^{-6}$	Pd(OH)$_2$ (97%)	Formation of metallic Pd^o
		pH$_2$(g)= 10^{-7} atm	$2.5\cdot10^{-6}$	Pd(OH)$_2$ (97%)	
		pH$_2$(g)= 10^2 atm	$2.5\cdot10^{-6}$	Pd(OH)$_2$ (97%)	

Element	Solubility limiting phase and reaction	Redox states	M(mol·dm^{-3})	Main complexes formed	Associated uncertainty parameters
Sm	SmPO$_4$(s) SmPO$_4$ +2H$^+$ = H$_2$PO$_4^-$ +Sm^{3+}	Eh gw	7.8·10^{-9}	Sm^{3+} (75%), SmCO$_3^+$ (8.5%), SmCl^{2+} (7.5%)	
		pH$_2$(g)= 10^{-7} atm	7.8·10^{-9}	Sm^{3+} (75%), SmCO$_3^+$ (8.5%), SmCl^{2+} (7.5%)	Reliability of phosphate measurements
		pH$_2$(g)= 10^2 atm	7.8·10^{-9}	Sm^{3+} (75%), SmCO$_3^+$ (8.5%), SmCl^{2+} (7.5%)	
Th	ThO$_2$:2H$_2$O(am) + 4H$^+$ = Th^{4+} + 4H$_2$O	Eh gw	2.0·10^{-10}	ThCO$_3$(OH)$_3^-$ (70%), Th(OH)$_4$ (26%)	Stability of the solid phase Uncertain thermodynamic data for aqueous carbonates
		pH$_2$(g)= 10^{-7} atm	2.0·10^{-10}	ThCO$_3$(OH)$_3^-$ (70%), Th(OH)$_4$ (26%)	
		pH$_2$(g)= 10^2 atm	2.0·10^{-10}	ThCO$_3$(OH)$_3^-$ (70%), Th(OH)$_4$ (26%)	
Pa	Pa$_2$O$_5$(s) +2H$^+$ = 2PaO$_2^+$ +H$_2$O	Eh gw	2.8·10^{-7}	PaO$_2$OH(aq) (100%)	Lack of thermodynamic data
		pH$_2$(g)= 10^{-7} atm	2.8·10^{-7}	PaO$_2$OH(aq) (100%)	
		pH$_2$(g)= 10^2 atm	2.8·10^{-7}	PaO$_2$OH(aq) (100%)	
U	UO$_2$·2H$_2$O +4H$^+$ = U^{4+} +4H$_2$O	Eh gw	6.1·10^{-10}	U(OH)$_4$(aq) (98%)	Silicate solid precipitation TDB data on solid stability
		pH$_2$(g)= 10^{-7} atm	6.1·10^{-10}	U(OH)$_4$(aq) (98.6%)	
		pH$_2$(g)= 10^2 atm	6.1·10^{-10}	U(OH)$_4$(aq) (99.6%)	
Np	NpO$_2$:2H$_2$O(am) NpO$_2$:2H$_2$O +4H$^+$ = Np^{4+} +4H$_2$O	Eh gw	6.9·10^{-10}	Np(OH)$_4$(aq) (97.6%)	Crystallinity of the solid phase
		pH$_2$(g)= 10^{-7} atm	6.9·10^{-10}	Np(OH)$_4$(aq) (97.6%)	
		pH$_2$(g)= 10^2 atm	6.9·10^{-10}	Np(OH)$_4$(aq) (97.6%)	
Pu	Pu(OH)$_4$(am) +4H$^+$ = Pu^{4+} + 4H$_2$O	Eh gw	1.3·10^{-9}	Pu^{3+} (45%), PuOH^{2+} (41%), Pu(OH)$_4$(aq) (8%)	Reliability of phosphate measurements

Element	Solubility limiting phase and reaction	Redox states	$M(\text{mol}\cdot\text{dm}^{-3})$	Main complexes formed	Associated uncertainty parameters
	$Pu(OH)_4(am) + 4H^+ = Pu^{4+} + 4H_2O$	$pH_2(g) = 10^{-7}$ atm	$1.8\cdot10^{-9}$	Pu^{3+} (46%), $PuOH^{2+}$ (42%), $Pu(OH)_4(aq)$ (6%)	
	$PuPO_4(s) + 2H^+ = Pu^{3+} + H_2PO_4^-$	$pH_2(g) = 10^{2}$ atm	$9.5\cdot10^{-9}$	Pu^{3+} (49%), $PuOH^{2+}$ (45%), $Pu(CO_3)^+$ (5%)	
Am/Cm	$AmPO_4{:}xH_2O(am)$ $AmPO_4 + 2H^+ = Am^{3+} + H_2PO_4$	Eh gw	$4.4\cdot10^{-7}$	$AmOSi(OH)_3^{2+}$(98.7%)	Reliability of phosphate measurements
		$pH_2(g) = 10^{-7}$ atm	$4.4\cdot10^{-7}$	$AmOSi(OH)_3^{2+}$ 98.7%	
		$pH_2(g) = 10^{2}$ atm	$4.4\cdot10^{-7}$	$AmOSi(OH)_3^{2+}$ 98.7%	

Table 5-3. *Solubilities for elements of interest. Dilute Brackish groundwater (KR6/58/1).*

Element	Solubility limiting phase and reaction	Redox states	M(mol·dm^{-3})	Main complexes formed	Associated uncertainty parameters
Cs		Eh gw	n.s.l.	Cs$^+$(99.9%)	
		pH$_2$(g) = 10^{-7} atm	n.s.l.	Cs$^+$(99.9%)	
		pH$_2$(g) = 10^2 atm	n.s.l.	Cs$^+$(99.9%)	
Sr	Strontianite $SrCO_3 + H^+ = Sr^{2+} + HCO_3^-$	Eh gw	3.1·10^{-4}	Sr^{2+}(92.9%), SrSO$_4$(6%)	Possibility of coprecipitation with other elements' carbonates SO$_4^{2-}$ to HS$^-$ reduction
		pH$_2$(g)= 10^{-7} atm	3.1·10^{-4}	Sr^{2+}(92.9%), SrSO$_4$(6%)	
		pH$_2$(g)= 10^2 atm	3.1·10^{-4}	Sr^{2+}(92.9%), SrSO$_4$(6%)	
Ra	RaSO$_4$(s) = Ra^{2+} + SO$_4^{2-}$	Eh gw	1.1·10^{-7}	Ra^{2+}(84%),RaSO$_4$(15%)	Possibility of coprecipitation with other elements' carbonates SO$_4^{2-}$ to HS$^-$ reduction
		pH$_2$(g)= 10^{-7} atm	1.1·10^{-7}	Ra^{2+}(84%),RaSO$_4$(15%)	
		pH$_2$(g)= 10^2 atm	1.1·10^{-7}	Ra^{2+}(84%),RaSO$_4$(15%)	
Sn	SnO$_2$ (am) + 4H$^+$ = 2H$_2$O + Sn^{4+}	Eh gw	1.1·10^{-7}	Sn(OH)$_4$ (77%), Sn(OH)$_5^-$ (23%)	SO$_4^{2-}$ to HS$^-$ reduction
		pH$_2$(g)= 10^{-7} atm	1.1·10^{-7}	Sn(OH)$_4$ (77%), Sn(OH)$_5^-$ (23%)	
		pH$_2$(g)= 10^2 atm	1.4·10^{-7}	Sn(OH)$_4$ (59%), Sn(OH)$_2$ (22%) Sn(OH)$_5^-$ (17%),	
Se	FeSe$_2$(s) +2H$^+$ +2e$^-$ =Fe^{2+} +2HSe$^-$	Eh gw	6.6·10^{-14}	HSe$^-$ (99.9%)	Formayion of native Se^o SO$_4^{2-}$ to HS$^-$ reduction Possibility of coprecipitation with sulphides Uncertainty in measured iron concentrations
	FeSe$_2$(s) +2H$^+$ +2e$^-$ =Fe^{2+} +2HSe$^-$	pH$_2$(g)= 10^{-7} atm	2.1·10^{-10}	HSe$^-$ (99.9%)	
	Fe$_{1.04}$Se + H$^+$ = 1.04 Fe^{2+} + HSe$^-$ + 0.08 e$^-$	pH$_2$(g)= 10^2 atm	3.8·10^{-7}	HSe$^-$ (99.9%)	

Element	Solubility limiting phase and reaction	Redox states	$M(mol \cdot dm^{-3})$	Main complexes formed	Associated uncertainty parameters
Zr	$Zr(OH)_4$ (aged) $Zr(OH)_4 + 4\ H^+ = 4\ H_2O + Zr^{4+}$	Eh gw	$1.8 \cdot 10^{-8}$	$Zr(OH)_4$ (99.9%)	Crystallinity of the solid phase
		$pH_2(g)= 10^{-7}$ atm	$1.8 \cdot 10^{-8}$	$Zr(OH)_4$ (99.9%)	
		$pH_2(g)= 10^{2}$ atm	$1.8 \cdot 10^{-8}$	$Zr(OH)_4$ (99.9%)	
Nb	$Nb_2O_5 + H_2O = 2\ NbO_3^- + 2\ H^+$	Eh gw	$4.6 \cdot 10^{-5}$	NbO_3^- (68%), $Nb(OH)_5$ (32%)	Scarcity of TDB
		$pH_2(g)= 10^{-7}$ atm	$4.6 \cdot 10^{-5}$	NbO_3^- (68%), $Nb(OH)_5$ (32%)	
		$pH_2(g)= 10^{2}$ atm	$4.6 \cdot 10^{-5}$	NbO_3^- (68%), $Nb(OH)_5$ (32%)	
Mo	$CaMoO_4\ (s) = MoO_4^{2-} + Ca^{2+}$	Eh gw	$1.9 \cdot 10^{-5}$	MoO_4^{2-} (99.9%)	Scarcity of TDB
	$MoO_2 +2H_2O=MoO_4^{2-} +4H^+ +2e^-$	$pH_2(g)= 10^{-7}$ atm	$3.7 \cdot 10^{-9}$	MoO_4^{2-} (99.9%)	
	$MoO_2 +2H_2O=MoO_4^{2-} +4H^+ +2e^-$	$pH_2(g)= 10^{2}$ atm	-		
Tc	$TcO_2 \cdot 1.6H_2O = TcO(OH)_2 +0.6H_2O$	Eh gw	$5 \cdot 10^{-9}$	$TcO(OH)_2(aq)$ (95%)	Formation of metallic Tc^o
		$pH_2(g)= 10^{2}$ atm	$4.2 \cdot 10^{-9}$	$TcO(OH)_2(aq)$ (95%)	
		$pH_2(g)= 10^{-7}$ atm	$4.2 \cdot 10^{-9}$	$TcO(OH)_2(aq)$ (95%)	
Ni	$Ni(OH)_2 + 2\ H^+ = Ni^{2+} + 2\ H_2O$	Eh gw	$4.4 \cdot 10^{-4}$	Ni^{+2}(87%), $NiSO_4$(6%)	SO_4^{2-} to HS^- reduction
		$pH_2(g)= 10^{-7}$ atm	$4.4 \cdot 10^{-4}$	Ni^{+2}(87%), $NiSO_4$(6%)	
		$pH_2(g)= 10^{2}$ atm	$4.4 \cdot 10^{-4}$	Ni^{+2}(87%), $NiSO_4$(6%)	
Pd	$Pd(OH)_2 + 2\ H^+ = 2\ H_2O + Pd^{2+}$	Eh gw	$2.7 \cdot 10^{-6}$	$Pd(OH)_2(aq)$ (99.9%)	Formation of metallic Pd^o
		$pH_2(g)= 10^{-7}$ atm	$2.7 \cdot 10^{-6}$	$Pd(OH)_2(aq)$ (99.9%)	
		$pH_2(g)= 10^{2}$ atm	$2.7 \cdot 10^{-6}$	$Pd(OH)_2(aq)$ (99.9%)	
Sm	$SmPO_4(s) +2H^+ =H_2PO_4^- +Sm^{3+}$	Eh gw	$9.2 \cdot 10^{-10}$	$Sm(CO_3)_2^-$(72%) $SmCO_3^+$(22%)	

Element	Solubility limiting phase and reaction	Redox states	M(mol·dm^{-3})	Main complexes formed	Associated uncertainty parameters
		pH$_2$(g)= 10^{-7} atm	$9.2 \cdot 10^{-10}$	Sm(CO$_3$)$_2^-$ (72%) SmCO$_3^+$ (22%)	Reliability of phosphate measurements
		pH$_2$(g)= 10^2 atm	$9.2 \cdot 10^{-10}$	Sm(CO$_3$)$_2^-$ (72%) SmCO$_3^+$ (22%)	
Th	ThO$_2$:2H$_2$O +4H$^+$ = Th^{4+} +4H$_2$O	Eh gw	$6.9 \cdot 10^{-9}$	ThCO$_3$(OH)$_3^-$ (69%), Th(CO$_3$)$_2$(OH)$_2^{2-}$ (27%)	Stability of the solid phase Uncertain thermodynamic data for aqueous carbonates
		pH$_2$(g)= 10^{-7} atm	$6.9 \cdot 10^{-9}$	ThCO$_3$(OH)$_3^-$ (69%), Th(CO$_3$)$_2$(OH)$_2^{2-}$ (27%)	
		pH$_2$(g)= 10^2 atm	$6.9 \cdot 10^{-9}$	ThCO$_3$(OH)$_3^-$ (69%), Th(CO$_3$)$_2$(OH)$_2^{2-}$ (27%)	
Pa	Pa$_2$O$_5$ + 2H$^+$ = 2PaO$_2^+$ +H$_2$O	Eh gw	$3.1 \cdot 10^{-7}$	PaO$_2$OH(aq) (99.9%)	Lack of thermodynamic data
		pH$_2$(g)= 10^{-7} atm	$3.1 \cdot 10^{-7}$	PaO$_2$OH(aq) (99.9%)	
		pH$_2$(g)= 10^2 atm	$3.1 \cdot 10^{-7}$	PaO$_2$OH(aq) (99.9%)	
U	Ca(UO$_2$)$_2$(SiO$_3$OH)$_2$·5H$_2$O + 6H$^+$= Ca^{2+}+2UO$_2^{2+}$ +2Si(OH)$_4$ +5H$_2$O	Eh gw	$2.7 \cdot 10^{-7}$	UO$_2$(CO$_3$)$_3^{4-}$ (86%), UO$_2$(CO$_3$)$_2^{2-}$ (13%)	Silicate solid precipitation TDB data on solid stability
	UO$_2$·2H$_2$O + 4 H$^+$ = U^{4+} + 4.H$_2$O	pH$_2$(g)= 10^{-7} atm	$8.0 \cdot 10^{-10}$	U(OH)$_4$ (84%), UO$_2$(CO$_3$)$_3^{4-}$ (12%)	
	UO$_2$·2H$_2$O + 4 H$^+$ = U^{4+} + 4.H$_2$O	pH$_2$(g)= 10^2 atm	$6.8 \cdot 10^{-10}$	U(OH)$_4$ (99%),	
Np	NpO$_2$:2H$_2$O(am)+ 4H$^+$ = Np^{4+} +4H$_2$O	Eh gw	$1.2 \cdot 10^{-9}$	Np(OH)$_4$ (64%) NpCO$_3$(OH)$_3^-$ (34%)	Crystallinity of the solid phase
		pH$_2$(g)= 10^{-7} atm	$1.2 \cdot 10^{-9}$	Np(OH)$_4$ (64%) NpCO$_3$(OH)$_3^-$ (34%)	
		pH$_2$(g)= 10^2 atm	$1.2 \cdot 10^{-9}$	Np(OH)$_4$ (64%) NpCO$_3$(OH)$_3^-$ (34%)	
Pu	Pu(OH)$_4$(am) +4H$^+$ = Pu^{4+} +4H$_2$O	Eh gw	$1.5 \cdot 10^{-10}$	Pu(OH)$_4$ (82%), Pu(CO$_3$)$_2^-$ (7%), Pu(OH)$_3^+$(7%)	Reliability of phosphate measurements

Element	Solubility limiting phase and reaction	Redox states	$M(mol \cdot dm^{-3})$	Main complexes formed	Associated uncertainty parameters
	$PuPO_4(s) + 2H^+ = Pu^{3+} + H_2PO_4^-$	$pH_2(g)= 10^{-7}$ atm	$5.1 \cdot 10^{-10}$	$Pu(CO_3)_2^-$ (57%), $PuCO_3^+$(25%), $PuSO_4^+$ (6%)	
	$PuPO_4(s) + 2H^+ = Pu^{3+} + H_2PO_4^-$	$pH_2(g)= 10^2$ atm	$5.1 \cdot 10^{-10}$	$Pu(CO_3)_2^-$ (57%), $PuCO_3^+$ (25%), $PuSO_4^+$ (6%)	
Am/Cm	$AmPO_4:xH_2O(am)$ $AmPO_4 +2H^+ = Am^{3+} + H_2PO_4$	Eh gw	$3.2 \cdot 10^{-9}$	$AmOSi(OH)_3^{2+}$ (80%), $Am(CO_3)_2^-$ (13%), $AmCO_3^+$(6%)	Reliability of phosphate measurements
		$pH_2(g)= 10^{-7}$ atm	$3.2 \cdot 10^{-9}$	$AmOSi(OH)_3^{2+}$ (80%), $Am(CO_3)_2^-$ (13%), $AmCO_3^+$(6%)	
		$pH_2(g)= 10^2$ atm	$3.2 \cdot 10^{-9}$	$AmOSi(OH)_3^{2+}$ (80%), $Am(CO_3)_2^-$ (13%), $AmCO_3^+$(6%)	

Table 5-4. Solubilities for elements of interest. Brine type groundwater (KR12/741/1).

Element	Solubility limiting phase and reaction	Redox states	M(mol·dm^{-3})	Main complexes formed	Associated uncertainty parameters
Cs		Eh gw	n.s.l.	Cs$^+$(80%) CsCl(20%)	
		pH$_2$(g) = 10^{-7} atm	n.s.l.	Cs$^+$(80%) CsCl(20%)	
		pH$_2$(g) = 10^2 atm	n.s.l.	Cs$^+$(80%) CsCl(20%)	
Sr	Strontianite SrCO$_3$ + H$^+$ = Sr^{2+} + HCO$_3^-$	Eh gw	1.6·10^{-2}	Sr^{2+} (100%)	Possibility of coprecipitation with other elements' carbonates SO$_4^{2-}$ to HS$^-$ reduction
		pH$_2$(g) = 10^{-7} atm	1.6·10^{-2}	Sr^{2+} (100%)	
		pH$_2$(g) = 10^2 atm	1.6·10^{-2}	Sr^{2+} (100%)	
Ra	RaSO$_4$(s) = Ra^{2+} + SO$_4^{2-}$	Eh gw	3.0·10^{-5}	Ra^{2+} (80%), RaCl$^+$ (19%)	Possibility of coprecipitation with other elements' carbonates SO$_4^{2-}$ to HS$^-$ reduction
		pH$_2$(g) = 10^{-7} atm	3.0·10^{-5}	Ra^{2+} (80%), RaCl$^+$ (19%)	
		pH$_2$(g) = 10^2 atm	3.0·10^{-5}	Ra^{2+} (80%), RaCl$^+$ (19%)	
Sn	SnO$_2$ (am) + 4H$^+$ = 2 H$_2$O + Sn^{4+}	Eh gw	1.5·10^{-7}	Sn(OH)$_5^-$ (61%), Sn(OH)$_4$ (38%)	
		pH$_2$(g) = 10^{-7} atm	1.5·10^{-7}	Sn(OH)$_5^-$ (61%), Sn(OH)$_4$ (38%)	SO$_4^{2-}$ to HS$^-$ reduction
		pH$_2$(g) = 10^2 atm	1.8·10^{-7}	Sn(OH)$_5^-$ (52%), Sn(OH)$_4$ (33%), Sn(OH)$_2$ (13%)	
Se	FeSe$_2$ + 2 H$^+$ + 2e$^-$ = Fe^{2+} + 2HSe$^-$	Eh gw	6.3·10^{-9}	HSe$^-$ (100%)	Formation of native Se^o SO$_4^{2-}$ to HS$^-$ reduction
	FeSe$_2$ + 2 H$^+$ + 2e$^-$ = Fe^{2+} + 2HSe$^-$	pH$_2$(g) = 10^{-7} atm	2.7·10^{-9}	HSe$^-$ (100%)	Possibility of coprecipitation with

Element	Solubility limiting phase and reaction	Redox states	M(mol·dm^{-3})	Main complexes formed	Associated uncertainty parameters
	$Fe_{1.04}Se + H^+ = 1.04Fe^{2+} + HSe^- + 0.08e^-$	$pH_2(g) = 10^2$ atm	$1.7 \cdot 10^{-5}$	HSe^- (100%)	coprecipitation with sulphides Uncertainty in measured iron concentrations
Zr	$Zr(OH)_4$ (am) $Zr(OH)_4 + 4 H^+ = 4 H_2O + Zr^{4+}$	Eh gw	$1.4 \cdot 10^{-8}$	$Zr(OH)_4$ (100%)	Crystallinity of the solid phase
		$pH_2(g) = 10^{-7}$ atm	$1.4 \cdot 10^{-8}$	$Zr(OH)_4$ (100%)	
		$pH_2(g) = 10^2$ atm	$1.4 \cdot 10^{-8}$	$Zr(OH)_4$ (100%)	
Nb	$Nb_2O_5 + H_2O = 2 NbO_3^- + 2 H^+$	Eh gw	$2.0 \cdot 10^{-4}$	NbO_3^- (95%), $Nb(OH)_5$ (5%)	Scarcity of TDB
		$pH_2(g) = 10^{-7}$ atm	$2.0 \cdot 10^{-4}$	NbO_3^- (95%), $Nb(OH)_5$ (5%)	
		$pH_2(g) = 10^2$ atm	$2.0 \cdot 10^{-4}$	NbO_3^- (95%), $Nb(OH)_5$ (5%)	
Mo	$MoO_2(s) + 2 H_2O = MoO_4^{2-} + 4H^+ + 2e^-$	Eh gw	$1.3 \cdot 10^{-8}$	MoO_4^{2-} (100%)	Scarcity of TDB
		$pH_2(g) = 10^{-7}$ atm	$6.7 \cdot 10^{-8}$	MoO_4^{2-} (100%)	
		$pH_2(g) = 10^2$ atm	$6.7 \cdot 10^{-17}$	MoO_4^{2-} (100%)	
Tc	$TcO_2 \cdot 1.6H_2O = TcO(OH)_2 + 0.6 H_2O$	Eh gw	$4.1 \cdot 10^{-9}$	$TcO(OH)_2$ (100%)	Formation of metallic Tc^o
		$pH_2(g) = 10^{-7}$ atm	$4.1 \cdot 10^{-9}$	$TcO(OH)_2$ (100%)	
		$pH_2(g) = 10^2$ atm	$4.0 \cdot 10^{-9}$	$TcO(OH)_2$ (100%)	
Ni	$Ni(OH)_2(s) + 2 H^+ = Ni^{2+} + 2 H_2O$	Eh gw	$4.4 \cdot 10^{-5}$	Ni^{2+}(70%), $NiCl^+$(26%)	SO_4^{2-} to HS^- reduction
		$pH_2(g) = 10^{-7}$ atm	$4.4 \cdot 10^{-5}$	Ni^{2+}(70%), $NiCl^+$(26%)	
		$pH_2(g) = 10^2$ atm	$4.4 \cdot 10^{-5}$	Ni^{+2}(70%), $NiCl^+$(26%)	
Pd	$Pd(OH)_2(s) + 2 H^+ = 2 H_2O + Pd^{2+}$	Eh gw	$2.4 \cdot 10^{-6}$	$Pd(OH)_2$ (83%), $PdCl_4^{2-}$ (15%)	Formation of metallic Pd^o

Element	Solubility limiting phase and reaction	Redox states	M(mol·dm^{-3})	Main complexes formed	Associated uncertainty parameters
		pH$_2$(g) = 10^{-7} atm	2.4·10^{-6}	Pd(OH)$_2$ (83%), PdCl$_4^{2-}$ (15%)	
		pH$_2$(g) = 10^2 atm	2.4·10^{-6}	Pd(OH)$_2$ (83%), PdCl$_4^{2-}$ (15%)	
Sm	SmPO$_4$(s) +2H$^+$ = H$_2$PO$_4^-$ + Sm^{3+}	Eh gw	1.2·10^{-10}	Sm^{3+} (56%), SmCl^{2+} (22%), SmOH^{2+}(14%) SmCO$_3^+$ (6%)	Reliability of phosphate measurements
		pH$_2$(g) = 10^{-7} atm	1.2·10^{-10}	Sm^{3+} (56%), SmCl^{2+} (22%), SmOH^{2+} (14%) SmCO$_3^+$ (6%)	
		pH$_2$(g) = 10^2 atm	1.2·10^{-10}	Sm^{3+} (56%), SmCl^{2+} (22%), SmOH^{2+} (14%) SmCO$_3^+$ (6%)	
Th	ThO$_2$·2H$_2$O +4H$^+$ = Th^{4+} + 4H$_2$O	Eh gw	7.5·10^{-11}	Th(OH)$_4$ (59%), ThCO$_3$(OH)$_3^-$ (38%)	Stability of the solid phase Uncertain thermodynamic data for aqueous carbonates
		pH$_2$(g) = 10^{-7} atm	7.5·10^{-11}	Th(OH)$_4$ (59%), ThCO$_3$(OH)$_3^-$ (38%)	
		pH$_2$(g) = 10^2 atm	7.5·10^{-11}	Th(OH)$_4$ (59%), ThCO$_3$(OH)$_3^-$ (38%)	
Pa	Pa$_2$O$_5$(s) + 2H$^+$ = 2PaO$_2^+$ + H$_2$O	Eh gw	2.4·10^{-7}	PaO$_2$OH (100%)	Lack of thermodynamic data
		pH$_2$(g) = 10^{-7} atm	2.4·10^{-7}	PaO$_2$OH (100%)	
		pH$_2$(g) = 10^2 atm	2.3·10^{-7}	PaO$_2$OH (100%)	
U	UO$_2$·2H$_2$O + 4H$^+$ = U^{4+} + 4H$_2$O	Eh gw	5.2·10^{-10}	U(OH)$_4$ (100%)	Silicate solid precipitation TDB data on solid stability
		pH$_2$(g) = 10^{-7} atm	5.2·10^{-10}	U(OH)$_4$ (100%)	
		pH$_2$(g) = 10^2 atm	5.1·10^{-10}	U(OH)$_4$ (100%)	
Np	NpO$_2$·2H$_2$O + 4H$^+$ = Np^{4+} + 4H$_2$O	Eh gw	5.7·10^{-10}	Np(OH)$_4$ (99%)	

Element	Solubility limiting phase and reaction	Redox states	M(mol·dm^{-3})	Main complexes formed	Associated uncertainty parameters
		pH$_2$(g) = 10^{-7} atm	5.7·10^{-10}	Np(OH)$_4$ (99%)	Crystallinity of the solid phase
		pH$_2$(g) = 10^2 atm	5.7·10^{-10}	Np(OH)$_4$ (99%)	
Pu	PuPO$_4$(s) + 2H$^+$ = Pu^{3+} + H$_2$PO$_4^-$	Eh gw	2.3·10^{-10}	PuOH^{2+} (60%), Pu^{3+} (23%), Pu(OH)$_4$ (13%)	
		pH$_2$(g) = 10^{-7} atm	2.7·10^{-10}	PuOH^{2+} (51%), Pu^{3+} (20%), Pu(OH)$_4$ (25%)	Reliability of phosphate measurements
		pH$_2$(g) = 10^2 atm	2.0·10^{-10}	PuOH^{2+} (69%), Pu^{3+} (27%)	
Am/Cm	AmPO$_4$·xH$_2$O(am) AmPO$_4$ +2 H$^+$ = Am^{3+} + H$_2$PO$_4^-$	Eh gw	1.2·10^{-8}	AmOSi(OH)$_3^{2+}$ (99%)	
		pH$_2$(g) = 10^{-7} atm	1.2·10^{-8}	AmOSi(OH)$_3^{2+}$ (99%)	Reliability of phosphate measurements
		pH$_2$(g) = 10^2 atm	1.2·10^{-8}	AmOSi(OH)$_3^{2+}$ (99%)	

5.2   Bentonite waters

The following tables summarize the solid phase assumed to control the concentration of the element in question, the concentration limit of this element, the underlying aqueous speciation and the uncertainty parameters associated for bentonite water type and redox state defined.

Table 5-5. *Solubilities for elements of interest. Brackish saline Bentonite water.*

Element	Solubility limiting phase and reaction	Redox states	M (mol·dm^{-3})	Main complexes formed	Associated uncertainty parameters
Cs		Eh gw	n.s.l.	Cs$^+$ (93%), CsCl (7%)	
		pH$_2$(g)=10^{-7} atm	n.s.l.	Cs$^+$ (93%), CsCl (7%)	
		pH$_2$(g)= 10^2 atm	n.s.l.	Cs$^+$ (93%), CsCl (7%)	
Sr	Celestite $SrSO_4 = Sr^{2+} +SO_4^{2-}$	Eh gw	1.9·10^{-4}	Sr^{2+} (79%), SrSO$_4$ (21%)	Possibility of coprecipitation with other elements carbonates SO$_4$$^{2-}$ to HS$^-$ reduction
		pH$_2$(g)=10^{-7} atm	1.9·10^{-4}	Sr^{2+} (79%), SrSO$_4$ (21%)	
		pH$_2$(g)= 10^2 atm	1.9·10^{-4}	Sr^{2+} (79%), SrSO$_4$ (21%)	
Ra	$RaSO_4(s) = Ra^{2+} + SO_4^{2-}$	Eh gw	3.5·10^{-8}	Ra^{2+} (55%), RaSO$_4$(43%)	Possibility of coprecipitation with other elements carbonates SO$_4$$^{2-}$ to HS$^-$ reduction
		pH$_2$(g)=10^{-7} atm	3.5·10^{-8}	Ra^{2+} (55%), RaSO$_4$(43%)	
		pH$_2$(g)= 10^2 atm	3.6·10^{-8}	Ra^{2+} (55%), RaSO$_4$(43%)	
Sn	$SnO_2(am) + 4H^+ = 2 H_2O + Sn^{4+}$	Eh gw	1.2·10^{-7}	Sn(OH)$_4$ (62%), Sn(OH)$_5^-$ (38%)	SO$_4$$^{2-}$ to HS$^-$ reduction
		pH$_2$(g)= 10^{-7} atm	1.2·10^{-7}	Sn(OH)$_4$ (62%), Sn(OH)$_5^-$ (38%)	
		pH$_2$(g)= 10^2 atm	1.5·10^{-7}	Sn(OH)$_4$ (50%), Sn(OH)$_5^-$ (31%), Sn(OH)$_2$ (19%)	
Se	$FeSe_2 + 2H^+ + 2e^- = Fe^{2+} + 2HSe^-$	Eh gw	4.3·10^{-11}	HSe$^-$ (100%)	Effect of iron in water
	$FeSe_2 + 2H^+ + 2e^- = Fe^{2+} + 2HSe^-$	pH$_2$(g)= 10^{-7} atm	1.2·10^{-9}	HSe$^-$ (100%)	Formation of native Se^o

Element	Solubility limiting phase and reaction	Redox states	M (mol·dm^{-3})	Main complexes formed	Associated uncertainty parameters
	$Fe_{1.04}Se + H^+ = 1.04Fe^{2+} + HSe^- + 0.08e^-$	pH$_2$(g)= 10^2 atm	$6.4·10^{-6}$	HSe$^-$ (100%)	Possibility of coprecipitation with sulphides Uncertainty in measured iron concentrations
Zr	$Zr(OH)_4$ (am) $Zr(OH)_4 + 4 H^+ = 4 H_2O + Zr^{4+}$	Eh gw	$1.7·10^{-8}$	$Zr(OH)_4$ (100%)	Crystallinity of the solid phase
		pH$_2$(g)= 10^{-7} atm	$1.7·10^{-8}$	$Zr(OH)_4$ (100%)	
		pH$_2$(g)= 10^2 atm	$1.7·10^{-8}$	$Zr(OH)_4$ (100%)	
Nb	Nb_2O_5(cr) $+ H_2O = 2 NbO_3^- + 2 H^+$	Eh gw	$8.1·10^{-5}$	NbO$_3^-$ (83%), Nb(OH)$_5$ (17%)	Scarcity of TDB
		pH$_2$(g)= 10^{-7} atm	$8.1·10^{-5}$	NbO$_3^-$ (83%), Nb(OH)$_5$ (17%)	
		pH$_2$(g)= 10^2 atm	$8.1·10^{-5}$	NbO$_3^-$ (83%), Nb(OH)$_5$ (17%)	
Mo	$CaMoO_4$ (s) $= MoO_4^{2-} + Ca^{2+}$	Eh gw	$8.9·10^{-6}$	MoO$_4^{2-}$ (100%)	Scarcity of TDB
	MoO_2(s) $+2H_2O = MoO_4^{2-} + 4H^+ +2e^-$	pH$_2$(g)= 10^{-7} atm	$2.0·10^{-8}$	MoO$_4^{2-}$ (100%)	
		pH$_2$(g)= 10^2 atm	-		
Tc	$TcO_2·1.6H_2O = TcO(OH)_2 +0.6 H_2O$	Eh gw	$4.0·10^{-9}$	TcO(OH)$_2$ (99.4%)	Formation of metallic Tc^o
		pH$_2$(g)= 10^{-7} atm	$4.0·10^{-9}$	TcO(OH)$_2$ (99.4%)	
		pH$_2$(g)= 10^2 atm	$4.0·10^{-9}$	TcO(OH)$_2$ (99.4%)	
Ni	$Ni(OH)_2$(s) $+ 2 H^+ = Ni^{2+} + 2 H_2O$	Eh gw	$3.9·10^{-4}$	Ni^{2+} (70%), NiSO$_4$(22%)	SO$_4^{2-}$ to HS$^-$ reduction
		pH$_2$(g)= 10^{-7} atm	$3.9·10^{-4}$	Ni^{2+} (70%), NiSO$_4$(22%)	
		pH$_2$(g)= 10^2 atm	$3.9·10^{-4}$	Ni^{2+} (71%), NiSO$_4$(22%)	
Pd	$Pd(OH)_2$(s) $+ 2 H^+ = 2 H_2O + Pd^{2+}$	Eh gw	$2.5·10^{-6}$	Pd(OH)$_2$ (99.4%)	Formation of metallic Pd^o
		pH$_2$(g)= 10^{-7} atm	$2.5·10^{-6}$	Pd(OH)$_2$ (99.4%)	

Element	Solubility limiting phase and reaction	Redox states	M (mol·dm^{-3})	Main complexes formed	Associated uncertainty parameters
		pH$_2$(g)= 10^2 atm	2.5·10^{-6}	Pd(OH)$_2$ (99.4%)	
Sm	SmOHCO$_3$(s) + H$^+$ = Sm^{3+} + CO$_3{}^{2-}$ + H$_2$O	Eh gw	2.1·10^{-8}	SmSO$_4{}^+$ (35%), Sm^{3+} (29%), Sm(CO$_3$)$^+$ (13%), Sm(CO$_3$)$_2{}^-$ (10%), Sm(SO$_4$)$_2{}^-$ (9%)	Effects of phosphates in water; stability of the solid hydroxo-carbonate
		pH$_2$(g)= 10^{-7} atm	2.1·10^{-8}	SmSO$_4{}^+$ (35%), Sm^{3+} (29%), Sm(CO$_3$)$^+$ (13%), Sm(CO$_3$)$_2{}^-$ (10%), Sm(SO$_4$)$_2{}^-$ (9%)	
		pH$_2$(g)= 10^2 atm	2.1·10^{-8}	SmSO$_4{}^+$ (35%), Sm^{3+} (29%), Sm(CO$_3$)$^+$ (13%), Sm(CO$_3$)$_2{}^-$ (10%), Sm(SO$_4$)$_2{}^-$ (9%)	
Th	ThO$_2$·2H$_2$O +4H$^+$ = Th^{4+} + 4H$_2$O	Eh gw	9.8·10^{-10}	ThCO$_3$(OH)$_3{}^-$ (84%), Th(CO$_3$)$_2$(OH)$_2{}^{-2}$ (8%), Th(OH)$_4$ (5%)	Stability of the solid phase Uncertain thermodynamic data for aqueous carbonates
		pH$_2$(g)= 10^{-7} atm	9.8·10^{-10}	ThCO$_3$(OH)$_3{}^-$ (84%), Th(CO3)$_2$(OH)$_2{}^{-2}$ (8%), Th(OH)$_4$ (5%)	
		pH$_2$(g)= 10^2 atm	9.8·10^{-10}	ThCO$_3$(OH)$_3{}^-$ (84%), Th(CO3)$_2$(OH)$_2{}^{-2}$ (8%), Th(OH)$_4$ (5%)	
Pa	Pa$_2$O$_5$(s) + 2H$^+$ = 2PaO$_2{}^+$ + H$_2$O	Eh gw	2.9·10^{-7}	PaO$_2$OH (100%)	Lack of thermodynamic data
		pH$_2$(g)= 10^{-7} atm	2.9·10^{-7}	PaO$_2$OH (100%)	
		pH$_2$(g)= 10^2 atm	2.9·10^{-7}	PaO$_2$OH (100%)	

Element	Solubility limiting phase and reaction	Redox states	M (mol·dm^{-3})	Main complexes formed	Associated uncertainty parameters
U	$UO_2 \cdot 2H_2O + 4H^+ = U^{4+} + 4H_2O$	Eh gw	$6.7 \cdot 10^{-9}$	$UO_2(CO_3)_3^{4-}$ (80%), $UO_2(CO_3)_2^{2-}$ (7%), $U(OH)_4$ (10%)	Silicate solid precipitation TDB data on solid stability
		$pH_2(g)= 10^{-7}$ atm	$6.5 \cdot 10^{-10}$	$U(OH)_4$ (99.4%)	
		$pH_2(g)= 10^2$ atm	$6.3 \cdot 10^{-10}$	$U(OH)_4$ (99.4%)	
Np	$NpO_2 \cdot 2H_2O + 4H^+ = Np^{4+} + 4H_2O$	Eh gw	$7.8 \cdot 10^{-10}$	$Np(OH)_4$ (90%), $NpCO_3(OH)_3^-$ (9%)	Crystallinity of the solid phase
		$pH_2(g)= 10^{-7}$ atm	$7.8 \cdot 10^{-10}$	$Np(OH)_4$ (90%), $NpCO_3(OH)_3^-$ (9%)	
		$pH_2(g)= 10^2$ atm	$7.8 \cdot 10^{-10}$	$Np(OH)_4$ (90%), $NpCO_3(OH)_3^-$ (9%)	
Pu	$Pu(OH)_4(am) + 4H^+ = Pu^{4+} + 4H_2O$	Eh gw	$8.0 \cdot 10^{-10}$	$PuSO_4^+$ (41%), $Pu(SO_4)_2^-$ (15%), Pu^{3+} (13%), $PuOH^{2+}$ (8%), $PuCO_3^+$ (5%), $Pu(OH)_4$ (15%)	Effect of phosphates in water; stability of the solid hydroxo-carbonate; SO_4^{2-} to HS^- reduction
	$Pu(OH)_4(am) + 4H^+ = Pu^{4+} + 4H_2O$	$pH_2(g)= 10^{-7}$ atm	$1.8 \cdot 10^{-8}$	$PuSO_4^+$ (48%), $Pu(SO_4)_2^{2-}$ (18%), Pu^{3+} (16%), $PuOH^{2+}$ (9%), $PuCO_3^+$ (5%)	
	$PuCO_3OH(s) +H^+ = Pu^{3+} + H_2O + CO_3^{2-}$	$pH_2(g)= 10^2$ atm	$3.4 \cdot 10^{-6}$	$PuSO_4^+$ (48%), $Pu(SO_4)_2^{2-}$ (17%), Pu^{3+} (16%), $PuOH^{2+}$ (10%), $PuCO_3^+$ (6%)	
Am/Cm	$Am(CO_3)_2Na \cdot 5H_2O = Am^{3+} + 2CO_3^{2-} + 5H_2O + Na^+$	Eh gw	$4.5 \cdot 10^{-7}$	Am^{3+} (29%), $AmSO_4$ (23%), $AmCO_3^+$ (22%), $Am(CO_3)_2^-$ (13%), $AmOH^{2+}$ (9%)	Effect of phosphates in water;(there is no phosphate defined in

Element	Solubility limiting phase and reaction	Redox states	M (mol·dm^{-3})	Main complexes formed	Associated uncertainty parameters
		$pH_2(g)= 10^{-7}$ atm	$4.5 \cdot 10^{-7}$	Am^{3+} (29%), AmSO$_4$ (23%), AmCO$_3^+$ (22%), Am(CO$_3$)$_2^-$ (13%), AmOH^{2+} (9%)	phosphate defined in this water, but the Am speciation would change in case of having phosphates, as in the case of Sm) Stability of the solid hydroxo-carbonate
		$pH_2(g)= 10^{2}$ atm	$4.5 \cdot 10^{-7}$	Am^{3+} (29%), AmSO$_4$ (23%), AmCO$_3^+$ (22%), Am(CO$_3$)$_2^-$ (13%), AmOH^{2+} (9%)	

Table 5-6. *Solubilities for elements of interest. Saline type bentonite water.*

Element	Solubility limiting phase and reaction	Redox states	M(mol·dm^{-3})	Main complexes formed	Associated uncertainty parameters
Cs		Eh gw	n.s.l.	Cs$^+$ (88%), CsCl (12%)	
		pH$_2$(g)= 10^{-7} atm	n.s.l.	Cs$^+$ (88%), CsCl (12%)	
		pH$_2$(g)= 10^2 atm	n.s.l.	Cs$^+$ (88%), CsCl (12%)	
Sr	Celestite $SrSO_4 = Sr^{2+} + SO_4^{2-}$	Eh gw	3.6·10^{-4}	Sr^{2+} (89%), SrSO$_4$ (11%)	Possibility of coprecipitation with other elements carbonates SO$_4^{2-}$ to HS$^-$ reduction
		pH$_2$(g)= 10^{-7} atm	3.6·10^{-4}	Sr^{2+} (89%), SrSO$_4$ (11%)	
		pH$_2$(g)= 10^{-7} atm	3.7·10^{-4}	Sr^{2+} (90%), SrSO$_4$ (10%)	
Ra	$RaSO_4(s) = Ra^{2+} + SO_4^{2-}$	Eh gw	5.9·10^{-8}	Ra^{2+} (69%), RaSO$_4$(25%), RaCl$^+$(6%)	Possibility of coprecipitation with other elements' carbonates SO$_4^{2-}$ to HS$^-$ reduction
		pH$_2$(g)= 10^{-7} atm	5.9·10^{-8}	Ra^{2+} (69%), RaSO$_4$(25%), RaCl$^+$(6%)	
		pH$_2$(g)= 10^2 atm	6.0·10^{-8}	Ra^{2+} (69%), RaSO$_4$(24%), RaCl$^+$(6%)	
Sn	SnO_2 (am) + 4H$^+$ = 2 H$_2$O + Sn^{4+}	Eh gw	1.0·10^{-7}	Sn(OH)$_4$ (69%), Sn(OH)$_5^-$ (31%)	SO$_4^{2-}$ to HS$^-$ reduction
		pH$_2$(g)= 10^{-7} atm	1.0·10^{-7}	Sn(OH)$_4$ (69%), Sn(OH)$_5^-$ (31%)	
		pH$_2$(g)= 10^2 atm	1.3·10^{-7}	Sn(OH)$_4$ (55%), Sn(OH)$_5^-$ (24%), Sn(OH)$_2$ (21%)	
Se	FeSe$_2$ + 2H$^+$ + 2e$^-$ = Fe^{2+} + 2HSe$^-$	Eh gw	3.0·10^{-11}	HSe$^-$ (100%)	Effect of iron in water Formation of native Se^o
	FeSe$_2$ + 2H$^+$ + 2e$^-$ = Fe^{2+} + 2HSe$^-$	pH$_2$(g)= 10^{-7} atm	8.8·10^{-10}	HSe$^-$ (100%)	Possibility of coprecipitation with

Element	Solubility limiting phase and reaction	Redox states	$M(mol \cdot dm^{-3})$	Main complexes formed	Associated uncertainty parameters
	$Fe_{1.04}Se + H^+ = 1.04Fe^{2+} + HSe^- + 0.08e^-$	$pH_2(g) = 10^2$ atm	$5.2 \cdot 10^{-6}$	HSe^- (100%)	sulphides Uncertainty in measured iron concentrations
Zr	$Zr(OH)_4$ (am) $Zr(OH)_4 + 4 H^+ = 4 H_2O + Zr^{4+}$	Eh gw	$1.6 \cdot 10^{-8}$	$Zr(OH)_4$ (100%)	Crystallinity of the solid phase
		$pH_2(g) = 10^{-7}$ atm	$1.6 \cdot 10^{-8}$	$Zr(OH)_4$ (100%)	
		$pH_2(g) = 10^2$ atm	$1.6 \cdot 10^{-8}$	$Zr(OH)_4$ (100%)	
Nb	$Nb_2O_5 + H_2O = 2 NbO_3^- + 2 H^+$	Eh gw	$6.2 \cdot 10^{-5}$	NbO_3^- (80%), $Nb(OH)_5$ (20%)	Scarcity of TDB
		$pH_2(g) = 10^{-7}$ atm	$6.2 \cdot 10^{-5}$	NbO_3^- (80%), $Nb(OH)_5$ (20%)	
		$pH_2(g) = 10^2$ atm	$6.2 \cdot 10^{-5}$	NbO_3^- (80%), $Nb(OH)_5$ (20%)	
Mo	$CaMoO_4 (s) = MoO_4^{2-} + Ca^{2+}$	Eh gw	$4.1 \cdot 10^{-6}$	MoO_4^{2-} (100%)	Scarcity of TDB
	$MoO_2 + 2 H_2O = MoO_4^{2-} + 4 H^+ + 2 e^-$	$pH_2(g) = 10^{-7}$ atm	$9.2 \cdot 10^{-9}$	MoO_4^{2-} (100%)	
		$pH_2(g) = 10^2$ atm	-		
Tc	$TcO_2 \cdot 1.6H_2O = TcO(OH)_2 + 0.6 H_2O$	Eh gw	$4.0 \cdot 10^{-9}$	$TcO(OH)_2$ (100%)	Formation of metallic Tc^o
		$pH_2(g) = 10^{-7}$ atm	$4.0 \cdot 10^{-9}$	$TcO(OH)_2$ (100%)	
		$pH_2(g) = 10^2$ atm	$4.0 \cdot 10^{-9}$	$TcO(OH)_2$ (100%)	
Ni	$Ni(OH)_2 + 2 H^+ = Ni^{2+} + 2 H_2O$	Eh gw	$7.4 \cdot 10^{-4}$	Ni^{2+} (79%), $NiSO_4$(11%), $NiCl^+$(10%)	SO_4^{2-} to HS^- reduction
		$pH_2(g) = 10^{-7}$ atm	$7.4 \cdot 10^{-4}$	Ni^{2+} (79%), $NiSO_4$(11%), $NiCl^+$(10%)	
		$pH_2(g) = 10^2$ atm	$7.4 \cdot 10^{-4}$	Ni^{2+} (79%), $NiSO_4$(11%), $NiCl^+$(10%)	
Pd	$Pd(OH)_2 + 2 H^+ = 2 H_2O + Pd^{2+}$	Eh gw	$2.8 \cdot 10^{-6}$	$Pd(OH)_2$ (87%), $PdCl_4^{2-}$(13%)	Formation of metallic Pd^o

Element	Solubility limiting phase and reaction	Redox states	$M(\text{mol} \cdot \text{dm}^{-3})$	Main complexes formed	Associated uncertainty parameters
		$pH_2(g)= 10^{-7}$ atm	$2.8 \cdot 10^{-6}$	$Pd(OH)_2$ (87%), $PdCl_4^{2-}$(13%)	
		$pH_2(g)= 10^{2}$ atm	$2.8 \cdot 10^{-6}$	$Pd(OH)_2$ (87%), $PdCl_4^{2-}$(13%)	
Sm	$SmOHCO_3 + H^+ = Sm^{3+} + CO_3^{2-} + H_2O$	Eh gw	$3.8 \cdot 10^{-8}$	Sm^{3+} (48%), $SmSO_4^+$ (28%), $SmCO_3^+$ (10%)	Effects of phosphates in water; stability of the solid hydroxo-carbonate
		$pH_2(g)= 10^{-7}$ atm	$3.8 \cdot 10^{-8}$	Sm^{3+} (48%), $SmSO_4^+$ (28%), $SmCO_3^+$ (10%)	
		$pH_2(g)= 10^{2}$ atm	$3.8 \cdot 10^{-8}$	Sm^{3+} (48%), $SmSO_4^+$ (28%), $SmCO_3^+$ (10%)	
Th	$ThO_2 \cdot 2H_2O$ (am) $+ 4 H^+ = Th^{4+} + 4 H_2O$	Eh gw	$6.8 \cdot 10^{-10}$	$ThCO_3(OH)_3^-$ (84%), $Th(OH)_4$ (8%), $Th(CO_3)_2(OH)_2^{2-}$ (5%)	Stability of the solid phase Uncertain thermodynamic data for aqueous carbonates
		$pH_2(g)= 10^{-7}$ atm	$6.8 \cdot 10^{-10}$	$ThCO_3(OH)_3^-$ (84%), $Th(OH)_4$ (8%), $Th(CO3)_2(OH)_2^{2-}$ (5%)	
		$pH_2(g)= 10^{2}$ atm	$6.8 \cdot 10^{-10}$	$ThCO_3(OH)_3^-$ (84%), $Th(OH)_4$ (8%), $Th(CO_3)_2(OH)_2^{2-}$ (5%)	
Pa	Pa_2O_5 (s) $+ 2 H^+ = 2 PaO_2^+ + H_2O$	Eh gw	$2.8 \cdot 10^{-7}$	PaO_2OH (100%)	Lack of thermodynamic data
		$pH_2(g)= 10^{-7}$ atm	$2.8 \cdot 10^{-7}$	PaO_2OH (100%)	
		$pH_2(g)= 10^{2}$ atm	$2.8 \cdot 10^{-7}$	PaO_2OH (100%)	
U	$UO_2 \cdot 2H_2O + 4 H^+ = U^{4+} + 4.H_2O$	Eh gw	$2.5 \cdot 10^{-9}$	$UO_2(CO_3)_3^{4-}$ (51%), $U(OH)_4$ (25%), UO_2^+ (14%), $UO_2(CO_3)_2^{2-}$ (9%)	Silicate solid precipitation TDB data on solid stability
		$pH_2(g)= 10^{-7}$ atm	$6.2 \cdot 10^{-10}$	$U(OH)_4$ (97%)	
		$pH_2(g)= 10^{-7}$ atm	$6.1 \cdot 10^{-10}$	$U(OH)_4$ (99%)	

Element	Solubility limiting phase and reaction	Redox states	$M(mol \cdot dm^{-3})$	Main complexes formed	Associated uncertainty parameters
Np	$NpO_2 \cdot 2H_2O(am) + 4\ H^+ = Np^{4+} + 4\ H_2O$	Eh gw	$7.2 \cdot 10^{-10}$	$Np(OH)_4$ (92%), $NpCO_3(OH)_3^-$ (6%)	Crystallinity of the solid phase
		$pH_2(g) = 10^{-7}$ atm	$7.2 \cdot 10^{-10}$	$Np(OH)_4$ (92%), $NpCO_3(OH)_3^-$ (6%)	
		$pH_2(g) = 10^{-7}$ atm	$7.2 \cdot 10^{-10}$	$Np(OH)_4$ (92%), $NpCO_3(OH)_3^-$ (6%)	
Pu	$Pu(OH)_4\ (am) + 4\ H^+ = Pu^{4+} + 4\ H_2O$	Eh gw	$1.0 \cdot 10^{-9}$	$PuSO_4^+$ (40%), Pu^{3+} (27%), $PuOH^{2+}$ (12%), $Pu(OH)_4$ (10%) $Pu(SO4)_2^-$ (7%), $PuCO_3^+$ (5%)	Effect of phosphates in water; stability of the solid hydroxo-carbonate; SO_4^{2-} to HS^- reduction
	$Pu(OH)_4\ (am) + 4\ H^+ = Pu^{4+} + 4\ H_2O$	$pH_2(g) = 10^{-7}$ atm	$2.9 \cdot 10^{-8}$	$PuSO_4^+$ (44%), Pu^{3+} (30%), $PuOH^{2+}$ (12%), $Pu(SO4)_2^-$ (7%), $PuCO_3^+$ (5%)	
	$PuCO_3OH + H^+ = Pu^{3+} + H_2O + CO_3^{2-}$	$pH_2(g) = 10^2$ atm	$5.4 \cdot 10^{-6}$	$PuSO_4^+$ (44%), Pu^{3+} (30%), $PuOH^{2+}$ (12%), $Pu(SO4)_2^-$ (7%), $PuCO_3^+$ (5%)	
Am/Cm	$Am(CO_3)_2Na \cdot 5H2O = Am^{3+} + 2\ CO_3^{2-} + 5\ H_2O + Na^+$	Eh	$9.2 \cdot 10^{-7}$	Am^{3+}, $AmSO_4$ (17%), $AmCO_3^+$ (17%), $AmOH^{2+}$ (9%)	Effect of phosphates in water; Stability of the solid hydroxo-carbonate
		$pH_2(g) = 10^{-7}$ atm	$9.2 \cdot 10^{-7}$	Am^{3+}, $AmSO_4$ (17%), $AmCO_3^+$ (17%), $AmOH^{2+}$ (9%)	
		$pH_2(g) = 10^2$ atm	$9.2 \cdot 10^{-7}$	Am^{3+}, $AmSO_4$ (17%), $AmCO_3^+$ (17%), $AmOH^{2+}$ (9%)	

Table 5-7. *Solubilities for elements of interest. Dilute brackish Bentonite water.*

Element	Solubility limiting phase and reaction	Redox states	M (mol·dm^{-3})	Main complexes formed	Associated uncertainty
Cs		Eh gw	n.s.l.	Cs^+(100%)	
		pH$_2$(g)= 10^{-7} atm	n.s.l.	Cs^+(100%)	
		pH$_2$(g)= 10^2 atm	n.s.l.	Cs^+(100%)	
Sr	Celestite $SrSO_4 = Sr^{2+} + SO4^{2-}$	Eh gw	9.1·10^{-5}	Sr^{2+}(55%), $SrSO_4$ (45%)	Possibility of coprecipitation with other elements' carbonates SO_4^{2-} to HS$^-$ reduction
		pH$_2$(g)= 10^{-7} atm	9.1·10^{-5}	Sr^{2+}(55%), $SrSO_4$ (45%)	
		pH$_2$(g)= 10^2 atm	9.3·10^{-5}	Sr^{2+}(56%), $SrSO_4$ (44%)	
Ra	$RaSO_4(s) = Ra^{2+} + SO_4^{2-}$	Eh gw	2.2·10^{-8}	$RaSO_4$(71%), Ra^{2+}(29%)	Possibility of coprecipitation with other elements' carbonates SO_4^{2-} to HS$^-$ reduction
		pH$_2$(g)= 10^{-7} atm	2.2·10^{-8}	$RaSO_4$(71%), Ra^{2+}(29%)	
		pH$_2$(g)= 10^2 atm	2.2·10^{-8}	$RaSO_4$(71%), Ra^{2+}(29%)	
Sn	SnO_2 (am) + 4H$^+$ = 2 H$_2$O + Sn^{4+}	Eh gw	9.6·10^{-8}	$Sn(OH)_4$(82%), $Sn(OH)_5^-$ (18%)	SO_4^{2-} to HS$^-$ reduction
		pH$_2$(g)= 10^{-7} atm	9.6·10^{-8}	$Sn(OH)_4$(82%), $Sn(OH)_5^-$ (18%)	
		pH$_2$(g)= 10^2 atm	1.2·10^{-7}	$Sn(OH)_4$(61%), $Sn(OH)_2$ (25%), $Sn(OH)_5^-$ (14%)	
Se	$FeSe_2 + 2H^+ + 2e^- = Fe^{2+} + 2HSe^-$	Eh gw	1.0·10^{-10}	HSe^- (100%)	Effect of iron in water Formation of native Se^o
	$FeSe_2 + 2H^+ + 2e^- = Fe^{2+} + 2HSe^-$	pH$_2$(g)= 10^{-7} atm	3.1·10^{-10}	HSe^- (100%)	Possibility of coprecipitation with sulphides
	$Fe_{1.04}Se + H^+ = 1.04Fe^{2+} + HSe^- + 0.08e^-$	pH$_2$(g)= 10^2 atm	1.2·10^{-6}	HSe^- (100%)	Uncertainty in measured iron concentrations
Zr	$Zr(OH)_4$ (aged)	pH$_2$(g)= 10^2 atm	1.7·10^{-8}	$Zr(OH)_4$ (100%)	Crystallinity of the solid

Element	Solubility limiting phase and reaction	Redox states	M (mol·dm^{-3})	Main complexes formed	Associated uncertainty
	$Zr(OH)_4 +4H^+ = 4H_2O +Zr^{4+}$	$pH_2(g)= 10^{-7}$ atm	$1.7 \cdot 10^{-8}$	$Zr(OH)_4$ (100%)	phase
		$pH_2(g)= 10^2$ atm	$1.7 \cdot 10^{-8}$	$Zr(OH)_4$ (100%)	
Nb	$Nb_2O_5 + H_2O = 2NbO_3^- +2H^+$	Eh gw	$3.8 \cdot 10^{-5}$	NbO_3^- (63%), $Nb(OH)_5$ (37%)	Scarcity of TDB
		$pH_2(g)= 10^{-7}$ atm	$3.8 \cdot 10^{-5}$	NbO_3^- (63%), $Nb(OH)_5$ (37%)	
		$pH_2(g)= 10^2$ atm	$3.8 \cdot 10^{-5}$	NbO_3^- (63%), $Nb(OH)_5$ (37%)	
Mo	$MoO_2 + 2 H_2O = MoO_4^{2-} + 4 H^+ + 2 e^-$	Eh gw	$2.4 \cdot 10^{-8}$	MoO_4^{2-} (100%)	Scarcity of TDB
		$pH_2(g)= 10^{-7}$ atm	$2.6 \cdot 10^{-9}$	MoO_4^{2-} (100%)	
		$pH_2(g)= 10^2$ atm	-		
Tc	$TcO_2 \cdot 1.6H_2O = TcO(OH)_2 +0.6 H_2O$	Eh gw	$4.2 \cdot 10^{-9}$	$TcO(OH)_2$ (99.9%)	Formation of metallic Tc°
		$pH_2(g)= 10^{-7}$ atm	$4.2 \cdot 10^{-9}$	$TcO(OH)_2$ (99.9%)	
		$pH_2(g)= 10^2$ atm	$4.2 \cdot 10^{-9}$	$TcO(OH)_2$ (99.9%)	
Ni	$Ni(OH)_2 + 2 H^+ = Ni^{2+} + 2 H_2O$	Eh gw	$4.3 \cdot 10^{-3}$	Ni^{2+}, $NiSO_4$ (43%), $Ni(SO_4)_2^{2-}$ (11%)	SO_4^{2-} to HS^- reduction
		$pH_2(g)= 10^{-7}$ atm	$4.3 \cdot 10^{-3}$	Ni^{2+}, $NiSO_4$ (43%), $Ni(SO_4)_2^{2-}$ (11%)	
		$pH_2(g)= 10^2$ atm	$4.1 \cdot 10^{-3}$	Ni^{2+} (47%), $NiSO_4$ (42%), $Ni(SO_4)_2^{2-}$ (11%)	
Pd	$Pd(OH)_2 + 2 H^+ = 2 H_2O + Pd^{2+}$	Eh gw	$2.5 \cdot 10^{-6}$	$Pd(OH)_2$ (100%)	Formation of metallic Pd°
		$pH_2(g)= 10^{-7}$ atm	$2.5 \cdot 10^{-6}$	$Pd(OH)_2$ (100%)	
		$pH_2(g)= 10^2$ atm	$2.5 \cdot 10^{-6}$	$Pd(OH)_2$ (100%)	
Sm	$SmOHCO_3 + H^+ = Sm^{3+} + CO_3^{2-} + H_2O$	Eh gw	$7.5 \cdot 10^{-8}$	$SmSO_4^+$ (39%), $Sm(SO_4)_2^-$ (28%), $Sm(CO_3)_2^-$ (14%), Sm^{3+} (10%), $SmCO_3^+$ (9%)	Effects of phosphates in water; stability of the solid hydroxo-carbonate
		$pH_2(g)= 10^{-7}$ atm	$7.5 \cdot 10^{-8}$	$SmSO_4^+$ (39%), $Sm(SO_4)_2^-$ (28%), $Sm(CO_3)_2^-$ (14%), Sm^{3+} (10%), $SmCO_3^+$ (9%)	

Element	Solubility limiting phase and reaction	Redox states	M (mol·dm^{-3})	Main complexes formed	Associated uncertainty
		pH$_2$(g)= 10^2 atm	7.2·10^{-8}	SmSO$_4^+$ (39%), Sm(SO$_4$)$_2^-$ (26%), Sm(CO$_3$)$_2^-$ (14%), Sm^{3+} (10%), SmCO$_3^+$ (9%)	
Th	ThO$_2$·2H$_2$O (am) + 4 H$^+$ = Th^{4+} + 4 H$_2$O	Eh gw	6.3·10^{-9}	ThCO$_3$(OH)$_3^-$ (65%), Th(CO$_3$)$_2$(OH)$_2^{2-}$ (30%)	Stability of the solid phase Uncertain thermodynamic data for aqueous carbonates
		pH$_2$(g)= 10^{-7} atm	6.3·10^{-9}	ThCO$_3$(OH)$_3^-$ (65%), Th(CO$_3$)$_2$(OH)$_2^{2-}$ (30%)	
		pH$_2$(g)= 10^2 atm	6.3·10^{-9}	ThCO$_3$(OH)$_3^-$ (65%), Th(CO$_3$)$_2$(OH)$_2^{2-}$ (30%)	
Pa	Pa$_2$O$_5$ (s) + 2 H$^+$ = 2 PaO$_2^+$ + H$_2$O	Eh gw	3.0·10^{-7}	PaO$_2$OH (100%)	Lack of thermodynamic data
		pH$_2$(g)= 10^{-7} atm	3.0·10^{-7}	PaO$_2$OH (100%)	
		pH$_2$(g)= 10^2 atm	3.0·10^{-7}	PaO$_2$OH (100%)	
U	UO$_2$·2H$_2$O + 4 H+ = U^{4+} + 4H$_2$O	Eh gw	3.3·10^{-9}	UO$_2$(CO$_3$)$_3^{4-}$ (78%), U(OH)$_4$ (19%),	Silicate solid precipitation TDB data on solid stability
		pH$_2$(g)= 10^{-7} atm	9.5·10^{-10}	U(OH)$_4$ (69%), UO$_2$(CO$_3$)$_3^{4-}$ (30%)	
		pH$_2$(g)= 10^2 atm	6.6·10^{-10}	U(OH)$_4$ (96%)	
Np	NpO$_2$·2H$_2$O(am) + 4 H$^+$ = Np^{4+} + 4 H$_2$O	Eh gw	1.1·10^{-9}	Np(OH)$_4$ (66%), NpCO$_3$(OH)$_3^-$ (32%)	Crystallinity of the solid phase
		pH$_2$(g)= 10^{-7} atm	1.1·10^{-9}	Np(OH)$_4$ (66%), NpCO$_3$(OH)$_3^-$ (32%)	
		pH$_2$(g)= 10^2 atm	1.1·10^{-9}	Np(OH)$_4$ (66%), NpCO$_3$(OH)$_3^-$ (32%)	
Pu	Pu(OH)$_4$ (am) +4 H$^+$ = Pu^{4+} + 4 H$_2$O	Eh gw	3.7·10^{-7}	Pu(SO$_4$)$_2^-$ (45%), PuSO$_4^+$ (42%)	Effect of phosphates in water; stability of the solid

Element	Solubility limiting phase and reaction	Redox states	M (mol·dm^{-3})	Main complexes formed	Associated uncertainty
	$Pu(OH)_4$ (am) $+4\ H^+ = Pu^{4+} + 4\ H_2O$	$pH_2(g)= 10^{-7}$ atm	$1.1 \cdot 10^{-6}$	$Pu(SO_4)_2^-$ (45%), $PuSO_4^+$ (42%)	water; stability of the solid hydroxo-carbonate; SO_4^{2-} to HS^- reduction
	$PuCO_3OH + H^+ = Pu^{3+} + H_2O + CO_3^{2-}$	$pH_2(g)= 10^2$ atm	$1.5 \cdot 10^{-5}$	$Pu(SO_4)_2^-$ (45%), $PuSO_4^+$ (42%)	
Am	$Am(CO_3)_2Na \cdot 5H_2O = Am^{3+} + 2\ CO_3^{2-} + 5\ H_2O + Na^+$	Eh gw	$4.0 \cdot 10^{-7}$	$AmSO_4$ (33%), $Am(CO_3)_2^-$ (23%), $AmCO_3^+$ (21%), Am^{3+} (13%)	Effect of phosphates in water; Stability of the solid hydroxo-carbonate
		$pH_2(g)= 10^{-7}$ atm	$4.0 \cdot 10^{-7}$	$AmSO_4$ (33%), $Am(CO_3)_2^-$ (23%), $AmCO_3^+$ (21%), Am^{3+} (13%)	
		$pH_2(g)= 10^2$ atm	$4.0 \cdot 10^{-7}$	$AmSO_4$ (33%), $Am(CO_3)_2^-$ (23%), $AmCO_3^+$ (21%), Am^{3+} (13%)	

5.3   Glacial meltwater and Ice-melting groundwater

The following tables summarize the solid phase assumed to control the concentration of the element in question, the concentration limit of this element, the underlying aqueous speciation and the uncertainty parameters associated for both glacial water types and redox state defined.

Table 5-8 *Solubilities for elements of interest. Glacial meltwater.*

Element	Solubility limiting phase and reaction	Redox states	M(mol·dm^{-3})	Main complexes formed	Associated uncertainty parameters
Cs		Eh gw	n.s.l.	Cs$^+$ (100%)	
		pH$_2$(g) = 10^{-7} atm	n.s.l.	Cs$^+$ (100%)	
Sr		Eh gw	n.s.l	Sr^{+2} (100%)	
		pH$_2$(g) = 10^{-7} atm	n.s.l	Sr^{+2} (100%)	
Ra	(*)RaSO$_4$(s) = Ra^{2+} + SO$_4^{2-}$	Eh gw	2.0·10^{-4}	Ra^{2+} (100%)	Possibility of coprecipitation with other elements' carbonates SO$_4^{2-}$ to HS$^-$ reduction
		pH$_2$(g) = 10^{-7} atm	7.1·10^{-5}	Ra^{2+} (100%)	
Sn	SnO$_2$ (am) + 4H$^+$ = 2 H$_2$O + Sn^{4+}	Eh gw	8.4·10^{-8}	Sn(OH)$_4$ (99%)	SO$_4^{2-}$ to HS$^-$ reduction
		pH$_2$(g) = 10^{-7} atm	8.4·10^{-8}	Sn(OH)$_4$ (99%)	
Se		Eh gw	n.s.l.	HSeO$_3^-$ (100%)	Formation of native Se^o SO$_4^{2-}$ to HS$^-$ reduction Possibility of coprecipitation with sulphides Uncertainty in measured iron concentrations
	FeSe$_2$ + 2 H$^+$ + 2 e$^-$ = Fe^{2+} + 2HSe$^-$	pH$_2$(g) = 10^{-7} atm	1.5·10^{-8}	HSe$^-$ (99%)	
Zr	Zr(OH)$_4$ (am) Zr(OH)$_4$ + 4 H$^+$ = 4 H$_2$O + Zr^{4+}	Eh gw	1.8·10^{-8}	Zr(OH)$_4$ (100%)	Crystallinity of the solid phase
		pH$_2$(g) = 10^{-7} atm	1.8·10^{-8}	Zr(OH)$_4$ (100%)	
Nb	(*)Nb$_2$O$_5$ + H$_2$O = 2 NbO$_3^-$ + 2 H$^+$	Eh gw	1.5·10^{-5}	Nb(OH)$_5$ (97%)	Scarcity of TDB
		pH$_2$(g) = 10^{-7} atm	1.5·10^{-5}	Nb(OH)$_5$ (97%)	

Element	Solubility limiting phase and reaction	Redox states	$M(mol \cdot dm^{-3})$	Main complexes formed	Associated uncertainty parameters
Mo		Eh gw	n.s.l	MoO_4^{2-} (99%)	Scarcity of TDB
	$MoO_2(s) + 2\ H_2O = MoO_4^{2-} + 4H^+ + 2e^-$	$pH_2(g) = 10^{-7}$ atm	$5.6 \cdot 10^{-13}$	MoO_4^{2-} (99%)	
Tc		Eh gw	n.s.l.	TcO_4^- (100%)	Formation of metallic Tc^o
	$TcO_2 \cdot 1.6H_2O = TcO(OH)_2 + 0.6\ H_2O$	$pH_2(g) = 10^{-7}$ atm	$4.0 \cdot 10^{-9}$	$TcO(OH)_2$ (100%)	
Ni		Eh gw	n.s.l	Ni^{2-} (100%)	
		$pH_2(g) = 10^{-7}$ atm	n.s.l	Ni^{2-} (100%)	
Pd	$Pd(OH)_2(s) + 2\ H^+ = 2\ H_2O + Pd^{2+}$	Eh gw	$2.7 \cdot 10^{-6}$	$Pd(OH)_2$ (100%)	Formation of metallic Pd^o
		$pH_2(g) = 10^{-7}$ atm	$2.7 \cdot 10^{-6}$	$Pd(OH)_2$ (100%)	
Sm	$SmPO_4(s) + 2H^+ = H_2PO_4^- + Sm^{3+}$	Eh gw	$1.0 \cdot 10^{-8}$	Sm^{3+} (100%)	Reliability of phosphate measurements
		$pH_2(g) = 10^{-7}$ atm	$1.0 \cdot 10^{-8}$	Sm^{3+} (100%)	
Th	$ThO_2 \cdot 2H_2O + 4H^+ = Th^{4+} + 4H_2O$	Eh gw	$6.4 \cdot 10^{-10}$	$Th(OH)_3^+$ (72%), $Th(OH)_2^{2+}$ (18%), $Th(OH)_4$ (9%)	Stability of the solid phase Uncertain thermodynamic data for aqueous carbonates
		$pH_2(g) = 10^{-7}$ atm	$6.4 \cdot 10^{-10}$	$Th(OH)_3^+$ (72%), $Th(OH)_2^{2+}$ (18%), $Th(OH)_4$ (9%)	
Pa	$Pa_2O_5(s) + 2H^+ = 2PaO_2^+ + H_2O$	Eh gw	$3.3 \cdot 10^{-7}$	PaO_2OH (95%), PaO_2^+ (5%)	Lack of thermodynamic data
		$pH_2(g) = 10^{-7}$ atm	$3.3 \cdot 10^{-7}$	PaO_2OH (95%), PaO_2^+ (5%)	

Element	Solubility limiting phase and reaction	Redox states	$M (\text{mol·dm}^{-3})$	Main complexes formed	Associated uncertainty parameters
U	Becquerelite $Ca(UO_2)_6O_4(OH)_6·8H_2O + 14H^+ = Ca^{+2} + UO_2^{2+} + 18H_2O$	Eh gw	$1.3·10^{-7}$	UO_2OH^+ (60%), UO_2^{2-} (31%)	Silicate solid precipitation TDB data on solid stability
	$UO_2·2H_2O + 4H^+ = U^{4+} + 4H_2O$	$pH_2(g) = 10^{-7}$ atm	$1.6·10^{-9}$	$U(OH)_4$ (42%), UO_2^+ (40%), $U(OH)_3^+$ (20%)	
Np		Eh gw	n.s.l	NpO_2^+ (100%)	Crystallinity of the solid phase
	$NpO_2·2H_2O + 4H^+ = Np^{4+} + 4H_2O$	$pH_2(g) = 10^{-7}$ atm	$1.3·10^{-9}$	$Np(OH)_4$ (58%), $Np(OH)_3^+$ (42%)	
Pu	(*)$PuO_2(OH)_2·H_2O + 2 H^+ = PuO_2^{2+} + 3H_2O$	Eh gw	$1.6·10^{-5}$	PuO_2^+ (69%), PuO_2^{2+} (17%), PuO_2OH^+ (15%)	Reliability of phosphate measurements
	$PuPO_4 + 2H^+ = Pu^{3+} + H_2PO_4^-$	$pH_2(g) = 10^{-7}$ atm	$8.3·10^{-9}$	Pu^{3+} (97%)	
Am/Cm	$AmPO_4·xH_2O$(am)	Eh gw	$5.4·10^{-9}$	Am^{+3} (99%)	Reliability of phosphate measurements
	$AmPO_4 + 2 H^+ = Am^{3+} + H_2PO_4^-$	$pH_2(g) = 10^{-7}$ atm	$5.3·10^{-9}$	Am^{+3} (99%)	

(*)The assumption of this limiting solid phase gives an important associated error in the balance charge due to the large solubility of the solid compared to the low ionic strength.

Table 5-9. *Solubilities for elements of interest. Ice melting groundwater.*

Element	Solubility limiting phase and reaction	M (mol·dm^{-3})	Main complexes formed	Associated uncertainty
Cs		n.s.l	Cs^+ (100%)	
Sr	*Strontianite* $SrCO_3 + H^+ = Sr^{2+} + HCO_3^-$	$1.4 \cdot 10^{-5}$	Sr^{2+} (97%)	Possibility of coprecipitation with other elements' carbonates SO_4^{2-} to HS^- reduction
Ra	$RaSO_4(s) = Ra^{2+} + SO_4^{2-}$	$8.8 \cdot 10^{-7}$	Ra^{2+} (97%)	Possibility of coprecipitation with other elements' carbonates SO_4^{2-} to HS^- reduction
Sn	$SnO_2 (am) + 4H^+ = 2 H_2O + Sn^{4+}$	$2.7 \cdot 10^{-6}$	$Sn(OH)_5^-$ (82%), $Sn(OH)_6^{2-}$ (15%)	SO_4^{2-} to HS^- reduction
Se	$FeSe_2(s) + 2 H^+ + 2 e^- = Fe^{2+} + 2 HSe^-$	$4.5 \cdot 10^{-11}$	HSe^- (100%)	Effect of iron in water Formation of native Se^o Possibility of coprecipitation with sulphides Uncertainty in measured iron concentrations
Zr	$Zr(OH)_4 (aged) + 4 H^+ = 4 H_2O + Zr^{4+}$	$1.8 \cdot 10^{-8}$	$Zr(OH)_4$ (100%)	Crystallinity of the solid phase
Nb	$Nb_2O_5 + H_2O = 2 NbO_3^- + 2 H^+$	$2.9 \cdot 10^{-3}$	NbO_3^- (100%)	Scarcity of TDB
Mo	$CaMoO_4 (s) = MoO_4^{2-} + Ca^{2+}$	$1.5 \cdot 10^{-4}$	MoO_4^{2-} (100%)	Scarcity of TDB
Tc	$TcO_2 \cdot 1.6H_2O = TcO(OH)_2 + 0.6 H_2O$	$4.5 \cdot 10^{-9}$	$TcO(OH)_2$ (89%), TcO_4^- (7%), $TcO(OH)_3^-$ (5%)	Formation of metallic Tc^o
Ni	$Ni(OH)_2 + 2 H^+ = Ni^{2+} + 2 H_2O$	$4.1 \cdot 10^{-7}$	$Ni(OH)_2$ (93%), Ni^{2+} (7%)	SO_4^{2-} to HS^- reduction
Pd	$Pd(OH)_2 + 2 H^+ = 2 H_2O + Pd^{2+}$	$2.7 \cdot 10^{-6}$	$Pd(OH)_2$ (100%)	Formation of metallic Pd^o

Element	Solubility limiting phase and reaction	M (mol·dm^{-3})	Main complexes formed	Associated uncertainty
Sm	$SmOHCO_3(s) + H^+ = Sm^{3+} + CO_3^{2-} + H_2O$	$1.8 \cdot 10^{-9}$	$Sm(CO_3)_2^-$ (100%)	Effects of phosphates in water; stability of the solid hydroxo-carbonate
Th	$ThO_2 \cdot 2H_2O$ (am) $+ 4 H^+ = Th^{4+} + 4 H_2O$	$8.1 \cdot 10^{-10}$	$ThCO_3(OH)_3^-$ (88%), $Th(OH)_4$ (7%)	Stability of the solid
Pa	Pa_2O_5 (s) $+ 2 H^+ = 2 PaO_2^+ + H_2O$	$3.2 \cdot 10^{-7}$	PaO_2OH (100%)	Lack of thermodynamic data
U	Uranophane $Ca(UO_2)_2(SiO_3OH)_2 \cdot 5H_2O + 6H^+ = Ca^{2+} + 2 UO_2^{2+} + 2 Si(OH)_4 + 5 H_2O$	$2.3 \cdot 10^{-9}$	$UO_2(CO_3)_3^{4-}$ (97%)	Silicate solid precipitation TDB data on solid stability
Np	$NpO_2 \cdot 2H_2O(am) + 4 H^+ = Np^{4+} + 4 H_2O$	$8.2 \cdot 10^{-10}$	$Np(OH)_4$ (93%), $NpCO_3(OH)_3^-$ (7%)	Crystallinity of the solid phase
Pu	$Pu(OH)_4$ (am) $+4 H^+ = Pu^{4+} + 4 H_2O$	$1.3 \cdot 10^{-10}$	$Pu(OH)_4$ (100%)	Stability of the solid hydroxo-carbonate; SO_4^{2-} to HS^- reduction
Am	$Am(OH)_3 + 3 H^+ = Am^{3+} + 3H_2O$	$5.6 \cdot 10^{-8}$	$Am(CO_3)_2^-$ (54%), $AmOSi(OH)_3^{2+}$ (46%)	Stability of the solid hydroxo-carbonate

REFERENCES

Altmaier, M., Neck, V., Denecke, M.A., Yin, R. & Fanghänel, Th. 2006. Solubility of $ThO_2 \cdot xH_2O(am)$ and the formation of ternary Th(IV) hydroxide-carbonate complexes in $NaHCO_3$-Na_2CO_3 solutions containing 0 - 4 M NaCl. Radiochim. Acta 94, 495-500.

Altmaier, M., Neck, V., Müller, R. & Fanghänel Th. 2005. Solubility of $ThO_2 \cdot xH_2O$ in carbonate solution and the formation of ternary Th(IV) hydroxide-carbonate complexes. Radiochim. Acta, 93, 83-92.

Aveston, J., Anacker, E.W. & Johnson, J.S. 1964. Hydrolyses of Molybdenum (IV). Ultracentrifugation, acidity measurements, and raman spectra of polymolybdates. Inorg. Chem., 3, 735-746.

Baeyens B. & Bradbury M. H. 1997. A mechanistic description of Ni and Zn sorption on Na-montmorillonite. Part I: Titration and sorption measurements. J. Contam. Hydrology 27, 199-222.

Bard, A.J., Parsons, R. & Jordan, J. 1985. Standard potentials in aqueous solution, International union of pure and applied chemistry. Oxford, U.K.

Brown, P.L., Curti, E & Grambow, B. 2005. Chemical Thermodynamics 8. Chemical Thermodynamics of Zirconium. NEA OECD, Elsevier.

Bruno, J., Duro, L. & Grivé, M. 2001. The applicability and limitations of the geochemical models and tools used in simulating radionuclide behaviour in natural waters. Lessons learned from the Blind Predictive Modelling exercises performed in conjunction with Natural Analoque studies. SKB Technical Report TR-01-20. Swedish Nuclear Fuel and Waste management Co. (SKB)., Stockholm, Sweden.

Cornell, R. M. & Schwertmann, U. 1996. The Iron Oxides. VCH, Weinheim, Germany.

Curti E. & Wersin P. 2002. Assessment of porewater chemistry in the bentonite backfill for the Swiss SF/HLW repository. Nagra Technical Report NTB 02-09, Wettingen, Switzerland.

Duro, L., Grivé, M., Cera, E., Domènech, C. & Bruno J. 2005. Update of a thermodynamic database for radionuclides to assist solubility limits calculation for PA. SKB Technical Report TR 06-17. Swedish Nuclear Fuel and Waste management Co. (SKB)., Stockholm, Sweden.

Duro, L., Grivé, M., Cera, E., Gaona, X., Domènech, C. & Bruno, J. 2006. Determination and assessment of the concentration limits to be used in SR-Can. SKB Technical Report TR 2006-30. Swedish Nuclear Fuel and Waste Management Co. (SKB), Stockholm, Sweden.

Gamsjäger, H., Bugajski, J., Lemire, R., Gajda, T. & Preis, W. 2005. Chemical Thermodynamics 6. Chemical Thermodynamics of Nickel. NEA OECD, Elsevier.

Grenthe, I. & Puigdomenech, I. 1997. Modelling in Aquatic Chemistry. NEA OECD, Paris.

Guillaumont, R., Fanghänel, J., Neck, V., Fuger, J., Palmer, D.A., Grenthe, I. & Rand, M.H. 2003. Chemical Thermodynamics 5. Update on the Chemical Thermodynamics of Uranium, Neptunium, Plutonium, Americium and Technetium. NEA OECD, Elsevier.

Hummel, W., Berner, U., Curti, E., Pearson, F.J. & Thoenen, T. 2002. Nagra/PSI Chemical Thermodynamic Data Base 01/01. ISBN: 1-58112-620-4. 565 p.

Iida, Y., Yamaguchi, T., Tanaka, T., Kitamura, A & Nakayama, S. 2007. Determination of the solubility limiting solid of Se in the presence of Fe under anoxic conditions in Book of Abstracts of Mobile Fision and Activation Products in Nuclear Waste Disposal International Workshop. La Baule (France) January 16-19 2007.

Johnson, L.H. & Tait, J.C. 1997. Release of segregated nuclides from spent fuel. SKB Technical Report TR-97-18. Swedish Nuclear Fuel and Waste management Co. (SKB), Stockholm, Sweden.

Johnson, L.H. and B.Schwyn (eds.) 2004. Proceedings of a workshop on the release and transport of C-14 in repository environments. NAGRA report Interner Bericht 04-03. 2004. Nagra, Wettingen, Switzerland.

Kaback, D.S. & Runnells, D. 1980. Geochemistry of molibdenum in some stream sediments and waters. Geochim et Cosmochim. Acta, 44, 447-456.

Kudo, K. & Komatsu, K. 1999. Reduction of alkali metal carbonate to methane with water in the presence of Raney alloy. Journal of Molecular Catalysis A: chemical, 145, 159-167.

Lemire, R.J. & Garisto, F. 1989. The solubility of U, Np, Pu, Th and Tc in a geological disposal vault for used nuclear fuel. AECL-10009.

Lemire, R.J., Fuger, J., Nitsche, H., Potter, P., Rand, M.H., Rydberg, J., Spahiu, K., Sullivan, J.C., Ullman, W.J., Vitorge, P. & Wanner, H. 2001. Chemical Thermodynamics 4. Chemical thermodynamics of neptunium and plutonium. NEA OECD, Elsevier.

Masurat, P. 2006: Potential for corrosion in disposal systems for high-level radioactive waste by *Meiothermus and Desulfovibrio*. Doctoral thesis. Göteborg University, Sweden.

Müller-Vonmoos, M. & Kahr, G. 1983. Mineralogische Untersuchungen von Wyoming Bentonit MX-80 und Montigel. Nagra Technical Report NTB 83-12, Wettingen, Switzerland.

Naumov, G.B., Ryzhenko, B.N. & Khodakovskiy, I.L. 1971. Handbook of thermodynamic data, Moscow: Atomizdat, in Russian; Engl. Transl.; Report USGSWRD+74-001 (Sikeunabu G.J., Barnes I., Spelts, V., eds.), U.S. Geological Survey, Menlo Park, California, USA, 1974, 328p.

Neck, V. & Kim, J.I. 1999. An electrostatic approach for the prediction of actinide complexation constants with inorganic ligands-application to carbonate complexes. Radiochim. Acta, 88, 815-822.

Neck, V. & Kim, J.I. 2001. Solubility and hydrolisis of tetravalent actinides. Radiochim. Acta, 89, 1-16.

Neck, V., Altmaier, M., Müller, R., Bauer, A., Fanghänel, Th. & Kim, J.I. 2003. Solubility of crystalline thorium dioxide. Radiochim. Acta, 91, 253-262.

Neck, V., Müller, R., Bouby, M., Altmaier, M., Rothe, J., Denecke, M.A. & Kim, J.I. 2002. Solubility of amorphous Th(IV) hydroxide – application of LIBD to determine the solubility product and EXAFS for aqueous speciation. Radiochim. Acta, 90, 485-494.

Olin, A., Noläng, B., Ohman, L-O. G., Osadchii, E. & Rosén E. 2005. Chemical Thermodynamics 7. Chemical Thermodynamics of Selenium NEA OECD, Elsevier.

Parkhurst, D.L. & Appelo, C.A.J. 2001. User's guide to PHREEQC (Version 2.4.6). A computer program for speciation, batch reaction, one dimensional transport and inverse geochemical calculations. U.S. Department of the Interior. U.S. Geological Survey. Water-Resources Investigations.

Pastina, B. & Hellä, P. 2006. Expected evolution of a spent fuel repository at Olkiluoto. POSIVA 2006-05. Posiva Oy, Olkikuoto, Finland.

Pitkänen P., Partamies S., & Luukkonen A. 2004. Hydrogeochemical interpretation of baseline groundwater conditions at the Olkiluoto site. POSIVA 2003-07. Posiva Oy, Olkiluoto, Finland.

Pitkänen, P., Ahokas, H., Ylä-Mella, M., Partamies, S., Snellman, M. & Hellä, P. 2007, Quality Review of Hydrochemical Baseline Data from the Olkiluoto Site, POSIVA 2007-05. Posiva Oy, Olkiluoto, Finland.

Puigdomènech, I. 2002. Chemical Equilibrium Software MEDUSA and Data Base HYDRA, http://www.kemi.kth.se/medusa/.

Rao D.V.R.J. 1954. Sci. Ind. Res. India, 13B, 309.

Robbie, R.A., Hemingway, B.S. & Fisher, J.R. 1979. Thermodynamicproperties of minerals and related substances at 298.15 K and 1 bar (105 Pascals) pressure and at higher temperatures. U.S. Geological Survey Bulletin 1452.

Sasaki, Y. & Sillén, L.G., 1968. Equilibrium studies of polyanions. XVI. Equilibriums of molybdates in 3M sodium perchlorate medium at 25º C. Ark. Kemi, 29, 253-277 Reported in: Cruywage J.J., Heyns J.B.B. & Rohwer E.F.C.H. 1976. Spectrophotometric investigation of the protonation of monomeric mollybdic acid in sodium perchlorate medium. J.Inorg. Nucl. Chem., 38, 203-206.

Shannon, R.D. 1976. Revised Effective ionic Radii and Systematic Studies of Interatomic Distances in Halides and Chalcogenides. cta Crystallographica, A32, 751-767.

Smith, P. Johnson, L., Snellman, M., Pastina, B & Gribi, P. 2007. Evolution of a KBS-3H repository at Olkiluoto site, POSIVA 2007-xx (in preparation). Posiva Oy, Olkiluoto, Finland.

Stroes-Gascoyne, S., Hamon, C. J., Kohle, C., & Dixon, D. A. 2006. The effects of dry density and porewater salinity on the physical and microbiological characteristics of highly compacted bentonite. Ontario Power Generation Report No: 06819-REP-01200-10016-R00.

Vaughn, D. J. & Craig, J. R. 1978. Mineral Chemistry of Metal Sulfides. Cambridge University Press.

Vogt, K. & Köster, H.M. 1978. Zur Mineralogie, Kristallchemie und Geochemie einiger Montmorillonite aus Bentoniten. Clay Minerals, 13, 25-43.

Wagman, D.D., Evans, W.H., Parker, V.B., Schumm, R.H., Halow, I., Bailey, S.M., Churney, K.L. & Nuttall, R.L. 1982. The NBS tables of chemicalthermodynamic properties, selected values for inorganic and c1 and c2 organicsubstances in SI units. J. Phys. Chem. Ref. Data, V. 11, supp. 2, 392p.

Wersin, P., Birgersson, M., Olsson, S., Karnland, O. & Snellman, M. 2007. Impact of corrosion-derived iron on the bentonite buffer within the KBS-3H disposal concept. The Olkiluoto site as case study. Posiva Working Report 2007-xx (in preparation). Posiva Oy, Olkiluoto, Finland.

Östhols, E., Bruno, J. & Grenthe, I. 1994. On the influence of carbonate on mineral dissolution: III. The solubility of microcrystalline ThO_2 in CO_2-H_2O media. Geochim. et Cosmochim. Acta, 58(2), 613-623.

APPENDIX A: GROUNDWATERS, BENTONITE WATERS AND GLACIAL MELTWATERS FOR SOLUBILITY CALCULATIONS

Three different types of waters have been considered for the assessment of solubility limits:

- Groundwater types currently found at the Olkiluoto site: Olkiluoto groundwaters;
- Olkiluoto groundwater modified by interaction with bentonite: Bentonite waters; and
- Glacial meltwaters.

A.1 Olkiluoto groundwaters

Based on the available data from deep boreholes (Pitkänen et al. 2004; Pitkänen et al. 2007) groundwaters representative of repository conditions at Olkiluoto have been defined:

i)   A brackish/saline water type that may contain water from outside the test section, but still representative for baseline conditions at Olkiluoto in the sampling depth of tens of meters (water sample reference: KR20/465/1)

ii)   A saline water type (water sample reference: KR10/498/1) describing baseline conditions at Olkiluoto,

iii)   The special case of upconing of brine water (water sample reference: KR12/741/1) which is dealt with in the calculations, and

iv)   A dilute/brackish water type (water sample reference: KR6/58/1) as a limiting composition of the expected possible variations in future chemical conditions.

The first two waters reflect the expected range of compositions at repository depth (465 m and 498 m) reasonably well for the present site conditions and the conditions once the site is constructed and natural conditions have been restored based on the discussion presented in the report by Pastina and Hellä (2006). The third and fourth type reflects brine type water conditions (represented by a sample at 740 m depth from borehole KR12) and dilute/brackish water conditions (represented by a sample taken at 58 m depth from borehole KR6) as limiting compositions of the expected possible variations in future chemical conditions. The properties of these Olkiluoto groundwater types are listed in Table A-1.

All of the samples presented in Table A-1 are classified as valid samples with no significant sampling or analysis uncertainties (Pitkänen et al. 2007). The classification is based on integrated interpretation of the hydrological background to the sampling and chemical analyses of groundwaters. Samples from KR10, KR12 and KR6 are all classified as the most representative samples (B1) describing the baseline conditions at Olkiluoto in a reliable way, whereas the sample from KR20 is classified as B2 and meaning it may contain water outside the test section, but is still representative for

baseline conditions at Olkiluoto in the sampling depth of tens of meters. The sample has slightly elevated alkalinity/DIC and SO$_4$ and also of C-14 and H-3.

Table A-1. Compositions of groundwaters taken from selected measurements in Pitkänen et al (2007). Calculated values obtained with PHREEQC assuming T = 15 °C. Concentrations in mmole l^{-1} unless otherwise indicated. SI: saturation index. (After Table 3.2.2 of Wersin et al. (2007), but with the addition of phosphate (PO$_4$) and fluoride (F)).

	Saline waters		Brine type water	Dilute/brackish water
Sample	**KR20/465/1**	**KR10/498/1**	**KR12/741/1**	**KR6/58/1**
Depth (m)	465	498	741	58
TDS (mg/l)	10544	22099	49483	1026
Ionic strength (meq/l)	218	478	1180	20
pH	7.4	8.0	8.2	7.6
Alkalinity	0.66	0.11	0.12	2.79
DIC	0.55	0.11	0.04	2.72
SO$_4$	0.21	0.01	0.05	1.31
Cl	180.5	380.8	863.2	10.4
Na	114.8	210.0	360.9	9.8
K	0.28	0.36	0.49	0.20
Ca	32.4	89.1	254.5	2.1
Mg	2.6	1.6	1.5	1.1
Sr	0.16	0.37	1.14	0.01
SiO$_2$	0.36	0.28	0.21	0.41
Mn	5.8E-03	7.3E-03	9.3E-03	
Fe	2.5E-03	2.0E-03	3.8E-04	0.024
S^{2-}tot	5.61E-03	<3.12E-04	1.25E-03	6.24E-04
F	1E-05	9.8E-05	6.3E-05	3.2E-05
PO$_4$	<3E-07	1E-07	2.6E-06	5E-06
Calculated data				
Eh (mV)	-217 S(6)/S(-2)	-258 S(6)/S(-2)	-299 C(4)/C(-4)	-35 Fe(OH)$_3$/Fe(2)
SI(calcite)	0.03	0.06	0.57	0.00
SI(FeS$_{am}$)	-0.34	-1.06	-0.11	0.00
SI(pyrite)	8.80	6.05	6.40	16.2
SI(siderite)	-1.72	-2.16	-2.11	0.34

A.2 Olkiluoto groundwater modified by interaction with bentonite: Bentonite waters

The composition of the groundwater in contact with the canister corresponds to the Olkiluoto groundwater modified to take into account its interaction with the bentonite and its interaction with the canister with respect to the redox conditions.

Table A-2, which is taken from Wersin et al. (2007), shows the porewater composition for bentonite equilibrated with the groundwaters given in Table A-1. The conventional model of Bradbury & Baeyens (1997), as applied by Curti & Wersin (2002), has been used under the constraint of constant pCO_2. The assumption that pCO_2 is constrained by the rock is justified if long term conditions are considered, because diffusion of dissolved CO_2 in bentonite is fast relative to the timescales of interest (>10 000 years). The results indicate that, due to cation exchange and dissolution of calcite and gypsum, some changes in composition relative to the groundwater will occur. The changes are obviously greatest in the case of the bentonite contacting the "dilute" groundwater where the equilibrium with the ion exchanger will lead to increased cation concentrations. However, because of the strong buffering of the clay surface and the presence of calcite, the pH conditions will remain remarkably stable (pH approx. 8). The main change predicted on long timescales is the enrichment of Ca relative to Na on the montmorillonite ion exchangeable sites.

The redox conditions for the bentonite waters have been calculated based on equilibrium with the corrosion products of the steel supercontainer in Olkiluoto groundwater conditions. Magnetite is the stable Fe phase at pH values higher than 8, and FeS is also thermodynamically stable under conditions expected for the repository. Siderite formation is in principle also possible but requires high carbonate and low sulphide activities in the groundwater, such as is the case for the dilute/brackish type groundwater.

In addition to the iron from the steel supercontainer and its impact on groundwater and bentonite, Wyoming bentonite as such generally contains Fe(II) mineral impurities, such as pyrite and siderite (e.g. Müller-Vonmoos & Kahr 1983). In addition, traces of iron oxides (Baeyens & Bradbury 1997) are present. Because of the variability in bentonite composition and possible oxidation of Fe^{2+} during processing of the raw material, the relative amounts of reactive iron phases may vary considerably. Moreover, the smectite fraction in MX80 typically contains about 2 wt% of structural iron, most of which is Fe(III) (Vogt & Köster 1978).

A.3 Glacial meltwaters

Large uncertainties exist with respect to the composition of glacial meltwater that could potentially penetrate at repository depth. To address these uncertainties, two different glacial water compositions have been used to carry out the solubility limit calculations: the "glacial meltwater" used by Pitkänen et al. (2004) and the "ice melting groundwater" used in SR-Can (see Duro et al. 2006). The former is the estimated Quaternary glacial melt water composition expected from ice melting processes, and the latter corresponds to the composition of a dilute granitic groundwater from ice melting

at Grimsel, sampled at the Grimsel Test Site, as an analogue for the diluted groundwater composition expected from ice melting processes. The chemical compositions of both groundwaters are given in Table A-3.

Table A-2. *Calculated bentonite porewater composition (bentonite waters) for different groundwater compositions. Concentrations in mM unless otherwise indicated (Wersin et al. 2007).*

	Saline type		Brine-type	Dilute/brackish type
Solution composition				
Ionic strength (meq/l)	315	507	1169	220
pH	7.82	7.66	8.03	7.39
Alkalinity	0.52	0.40	0.072	2.50
SO_4	34.9	22.6	11.9	74.2
Cl	185	386	924	15.1
Na	271	384	645	167
K	0.85	1.24	2.3	0.53
Ca	20.8	42.9	167	10.4
Mg	6.32	10.9	24.9	1.1
Surface species				
NaX	1990	1980	1890	1990
CaX_2	249	247	324	248
MgX_2	69.3	63.8	49.8	70.3
KX	23.4	23.0	22.1	23.5
SOH	221	234	203	250
SO^-	68.2	54.4	86.1	35.4
SOH_2^+	2.14	3.12	1.3	5.68
Eh calculation				
Fe	2.3E-3	4.2E-3	4E-03	0.04
$S^{2-}tot$	5.3E-3	4.8E-3	1.3E-03	-
Eh (mV)	-171	-160	-280	-202
	Fe_3O_4/FeS	Fe_3O_4/FeS	Fe_3O_4/FeS	$Fe_3O_4/FeCO_3$

Table A-3. *Two types of glacial meltwater compositions (i) ice-melting water (Table 2-1) and (ii) glacial meltwater Pitkänen et al. (2004). All concentrations in (mM) unless otherwise indicated.*

	Ice melting water (Table 2-1)	Glacial meltwater (Pitkänen et al. 2004)
T (°C)	15	1
pH	9.8	5.8
Alkalinity (meq/l)	0.45	$2.6 \cdot 10^{-3}$
SO_4	$6.1 \cdot 10^{-2}$	$5.2 \cdot 10^{-4}$
Cl	0.16	0.020
Na	0.69	$6.5 \cdot 10^{-3}$
K	$5 \cdot 10^{-3}$	$3.8 \cdot 10^{-3}$
Ca	0.14	$3.2 \cdot 10^{-3}$
Mg	$6.2 \cdot 10^{-4}$	$4.1 \cdot 10^{-3}$
Sr	$2 \cdot 10^{-3}$	$1 \cdot 10{-6}$
SiO_2	0.25	$1.7 \cdot 10^{-4}$
Mn	$5 \cdot 10^{-6}$	
Fe	$3 \cdot 10^{-6}$	$1.8 \cdot 10^{-6}$
F	0.36	
Eh (mV)	-200	920*
Eh (calculated)		-136*(magnetite/hematite)

*In the GMWV glacial meltwater, the Eh 920 mV was calculated taking into account the oxygen present in the original infiltrating glacial meltwater (7.2 mg/l). If the oxygen consumption by iron compounds and the long-term equilibrium between magnetite/hematite ($pH_2 = 10^{-7}$atm) are taken into account, the calculated Eh is –136 mV.

References

Baeyens B. & Bradbury M. H. 1997. A mechanistic description of Ni and Zn sorption on Na-montmorillonite. Part I: Titration and sorption measurements. J. Contam. Hydrology 27, 199-222.

Bradbury M. H. & Baeyens B. 1997. A mechanistic description of Ni and Zn sorption on Na-montmorillonite. J. Contam. Hydrol. 27, 223-248.

Curti E. & Wersin P. 2002. Assessment of porewater chemistry in the bentonite backfill for the Swiss SF/HLW repository. Nagra Technical Report NTB 02-09, Wettingen, Switzerland.

Duro, L., Grivé, M., Cera, E., Gaona, X., Domènech, C. & Bruno, J. 2006. Determination and assessment of the concentration limits to be used in SR-Can. SKB Technical Report TR 2006-30. Swedish Nuclear Fuel and Waste Management Co. (SKB), Stockholm, Sweden.

Müller-Vonmoos M., Kahr G. 1983. Mineralogische Untersuchungen von Wyoming Bentonit MX-80 und Montigel. Nagra Technical Report NTB 83-12, Wettingen, Switzerland.

Pastina, B. & Hellä, P. 2006. Expected evolution of a spent fuel repository at Olkiluoto, POSIVA 2006-05. Posiva Oy, Olkikuoto, Finland.

Pitkänen P., Partamies S. & Luukkonen A. 2004. Hydrogeochemical interpretation of baseline groundwater conditions at the Olkiluoto site. Posiva report 2003-07. Posiva Oy, Olkiluoto, Finland.

Pitkänen, P., Ahokas, H., Ylä-Mella, M., Partamies, S., Snellman, M. & Hellä, P. 2007, Quality Review of Hydrochemical Baseline Data from the Olkiluoto Site, POSIVA 2007-05. Posiva Oy, Olkiluoto, Finland.

Vogt K. & Köster H.M. 1978. Zur Mineralogie, Kristallchemie und Geochemie einiger Montmorillonite aus Bentoniten. Clay Minerals 13, 25-43.

Wersin, P., Birgersson, M., Olsson, S., Karnland, O. & Snellman, M. 2007. Impact of corrosion-derived iron on the bentonite buffer within the KBS-3H disposal concept. The Olkiluoto site as case study. Posiva Working Report 2007-xx (in preparation). Posiva Oy, Olkiluoto, Finland.

APPENDIX B: SOLUBILITIES

Solubilities for the elements of interest for POSIVA under the conditions of the nine groundwaters (4 groundwaters, 3 bentonite waters and 2 glacial waters). For the composition of the specific groundwaters the reader is referred to section 2.

Table B- 1. *Solubilities for elements of interest for the different groundwaters.*

		SOLUBILITY (mol·dm⁻³)								
		Olkiluoto groundwaters				*Bentonitic waters*			*Glacial waters*	
Element	Redox state	Brackish/ Saline KR20/465/1	Saline KR10/498/1	Dilute/ brackish KR6/58/1	Brine KR12/741/1	Brackish/ Saline	Saline	Dilute/ brackish	Glacial meltwater	Ice melting water
Cs	Eh gw	n.s.l	n.s.l	n.s.l	n.s.l	n.s.l	n.s.l	n.s.l	n.s.l	n.s.l
	$pH_2(g)=10^{-7}$ atm	n.s.l	n.s.l	n.s.l	n.s.l	n.s.l	n.s.l	n.s.l	n.s.l	
	$pH_2(g)=10^{2}$ atm	n.s.l	n.s.l	n.s.l	n.s.l	n.s.l	n.s.l	n.s.l		
Sr	Eh gw	$5.9 \cdot 10^{-3}$	$9.2 \cdot 10^{-3}$	$3.1 \cdot 10^{-4}$	$1.6 \cdot 10^{-2}$	$1.9 \cdot 10^{-4}$	$3.6 \cdot 10^{-4}$	$9.1 \cdot 10^{-5}$	n.s.l	$1.4 \cdot 10^{-5}$
	$pH_2(g)=10^{-7}$ atm	$5.9 \cdot 10^{-3}$	$9.2 \cdot 10^{-3}$	$3.1 \cdot 10^{-4}$	$1.6 \cdot 10^{-2}$	$1.9 \cdot 10^{-4}$	$3.6 \cdot 10^{-4}$	$9.1 \cdot 10^{-5}$	n.s.l	
	$pH_2(g)=10^{2}$ atm	$5.9 \cdot 10^{-3}$	$9.2 \cdot 10^{-3}$	$3.1 \cdot 10^{-4}$	$1.6 \cdot 10^{-2}$	$1.9 \cdot 10^{-4}$	$3.7 \cdot 10^{-4}$	$9.3 \cdot 10^{-5}$		
Ra	Eh gw	$3.2 \cdot 10^{-6}$	$1.1 \cdot 10^{-4}$	$1.1 \cdot 10^{-7}$	$3.0 \cdot 10^{-5}$	$3.5 \cdot 10^{-8}$	$5.9 \cdot 10^{-8}$	$2.2 \cdot 10^{-8}$	2.010^{-4}	$8.8 \cdot 10^{-7}$
	$pH_2(g)=10^{-7}$ atm	$3.2 \cdot 10^{-6}$	$1.1 \cdot 10^{-4}$	$1.1 \cdot 10^{-7}$	$3.0 \cdot 10^{-5}$	$3.5 \cdot 10^{-8}$	$5.9 \cdot 10^{-8}$	$2.2 \cdot 10^{-8}$	$7.1 \cdot 10^{-5}$	
	$pH_2(g)=10^{2}$ atm	$3.3 \cdot 10^{-6}$	$1.1 \cdot 10^{-4}$	$1.1 \cdot 10^{-7}$	$3.0 \cdot 10^{-5}$	$3.6 \cdot 10^{-8}$	$6.0 \cdot 10^{-8}$	$2.2 \cdot 10^{-8}$		
Sn	Eh gw	$9.6 \cdot 10^{-8}$	$1.4 \cdot 10^{-7}$	$1.1 \cdot 10^{-7}$	$1.5 \cdot 10^{-7}$	$1.2 \cdot 10^{-7}$	$1.0 \cdot 10^{-7}$	$9.6 \cdot 10^{-8}$	$8.4 \cdot 10^{-8}$	$2.7 \cdot 10^{-6}$
	$pH_2(g)=10^{-7}$ atm	$9.6 \cdot 10^{-8}$	$1.4 \cdot 10^{-7}$	$1.1 \cdot 10^{-7}$	$1.5 \cdot 10^{-7}$	$1.2 \cdot 10^{-7}$	$1.0 \cdot 10^{-7}$	$9.6 \cdot 10^{-8}$	$8.4 \cdot 10^{-8}$	
	$pH_2(g)=10^{2}$ atm	$1.2 \cdot 10^{-7}$	$1.7 \cdot 10^{-7}$	$1.4 \cdot 10^{-7}$	$1.8 \cdot 10^{-7}$	$1.5 \cdot 10^{-7}$	$1.3 \cdot 10^{-7}$	$1.2 \cdot 10^{-7}$		
Se	Eh gw	$6.0 \cdot 10^{-10}$	$8.8 \cdot 10^{-10}$	$6.6 \cdot 10^{-14}$	$6.3 \cdot 10^{-9}$	$4.3 \cdot 10^{-11}$	$3.0 \cdot 10^{-11}$	$1.0 \cdot 10^{-10}$	n.s.l	$4.5 \cdot 10^{-11}$
	$pH_2(g)=10^{-7}$ atm	$1.0 \cdot 10^{-9}$	$1.2 \cdot 10^{-9}$	$2.1 \cdot 10^{-10}$	$2.7 \cdot 10^{-9}$	$1.2 \cdot 10^{-9}$	$8.8 \cdot 10^{-10}$	$3.1 \cdot 10^{-10}$	$1.5 \cdot 10^{-8}$	
	$pH_2(g)=10^{2}$ atm	$1.4 \cdot 10^{-5}$	$4.5 \cdot 10^{-6}$	$3.8 \cdot 10^{-7}$	$1.7 \cdot 10^{-5}$	$6.4 \cdot 10^{-6}$	$5.2 \cdot 10^{-6}$	$1.2 \cdot 10^{-6}$		
Zr	Eh gw	$1.7 \cdot 10^{-8}$	$1.6 \cdot 10^{-8}$	$1.8 \cdot 10^{-8}$	$1.4 \cdot 10^{-8}$	$1.7 \cdot 10^{-8}$	$1.6 \cdot 10^{-8}$	$1.7 \cdot 10^{-8}$	$1.8 \cdot 10^{-8}$	$1.8 \cdot 10^{-8}$
	$pH_2(g)=10^{-7}$ atm	$1.7 \cdot 10^{-8}$	$1.6 \cdot 10^{-8}$	$1.8 \cdot 10^{-8}$	$1.4 \cdot 10^{-8}$	$1.7 \cdot 10^{-8}$	$1.6 \cdot 10^{-8}$	$1.7 \cdot 10^{-8}$	$1.8 \cdot 10^{-8}$	
	$pH_2(g)=10^{2}$ atm	$1.7 \cdot 10^{-8}$	$1.6 \cdot 10^{-8}$	$1.8 \cdot 10^{-8}$	$1.4 \cdot 10^{-8}$	$1.7 \cdot 10^{-8}$	$1.6 \cdot 10^{-8}$	$1.7 \cdot 10^{-8}$		
Nb	Eh gw	$3.9 \cdot 10^{-5}$	$1.2 \cdot 10^{-4}$	$4.6 \cdot 10^{-5}$	$2.0 \cdot 10^{-4}$	$8.1 \cdot 10^{-5}$	$6.2 \cdot 10^{-5}$	$3.8 \cdot 10^{-5}$	$1.5 \cdot 10^{-5}$	$2.9 \cdot 10^{-3}$
	$pH_2(g)=10^{-7}$ atm	$3.9 \cdot 10^{-5}$	$1.2 \cdot 10^{-4}$	$4.6 \cdot 10^{-5}$	$2.0 \cdot 10^{-4}$	$8.1 \cdot 10^{-5}$	$6.2 \cdot 10^{-5}$	$3.8 \cdot 10^{-5}$	$1.5 \cdot 10^{-5}$	
	$pH_2(g)=10^{2}$ atm	$3.9 \cdot 10^{-5}$	$1.2 \cdot 10^{-4}$	$4.6 \cdot 10^{-5}$	$2.0 \cdot 10^{-4}$	$8.1 \cdot 10^{-5}$	$6.2 \cdot 10^{-5}$	$3.8 \cdot 10^{-5}$		
Mo	Eh gw	$7.9 \cdot 10^{-9}$	$8.5 \cdot 10^{-8}$	$1.9 \cdot 10^{-5}$	$1.3 \cdot 10^{-8}$	$8.9 \cdot 10^{-6}$	$4.1 \cdot 10^{-6}$	$2.4 \cdot 10^{-8}$	n.s.l	$1.5 \cdot 10^{-4}$
	$pH_2(g)=10^{-7}$ atm	$2.8 \cdot 10^{-9}$	$4.5 \cdot 10^{-8}$	$3.7 \cdot 10^{-9}$	$6.7 \cdot 10^{-8}$	$2.0 \cdot 10^{-8}$	$9.2 \cdot 10^{-9}$	$2.6 \cdot 10^{-9}$	$5.6 \cdot 10^{-13}$	
	$pH_2(g)=10^{2}$ atm									

		SOLUBILITY (mol·dm^{-3})								
		Olkiluoto groundwaters				*Bentonitic waters*			*Glacial waters*	
Element	Redox state	Brackish/ Saline KR20/465/1	Saline KR10/498/1	Dilute/ brackish KR6/58/1	Brine KR12/741/1	Brackish/ Saline	Saline	Dilute/ brackish	Glacial meltwater	Ice melting water
Tc	Eh gw	$4.0·10^{-9}$	$4.0·10^{-9}$	$5.0·10^{-9}$	$4.1·10^{-9}$	$4.0·10^{-9}$	$4.0·10^{-9}$	$4.2·10^{-9}$	n.s.l	$4.5·10^{-9}$
	pH$_2$(g)=10^{-7} atm	$4.0·10^{-9}$	$4.0·10^{-9}$	$4.2·10^{-9}$	$4.1·10^{-9}$	$4.0·10^{-9}$	$4.0·10^{-9}$	$4.2·10^{-9}$	$4.0·10^{-9}$	
	pH$_2$(g)= 10^{2} atm	$4.0·10^{-9}$	$4.0·10^{-9}$	$4.2·10^{-9}$	$4.0·10^{-9}$	$4.0·10^{-9}$	$4.0·10^{-9}$	$4.2·10^{-9}$		
Ni	Eh gw	$2.0·10^{-3}$	$1.4·10^{-4}$	$4.4·10^{-4}$	$4.4·10^{-5}$	$3.9·10^{-4}$	$7.4·10^{-4}$	$4.3·10^{-3}$	n.s.l	$4.1·10^{-7}$
	pH$_2$(g)=10^{-7} atm	$2.0·10^{-3}$	$1.4·10^{-4}$	$4.4·10^{-4}$	$4.4·10^{-5}$	$3.9·10^{-4}$	$7.4·10^{-4}$	$4.3·10^{-3}$	n.s.l	
	pH$_2$(g)= 10^{2} atm	$2.0·10^{-3}$	$1.4·10^{-4}$	$4.4·10^{-4}$	$4.4·10^{-5}$	$3.9·10^{-4}$	$7.4·10^{-4}$	$4.1·10^{-3}$		
Pd	Eh gw	$2.6·10^{-6}$	$2.5·10^{-6}$	$2.7·10^{-6}$	$2.4·10^{-6}$	$2.5·10^{-6}$	$2.8·10^{-6}$	$2.5·10^{-6}$	$2.7·10^{-6}$	$2.7·10^{-6}$
	pH$_2$(g)=10^{-7} atm	$2.6·10^{-6}$	$2.5·10^{-6}$	$2.7·10^{-6}$	$2.4·10^{-6}$	$2.5·10^{-6}$	$2.8·10^{-6}$	$2.5·10^{-6}$	$2.7·10^{-6}$	
	pH$_2$(g)= 10^{2} atm	$2.6·10^{-6}$	$2.5·10^{-6}$	$2.7·10^{-6}$	$2.4·10^{-6}$	$2.5·10^{-6}$	$2.8·10^{-6}$	$2.5·10^{-6}$		
Sm	Eh gw	$9.3·10^{-9}$	$7.8·10^{-9}$	$9.2·10^{-10}$	$1.2·10^{-10}$	$2.1·10^{-8}$	$3.8·10^{-8}$	$7.5·10^{-8}$	$1.0·10^{-8}$	$1.8·10^{-9}$
	pH$_2$(g)=10^{-7} atm	$9.3·10^{-9}$	$7.8·10^{-9}$	$9.2·10^{-10}$	$1.2·10^{-10}$	$2.1·10^{-8}$	$3.8·10^{-8}$	$7.5·10^{-8}$	$1.0·10^{-8}$	
	pH$_2$(g)= 10^{2} atm	$9.3·10^{-9}$	$7.8·10^{-9}$	$9.2·10^{-10}$	$1.2·10^{-10}$	$2.1·10^{-8}$	$3.8·10^{-8}$	$7.2·10^{-8}$		
Th	Eh gw	$1.0·10^{-9}$	$2.0·10^{-10}$	$6.9·10^{-9}$	$7.5·10^{-11}$	$9.8·10^{-10}$	$6.8·10^{-10}$	$6.3·10^{-9}$	$6.4·10^{-10}$	$8.1·10^{-10}$
	pH$_2$(g)=10^{-7} atm	$1.0·10^{-9}$	$2.0·10^{-10}$	$6.9·10^{-9}$	$7.5·10^{-11}$	$9.8·10^{-10}$	$6.8·10^{-10}$	$6.3·10^{-9}$	$6.4·10^{-10}$	
	pH$_2$(g)= 10^{2} atm	$1.0·10^{-9}$	$2.0·10^{-10}$	$6.9·10^{-9}$	$7.5·10^{-11}$	$9.8·10^{-10}$	$6.8·10^{-10}$	$6.3·10^{-9}$		
Pa	Eh gw	$3.0·10^{-7}$	$2.8·10^{-7}$	$3.1·10^{-7}$	$2.4·10^{-7}$	$2.9·10^{-7}$	$2.8·10^{-7}$	$3.0·10^{-7}$	$3.3·10^{-7}$	$3.2·10^{-7}$
	pH$_2$(g)=10^{-7} atm	$3.0·10^{-7}$	$2.8·10^{-7}$	$3.1·10^{-7}$	$2.4·10^{-7}$	$2.9·10^{-7}$	$2.8·10^{-7}$	$3.0·10^{-7}$	$3.3·10^{-7}$	
	pH$_2$(g)= 10^{2} atm	$3.0·10^{-7}$	$2.8·10^{-7}$	$3.1·10^{-7}$	$2.3·10^{-7}$	$2.9·10^{-7}$	$2.8·10^{-7}$	$3.0·10^{-7}$		
U	Eh gw	$7.0·10^{-10}$	$6.1·10^{-10}$	$2.7·10^{-7}$	$5.2·10^{-10}$	$6.7·10^{-9}$	$2.5·10^{-9}$	$3.3·10^{-9}$	$1.3·10^{-7}$	$2.3·10^{-9}$
	pH$_2$(g)=10^{-7} atm	$6.8·10^{-10}$	$6.1·10^{-10}$	$8.0·10^{-10}$	$5.2·10^{-10}$	$6.5·10^{-10}$	$6.2·10^{-10}$	$9.5·10^{-10}$	$1.6·10^{-9}$	
	pH$_2$(g)= 10^{2} atm	$6.5·10^{-10}$	$6.1·10^{-10}$	$6.8·10^{-10}$	$5.1·10^{-10}$	$6.3·10^{-10}$	$6.1·10^{-10}$	$6.6·10^{-10}$		
Np	Eh gw	$8.0·10^{-10}$	$6.9·10^{-10}$	$1.2·10^{-9}$	$5.7·10^{-10}$	$7.8·10^{-10}$	$7.2·10^{-10}$	$1.1·10^{-9}$	n.s.l	$8.2·10^{-10}$
	pH$_2$(g)=10^{-7} atm	$8.0·10^{-10}$	$6.9·10^{-10}$	$1.2·10^{-9}$	$5.7·10^{-10}$	$7.8·10^{-10}$	$7.2·10^{-10}$	$1.1·10^{-9}$	$1.3·10^{-9}$	
	pH$_2$(g)= 10^{2} atm	$8.0·10^{-10}$	$6.9·10^{-10}$	$1.2·10^{-9}$	$5.7·10^{-10}$	$7.8·10^{-10}$	$7.2·10^{-10}$	$1.1·10^{-9}$		
Pu	Eh gw	$8.0·10^{-9}$	$1.3·10^{-9}$	$1.5·10^{-10}$	$2.3·10^{-10}$	$8.0·10^{-10}$	$1.0·10^{-9}$	$3.7·10^{-7}$	$1.6·10^{-5}$	$1.3·10^{-10}$
	pH$_2$(g)=10^{-7} atm	$8.0·10^{-9}$	$1.8·10^{-9}$	$5.1·10^{-10}$	$2.7·10^{-10}$	$1.8·10^{-8}$	$2.9·10^{-8}$	$1.1·10^{-6}$	$8.3·10^{-9}$	
	pH$_2$(g)= 10^{2} atm	$8.0·10^{-9}$	$9.5·10^{-9}$	$5.1·10^{-10}$	$2.0·10^{-10}$	$3.4·10^{-6}$	$5.4·10^{-6}$	$1.5·10^{-5}$		

		SOLUBILITY (mol·dm^{-3})								
		Olkiluoto groundwaters				Bentonitic waters			Glacial waters	
Element	Redox state	Brackish/ Saline KR20/465/1	Saline KR10/498/1	Dilute/ brackish KR6/58/1	Brine KR12/741/1	Brackish/ Saline	Saline	Dilute/ brackish	Glacial meltwater	Ice melting water
Am/Cm	Eh gw	$1.7 \cdot 10^{-7}$	$4.4 \cdot 10^{-7}$	$3.2 \cdot 10^{-9}$	$1.2 \cdot 10^{-8}$	$4.5 \cdot 10^{-7}$	$9.2 \cdot 10^{-7}$	$4.0 \cdot 10^{-7}$	$5.4 \cdot 10^{-9}$	$5.6 \cdot 10^{-8}$
	pH$_2$(g)=10^{-7} atm	$1.7 \cdot 10^{-7}$	$4.4 \cdot 10^{-7}$	$3.2 \cdot 10^{-9}$	$1.2 \cdot 10^{-8}$	$4.5 \cdot 10^{-7}$	$9.2 \cdot 10^{-7}$	$4.0 \cdot 10^{-7}$	$5.3 \cdot 10^{-9}$	
	pH$_2$(g)= 10^{2} atm	$1.7 \cdot 10^{-7}$	$4.4 \cdot 10^{-7}$	$3.2 \cdot 10^{-9}$	$1.2 \cdot 10^{-8}$	$4.5 \cdot 10^{-7}$	$9.2 \cdot 10^{-7}$	$4.0 \cdot 10^{-7}$		